Prying open a Thiele cage: discovery of an unprecedented extended pinacol rearrangement

Nathan Dao, Jonathan K. Sader, Allen G. Oliver, and Jeremy E. Wulff

2019

The final publication is available at:
https://doi.org/10.1039/C8CC08862D

ChemComm

COMMUNICATION

Prying Open a Thiele Cage: Discovery of an Unprecedented Extended Pinacol Rearrangement

Received 00th January 20xx,
Accepted 00th January 20xx

DOI: 10.1039/x0xx00000x

www.rsc.org/

Nathan Dao,‡[a] Jonathan K. Sader,‡[a] Allen G. Oliver,[b] and Jeremy E. Wulff *[a]

The first extended pinacol rearrangement across an sp3–sp3 bond is reported. The reaction appears to be both stereo- and regio-specific, and results in an extremely rare example of cage opening for a 1,3-bishomocubane structure derived from Thiele's ester.

Thiele's acid and ester are Diels-Alder heterodimers resulting from equilibrating mixtures of carboxylated cyclopentadiene (Figure 1A).[1] While in principle up to 72 different Diels-Alder adducts could be produced from such a reaction, in practice only a single major product predominates in both the acid and ester cases.[2,3] The rigid molecular architecture of Thiele's acid and derivatives thereof suggests as-yet unrealized opportunities in the synthesis of conformationally restricted drug candidates for biological screening applications.[4,5]

Our group recently described an improved synthesis of Thiele's ester,[6] established the first chiral resolution of the parent diacid,[7] and developed a suite of conformationally tuned molecular clefts based upon the Thiele framework (Figure 1B).[6] While these products have the appropriate structural characteristics for use in supramolecular applications or perhaps as ß-turn mimics, they all display essentially the same core structure, and therefore lack the deep-seated scaffold alterations that would be desirable for the development of a screening library.

Although Thiele's acid and ester have been known for over a century, relatively little reaction chemistry has been developed around them. Nevertheless, Dunn and Donohue showed many years ago that exposure of Thiele's ester to ultraviolet light results in an efficient intramolecular [2+2] reaction that transforms the 'open' Thiele's ester into a 'closed' 1,3-bishomocubane structure that we shall refer to here as a Thiele cage (Figure 2A).[8] Marchand and others have exploited this reaction to make a wide variety of structures

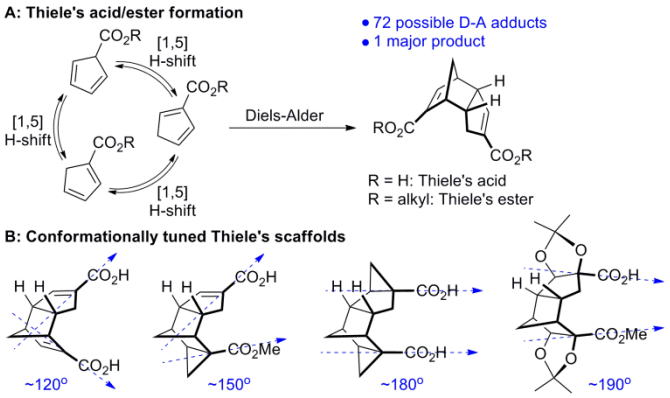

Figure 1. Origin of Thiele's acid and ester, and a series of conformationally tuned scaffolds derived from them. Blue arrows indicate angles of projection for the carboxylic acid or ester substituents, and numbers in blue indicate cleft angles calculated as in reference 6.

incorporating the 1,3-bishomocubane motif,[4,5,9-12] but here too, deep-seated structural changes for cages derived from Thiele's acid or ester are exceedingly rare.[13]

Containing two cyclobutane units, 1,3-bishomocubanes are strained systems, and in fact several 1,3-bishomocubane derivatives have been investigated as explosives and high energy density fuels.[12,14] More functionalized bishomocubanes —especially those incorporating ketone or acetoxy groups

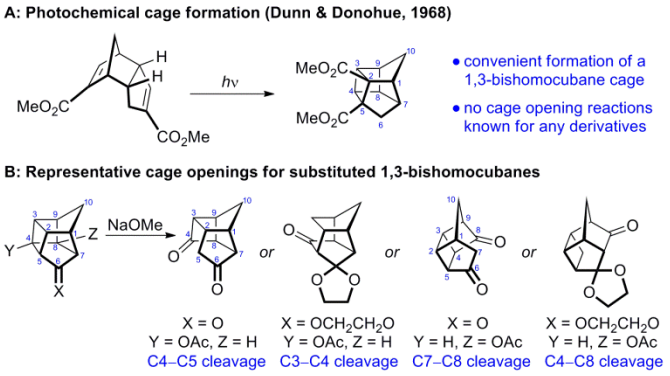

Figure 2. Generation of a 1,3-bishomocubane cage structure from Thiele's ester, and representative structural rearrangements for keto- and acetoxy-substituted 1,3-bishomocubanes.

[a] Dept. of Chemistry, University of Victoria, PO Box 3065 STN CSC, Victoria, British Columbia, Canada, V8W 3V6. E-mail: wulff@uvic.ca
[b] Molecular Structure Facility, Dept. of Chemistry and Biochemistry, University of Notre Dame, 251 Nieuwland Science Hall, Notre Dame, IN 46556, USA

† Electronic Supplementary Information (ESI) available: Figures S1 and S2, full experimental details, spectroscopic data for all new compounds. CCDC 1871599 (**3**). For ESI and crystallographic data in cif form, see DOI: 10.1039/x0xx00000x

‡ These authors contributed equally to the preparation of the manuscript.

within the pentacyclo[5.3.0.0^{2,5}.0^{3,9}.0^{4,8}]decane core—are known to undergo rearrangement reactions leading to partially open seco-cage structures.[15,16,17] Although such rearrangements have not previously been shown for Thiele's acid derivatives (which necessarily lack functionality within the 1,3-bishomocubane core), we hypothesized that a selective ring-opening reaction could be identified, which would result in deep-seated changes to the Thiele cage core structure.[18,19]

Here we report the results of our study aimed at the identification of such a reaction, culminating in the discovery of an unprecedented extended pinacol rearrangement that opens the Thiele cage. The reaction proceeds with perfect control over both regiochemistry and stereochemistry, and results in a substantial change to the three-dimensional structure of the overall scaffold architecture.

Operating under a hypothesis that increasing steric strain might favour ring opening of the Thiele cage, we began by preparing substrates of increasing steric bulk (**1a**–**1d**, Scheme 1). Thiele's methyl ester (**1b**) and benzyl ester (**1c**) were prepared from sodium cyclopentadienylide and the appropriate carbonate, following our previously developed route.[6] The methyl ester was saponified (using a hindered solvent to avoid unwanted conjugate addition) to afford Thiele's acid (**1a**). Accessing the corresponding adamantyl ester (**1d**) was more challenging, but we were ultimately able to achieve this substrate (albeit in low yield) through the use of Lebel's amine diazotization protocol.[20]

Compounds **1a**–**1d** were irradiated at 254 nm. Each of the substrates cyclized efficiently to the corresponding 1,3-bishomocubane (**2a**–**2d**). The conversion in each case was high although purification challenges contributed to modest isolated yields for three of the four products.

We next attempted thermal or photochemical ring opening for cages **2a**–**2d**. Photochemical irradiation at either 254, 300, or 350 nm in benzene-d_6 or methanol-d_4 led to no detectable reaction, and to recovery of starting material for all four cages.[21] Thermal activation was studied at 50 °C and 100 °C, in a variety of solvents (toluene, xylene, chloroform, ethyl acetate, ethanol, acetic acid, or dimethyl sulfoxide). Once again, however, no detectable ring opening was observed. In each case the substrate was recovered unchanged.

In an effort to further increase the steric demands for the system, we next reacted ester **2b** with phenyl lithium to afford the very hindered diol **3** (Scheme 2).[22] The constrained nature of this molecule is highlighted by the fact that the ß-proton at C10 of the pentacyclo[5.3.0.0^{2,5}.0^{3,9}.0^{4,8}]decane core appears at –0.65 ppm in the ^{1}H NMR spectrum—evidence of substantial magnetic shielding by the phenyl groups on C11.

Diol **3** also did not react under photochemical conditions, or upon heating in aprotic solvents. Gratifyingly, however, when the compound was incubated in acidic conditions (neat AcOH at 100 °C or 2.5 equiv of H_2SO_4 in various solvents) we observed rearrangement to a single major product. The less hindered analogue **6** did not undergo a similar reaction, affording only acetylated derivative **7** upon heating in acetic acid, or recovered starting material when exposed to H_2SO_4.

Isolation and characterization of the rearrangement product from **3** immediately revealed that the C2–C5 bond of the cage had been selectively cleaved, and that the two diphenylmethanol substituents had been exchanged for a diphenyl alkylidene (^{13}C NMR: δ 136 and 144 ppm) and a phenyl ketone (^{13}C NMR: δ 198 ppm; IR ν 1661 cm^{-1}). These observations (together with additional spectroscopic and MS data; refer to the Supplementary Information for full details) were sufficient to identify the product as arising from an extended pinacol rearrangement, from which two different regioisomeric products could be envisioned (**4** and **5**). For each regioisomer, two diastereomers were considered (i.e. **4a** and **4b**; **5a** and **5b**; structures shown in Scheme 3).

Detailed analysis of the ^{1}H, ^{13}C, COSY, DEPT-135, HSQC and HMBC data – together with comparison of ^{1}H and ^{13}C chemical shifts to estimated resonances for each structure (see Supplementary Information) allowed us to rule out regioisomer **5** and unambiguously confirm the connectivity shown in structure **4** as corresponding to the isolated product.

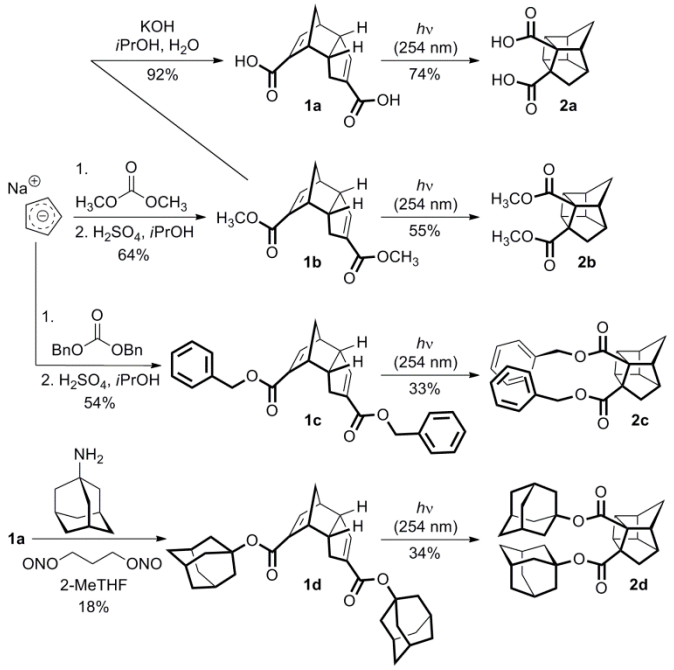

Scheme 1. Synthesis of Thiele acid and ester substrates of increasing steric demand, and photocyclization to the corresponding cage structures.

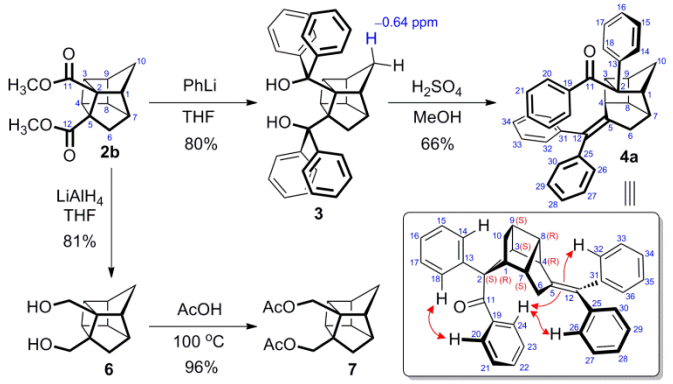

Scheme 2. Synthesis of diol substrates, and observation of a new extended pinacol rearrangement reaction. Red arrows indicate NOE interactions.

Establishing the relative stereochemistry for the molecule was more difficult, and required us to first use 1D TOCSY NMR to resolve the overlapping aromatic signals from the ^{1}H NMR spectrum. This revealed that the *ortho* protons on the four aromatic rings (i.e. H14/18, H20/24, H26/30, and H32/36 using the numbering system in Scheme 2) were all sufficiently well resolved in the ^{1}H NMR to permit cross-relaxation experiments. A series of 1D NOE spectra showed that the *ortho* protons on the phenyl ketone (H20/24) were in close proximity to the *ortho* protons of each of the other aromatic rings. This is only possible for the 1*R*, 2*S*, 3*S*, 4*R*, 7*S*, 8*R*, 9*S* diastereomer, which allowed us to conclusively establish the product from the rearrangement as **4a**.

In seeking to understand the reaction from a mechanistic perspective, we first considered the stepwise pathway described in Scheme 3A. In this putative mechanism, protonation of either of the two alcohol groups would lead to loss of water and formation of a pair of regioisomeric carbocation intermediates: **A** and **B**. Which intermediate forms first would probably be inconsequential in this case, since the two species could interconvert, either *via* tetrahydrofuran **C** or through recombination with water to regenerate the starting material. Fragmentation of the C2–C5 cyclobutane bond in either **A** or **B** would be accompanied by generation of an olefin, affording a new pair of regioisomeric carbocation intermediates: **D** and **E**. The preferential formation of either **D** or **E** would presumably dictate the regiochemical outcome for the reaction, since these two species are less likely to interconvert prior to the semipinacol rearrangement taking place. The last step—1,2-migration of the benzene ring—should be essentially irreversible and will dictate the stereochemical outcome for the overall process, by establishing the new stereogenic centre at C2.

We briefly investigated this mechanism computationally, but could find little purchase to support it on either thermodynamic or kinetic grounds. Compound **4a** is not the lowest in energy of the four potential rearrangement products shown in Scheme 3A, and there doesn't appear to be sufficient difference between the energies of **C** and **D** to account for the high degree of regiochemical control observed in the reaction. Moreover, the geometry-optimized structure of intermediate **D** provides no indication for why the preferred trajectory should be the one leading to **4a** over **4b**.

With the stepwise mechanism thus unable to explain the regio- and stereochemical outcome, we considered the possibility of a concerted reaction. Because the two alcohol groups are held near one another, we reasoned that protonation of either alcohol could be stabilized through hydrogen bonding to the other oxygen atom, akin to the situation with proton sponge base. The existence of this O–H–O hydrogen bond places an additional constraint on the system, limiting the number of accessible conformers.

DFT calculations on this equilibrating mixture (**F** and **G**) suggested the existence of a low-energy conformer wherein one of the two phenyl groups on C11 is held antiperiplanar to the C2–C5 bond (see Figure S1 for optimized structure). At the same time, the C12–O bond is approximately synperiplanar,

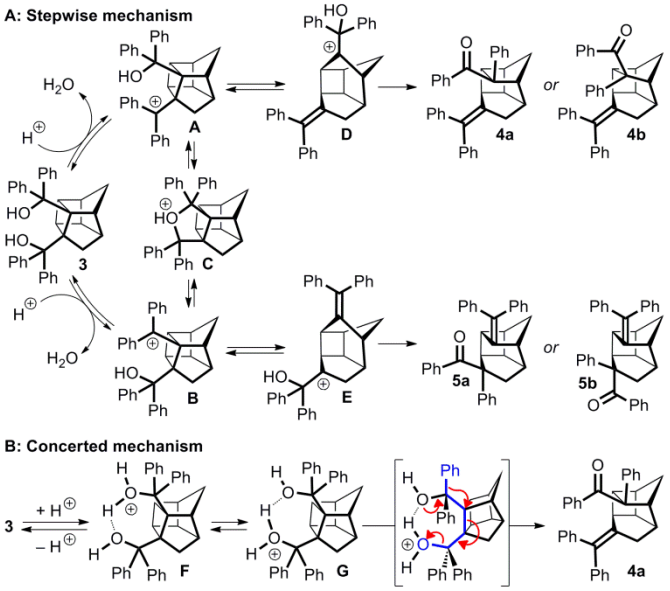

Scheme 3. Proposed mechanisms for the extended pinacol rearrangement. Bonds shown in blue are approximately coplanar.

something that presumably would facilitate the movement of electrons as shown in Scheme 3B. Reaction *via* this conformer would lead exclusively to species **4a**.

Seeking additional evidence, we obtained an X-ray structure of precursor **3** (Figure S2). This revealed that even in the unprotonated form, the molecule is pre-organized to undergo rearrangement, with the migrating phenyl group (C13–C18) held *anti* to the C2–C5 bond (θ = 177°), and with the C2–C5 bond itself exhibiting a significantly longer distance (1.66 Å) than the other six cyclobutane bonds in the structure (1.56 ± 0.01 Å)—a feature that was also predicted in our calculated structure of the putative reactive conformer (Table S1). This structure also explained the dramatic upfield shift for the C10 ß-proton (*vide infra*), since the latter is positioned directly in the π system of the C13–C18 phenyl group, which is notably distorted from planarity; the observation of this shift in the solution-state NMR thus supports the relevance of the solid state structure in interpreting solution-state reactivity.

These data would be consistent with a concerted extended pinacol pathway, but might also serve to rationalize the stereochemical outcome of a stepwise reaction, if the intermediate carbocation **D** is sufficiently short-lived as to facilitate the migration of the phenyl group before structural relaxation occurs. Further mechanistic study will be required to distinguish between the two related possibilities.

Pinacol (or semipinacol) rearrangements are among the most well-known structural reorganization reactions in organic chemistry, and have been extensively exploited in the synthesis of complex natural products and other targets.[23] π-Extended pinacol rearrangements (i.e. **8**→**9**, Scheme 4) are likewise well-studied,[24] and an enantioselective variant has been described.[24d] A single example of an analogous reaction across a cyclopropane ring (i.e. **10**→**11**) was reported,[25] but since the sp^{5} carbon atoms in the cyclopropane contribute significant π character to the bonds, this does not constitute a reaction across a true alkyl bond. Indeed, to the best of our

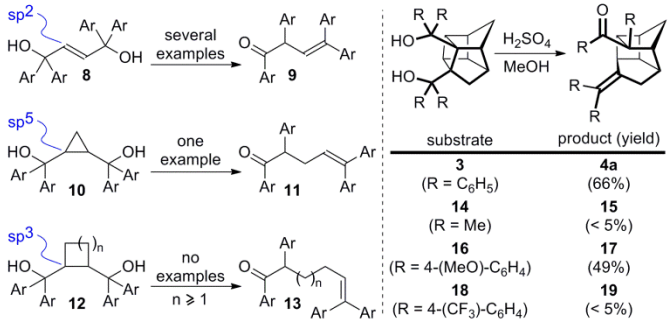

Scheme 4. Known, unknown, and novel extended pinacol rearrangements.

knowledge, there are no prior examples of extended pinacol rearrangements occurring across $sp^3C–sp^3C$ bonds.

To gain insight into the scope and limitations of the reaction, we prepared and tested three additional substrates: **14**, **16**, and **18** (Scheme 4). As with 1° alcohol **6**, the simple 3° alcohol **14** (containing four methyl groups) failed to produce a product analogous to **4a**. Likewise the very electron-poor **18** (containing four CF_3 groups at the *para*-positions of the aromatic rings) did not react, even at increased temperatures. However, the more electron-rich substrate **16** (containing four *p*-methoxy groups) efficiently rearranged to afford ketone **17**. These data would be consistent with carbocation character in the rate-determining step, but further study will be required to elucidate the precise mechanistic details.

In summary, the extended pinacol reaction described here represents a novel ring opening reaction for the Thiele bishomocubane, and constitutes one of the first selective cage openings for any pentacyclo[5.3.0.0^{2,5}.0^{3,9}.0^{4,8}]decane scaffold derived from the venerable Thiele acid scaffold. We envision that pairs of tetraarylated molecules before and after cage opening (i.e. derivatives of **3** and **4a**) will be interesting to evaluate for their biological properties, and plan to undertake such a study in the future. In addition to switching the hydrogen-bond donor and acceptor groups on the compounds' surface, the rearrangement reaction results in a substantial change in the shape of the rigid backbone, altering the projection vectors for the substituents. These changes will profoundly perturb interactions with protein targets.

Of perhaps even greater importance, the synthesis of **4a** represents a significant expansion of known pinacol-type processes. While extended pinacol reactions across π systems and cyclopropanes are described elsewhere, we believe this to be the first report of such a rearrangement occurring across an alkyl C–C bond. The apparent regio- and stereo-specificity indicates a constrained transition state in which an intramolecular hydrogen bond may serve to position a distal migrating group to control the reaction trajectory.

We acknowledge NSERC Canada for operating funds, and for a fellowship to J. S. We also thank the Canada Research Chairs program, the Michael Smith Foundation for Health Research, and the University of Victoria for ongoing support.

Conflicts of interest

There are no conflicts to declare.

Notes and references

1 J. Thiele, *Chem. Ber.*, 1901, **34**, 68.
2 (a) I. Fleming, Frontier Orbitals and Organic Chemical Reactions; John Wiley & Sons: Chichester, 1976; pp 136, 167-168; (b) I. Fleming, Molecular Orbitals and Organic Chemical Reactions, Reference Edition; John Wiley & Sons: Chichester, 2010; pp 321-322; (c) G. Deslongchamps and P. Deslongchamps, *Tetrahedron*, 2013, **69**, 6022; (d) J. Chen and J. E. Wulff, *Org. Biomol. Chem.*, 2016, **14**, 10170; (e) J. Chen, L. Lu and J. E. Wulff, *Synlett*, 2017, **28**, 2777.
3 A. P. Marchand, I. N. N. Namboothiri, S. B. Lewis, W. H. Watson and M. Krawiec, *Tetrahedron*, 1998, **54**, 1261.
4 O. Onajole, S. Sosibo, P. Govender, T. Govender, P. D. van Helden, G. E. M. Maguire, K. Mlinarić-Majerski, I. Wiid and H. G. Kruger, *Chem. Biol. Drug Des.*, 2011, **78**, 1022.
5 A. S. Sklyarova, V. N. Rodionov, C. G. Parsons, G. Quack, P. R. Schreiner, A. A. Fokin, *Med. Chem. Res.*, 2013, **22**, 360-366
6 J. Chen, B. Kilpatrick, A. G. Oliver and J. E. Wulff, *J. Org. Chem.*, 2015, **80**, 8979.
7 J. Chen, X. Sun, A. G. Oliver and J. E. Wulff, *Can. J. Chem.*, 2017, **95**, 234.
8 G. L. Dunn and J. K. Donohue, *Tetrahedron Lett.*, 1968, **31**, 3485.
9 A. P. Marchand, I. N. N. Namboothiri, B. Ganguly, W. H. Watson and S. G. Bodige, *Tetrahedron Lett.*, **1999**, *40*, 5105.
10 A. P. Marchand, H, K. Hariprakasha and I. N. N. Namboothiri, *Synth. Commun.*, 2001, **31**, 1863.
11 S. G. Bodige, W. H. Watson, A. P. Marchand and V. S. Kumar, *J. Chem. Crystallog.*, 1999, **29**, 1261.
12 (a) S. Rajkumar, R. S. Choudhari, A. Chowdhury, and I. N. N. Namboothiri, *Thermochimica Acta*, 2013, **563**, 38; (b) S. Lal, L. Mallick, S. Rajkumar, O. P. Oommen, S. Reshmi, N. Kumbhakarna, A. Chowdhury and I. N. N. Namboothiri, *J. Mat. Chem. A*, 2015, **3**, 22118.
13 A. P. Marchand, D. Zhao, T.-K. Ngooi and V. Vidyasagar, *Tetrahedron*, 1993, **49**, 2613.
14 L. Mallick, S. Lal, S. Reshmi, I. N. N. Namboothiri, A. Chowdhury and N. Kumbhakarna, *New J. Chem.*, 2017, **41**, 920.
15 (a) A. J. H. Klunder, W. C. G. M. de Valk, J. M. J. Verlaak, J. W. M. Schellekens, J. H. Noordik, V. Parthasarathi and B. Zwanenburg, *Tetrahedron*, 1985, **41**, 963; (b) P. M. Ivanov, P. M., E. Ōsawa, A. J. H. Klunder and B. Zwanenburg, *Tetrahedron*, 1985, **41**, 975.
16 T. Ogino, K. Awano and Y. Fukazawa, *J. Chem. Soc. Perkin Trans. 2*, 1990, 1735.
17 T. Hasegawa, T. Nigo, Y. Kuwatani, I. Ueda, *Bull. Chem. Soc. Jpn.*, 1993, **66**, 2068.
18 Simple reductions of the cyclobutane bonds in Thiele's ester and related 1,3-bishomocubanes are known, using either dissolving metal reductions (ref. 13) or hydrogenation (ref. 19). However, we opted not to pursue this strategy here.
19 K. Hirao, T. Iwakuma, M. Taniguchi, O. Yonemitsu, T. Date and K. Kotera, *J. Chem. Soc., Perkin Trans. 1*, 1980, 163.
20 C. Audubert and H. Lebel, *Org. Lett.*, 2017, **19**, 4407.
21 The broad spectrum n→π transition associated with carbonyl groups is known to facilitate activation with unfiltered light centred on 254 nm; see: Y. Liu, X. Lan, S. Gao, Z. Shen, J. Lu and X. Ni, *Proc. SPIE*, 2003, **5254**, 526.
22 I. N. N. Namboothiri and O. P. Oommenn, Indian Pat. Appl. IN 2008MU00098 A 20091002, 2009.
23 Z.-L. Song, C.-A. Fan and Y.-Q. Tu, *Chem. Rev.*, 2011, **111**, 7523.
24 (a) R. E. Lutz, R. G. Bass and D. W. Boykin, *J. Org. Chem.*, 1964, **29**, 3660; (b) K. Saito, Y. Horie, T. Mukai and T. Toda, *Bull. Chem. Soc. Jpn.*, 1985, **58**, 3118; (c) L.-L. Zhu, X.-X. Li, W. Zhou, X. Li and Z. Chen, *J. Org. Chem.*, 2011, **76**, 8814; (d) H.

Wu, Q. Wang and J. Zhu, *Angew. Chem.*, 2016, **55**, 15411.
25 R. A. Darby and R. E. Lutz, *J. Org. Chem.*, 1957, **22**, 1353.

Prying Open a Thiele Cage:
Discovery of an Unprecedented Extended Pinacol Rearrangement

Supplementary Information

Index:

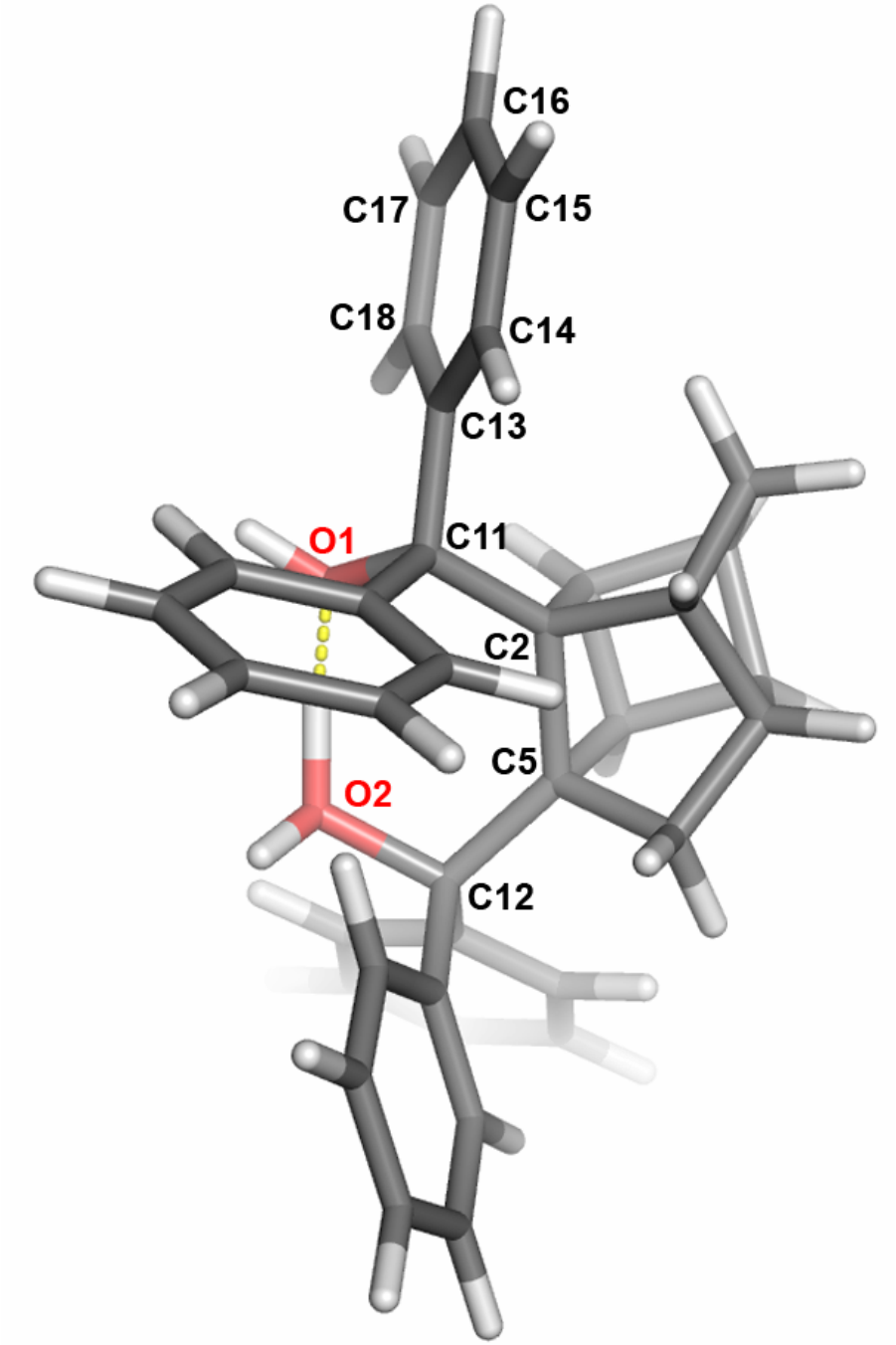

Figure S1. Possible reactive conformer of protonated diol **G**, leading to observed product **4a**. ΔH_f = +6.95 kJ/mol above minimum energy conformer (B3LYP/6-31G*). θ(C13-C11-C2-C5) = 169° (ideal antiperiplanar orientation = 180°); θ(C11-C2-C5-C12) = 14° (ideal synperiplanar orientation = 0°); θ(C2-C5-C12-O2) = 9° (ideal synperiplanar orientation = 0°). C2–C5 distance is 1.69 Å relative to 1.56±0.02 Å for the other six butane bonds. Intramolecular H-bond indicated with yellow dashes. The calculated geometry of the H-bond is similar to those determined within proton sponges.[1]

[1] H. A. Staab and T. Saupe, *Angewandte Chemie Int. Ed. Engl.*, 1988, **27**, 865.

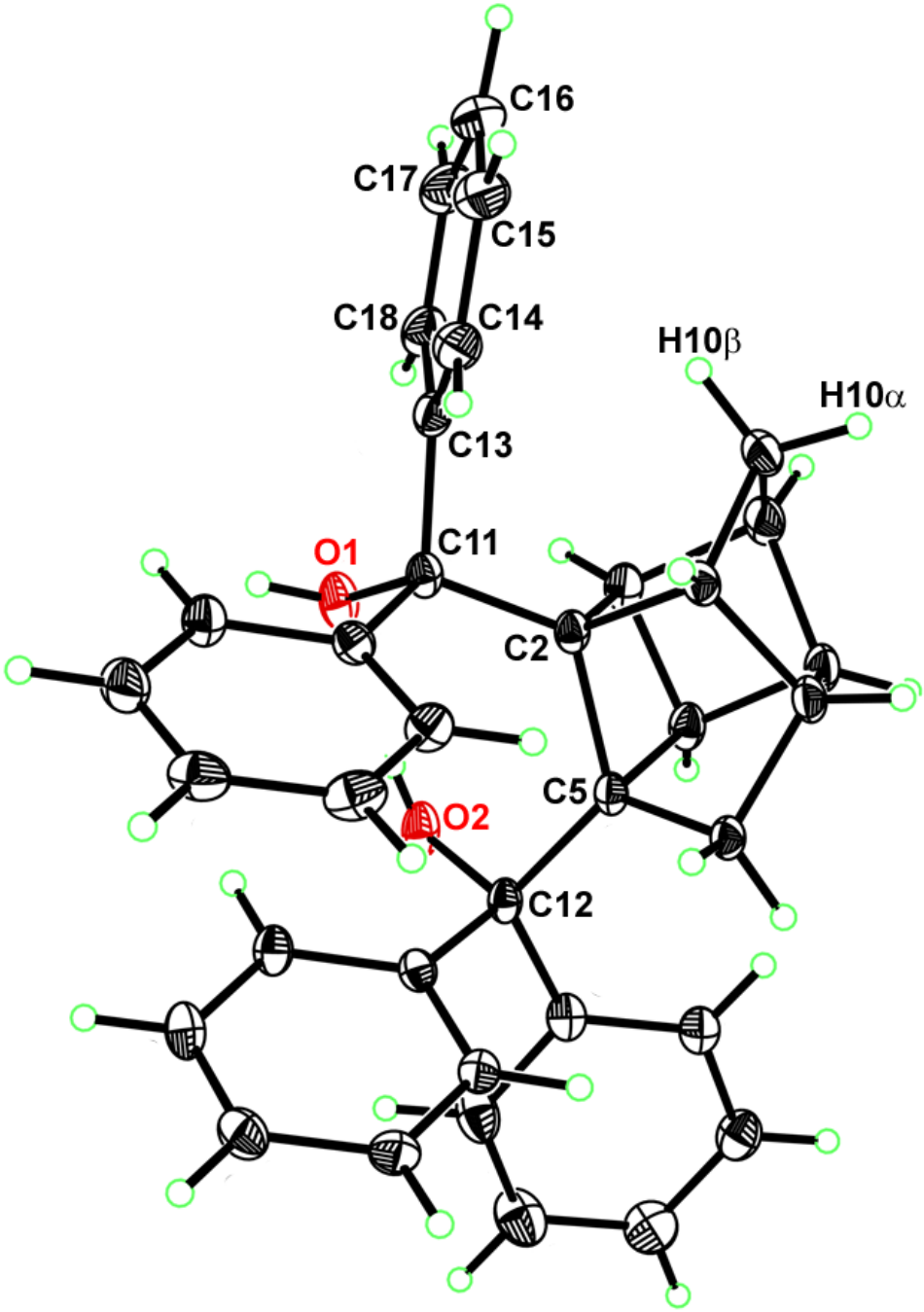

Figure S2A. X-ray structure of diol **3**. θ(C13-C11-C2-C5) = 177.04(8)° (ideal antiperiplanar orientation = 180°). Average distance between H10ß and C13–C18 = 2.905 Å. C2–C5 distance is 1.6610(13) Å relative to 1.56±0.01 Å for the other six butane bonds.

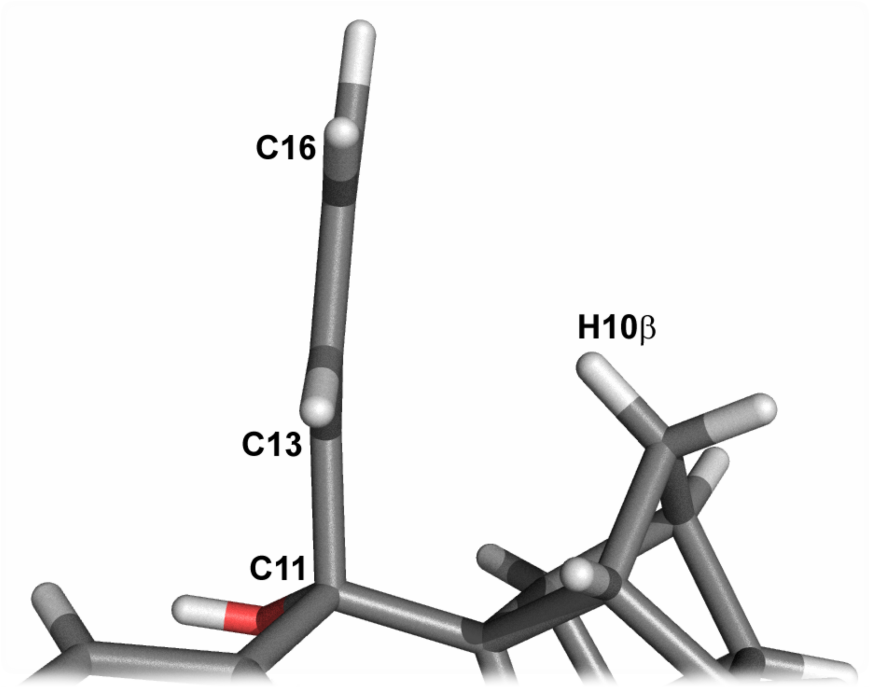

Figure S2B. Close-up view of the C13–C18 aromatic ring in the X-ray structure of diol **3**, showing the proximity to H10ß and the notable curvature of the phenyl group. ∠(C11-C13-C16) = 173.98(7)°.

Table S1. Comparison of Cyclobutane Bond Lengths in the Calculated Reactive Conformer of **G** (as in Figure S1) vs. the X-ray Structure of **3** (as in Figure S2).

bond	calculated reactive conformer **G** (DFT)	diol **3** (X-ray)
C2-C5	**1.688** Å	**1.6610(13)** Å
C2-C3	1.582 Å	1.5743(13) Å
C3-C4	1.534 Å	1.5360(14) Å
C4-C5	1.567 Å	1.5592(12) Å
C3-C9	1.553 Å	1.5500(14) Å
C8-C9	1.573 Å	1.5660(14) Å
C4-C8	1.567 Å	1.5663(14) Å
average:	**1.563 ± 0.017** Å	**1.559 ± 0.014** Å

Table S2. Full Chemical Shift Assignments for **4a** (CD_2Cl_2).

	Assigned ^{13}C Shift (ppm)	Assigned ^{1}H Shift(s) (ppm)		Assigned ^{13}C Shift (ppm)	Assigned ^{1}H Shift(s) (ppm)
C1	50.15	3.14	C7	48.86	2.79
C2	67.20	n/a	C8	45.69	2.72
C3	45.84	3.98	C9	40.87	3.05
C4	46.35	3.35	C10	38.37	1.09, 1.28
C5	144.44	n/a	C11	197.61	n/a
C6	37.39	2.63, 2.93	C12	135.95	n/a
C13	142.96	n/a	C25	143.39	n/a
C14/C18	127.02	7.24 or 7.36[a]	C26/C30	129.56	7.12
C15/C17	127.68	7.36 or 7.24[a]	C27/C29	128.36 or 128.51[a]	7.31
C16	127.22	7.19[b]	C28	126.73	7.21
C19	138.28	n/a	C31	143.18	n/a
C20/C24	130.56	7.76	C32/C36	128.93	6.21
C21/C23	128.36 or 128.51[a]	7.20	C33/C35	127.64	6.96
C22	132.23	7.28	C34	126.23	7.01

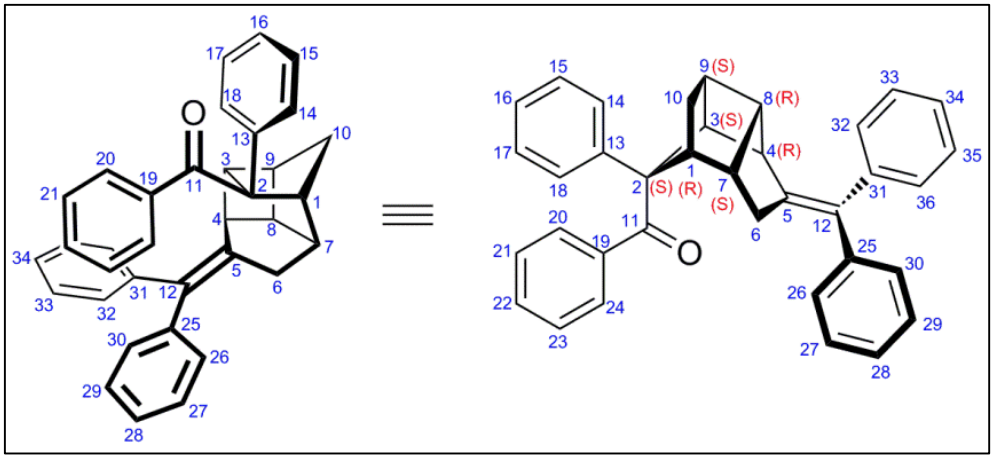

[a] poorly resolved signals in HSQC

[b] tentative assignment due to overlapping signals in HSQC

Table S3. Calculated Chemical Shifts for Structures **4a**–**4b** and **5a**–**5b**.

3A. Confirmed Assignments for **4a**: (all values in ppm)

	Assigned ^{13}C Shift	Assigned ^{1}H Shift(s)	MestReNova Estimates (Mnova Best) ^{13}C Shift	Δ(δ)	^{1}H Shift	Δ(δ)	DFT Estimates (B3LYP/6-31G*) ^{13}C Shift	Δ(δ)	^{1}H Shift	Δ(δ)
C1	50.15	3.14	47.51	2.6	2.84	0.3	52.64	2.5	3.22	0.1
C2	67.20	n/a	56.16	11.0	n/a	n/a	68.21	1.0	n/a	n/a
C3	45.84	3.98	51.47	5.6	3.80	0.2	49.04	3.2	3.62	0.4
C4	46.35	3.35	40.21	6.1	3.15	0.2	46.23	0.1	3.52	0.2
C5	144.44	n/a	131.39	13.1	n/a	n/a	142.40	2.0	n/a	n/a
C6	37.39	2.63, 2.93	38.88	1.5	2.47, 2.54	0.2, 0.4	36.79	0.6	2.25, 3.77	0.4, 0.8
C7	48.86	2.79	43.89	5.0	2.64	0.2	50.76	1.9	2.72	0.1
C8	45.69	2.72	48.64	3.0	2.92	0.2	45.83	0.1	2.62	0.1
C9	40.87	3.05	41.20	0.3	2.66	0.4	41.46	0.6	2.70	0.4
C10	38.37	1.09, 1.28	33.66	4.7	1.62, 1.70	0.5, 0.4	38.05	0.3	1.11, 1.23	0.0, 0.5
C11	197.61	n/a	199.59	2.0	n/a	n/a	190.39	7.2	n/a	n/a
C12	135.95	n/a	138.99	3.0	n/a	n/a	135.29	0.7	n/a	n/a
			average Δ(δ):	**4.8**		**0.29**		**1.7**		**0.24**

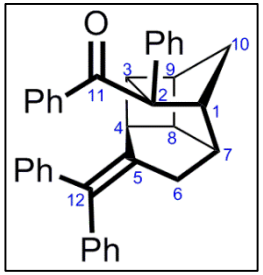

3B. Best-Fit* Assignments for **4b**: (all values in ppm)

	Assigned ^{13}C Shift	Assigned ^{1}H Shift(s)	MestReNova Estimates (Mnova Best) ^{13}C Shift	Δ(δ)	^{1}H Shift	Δ(δ)	DFT Estimates (B3LYP/6-31G*) ^{13}C Shift	Δ(δ)	^{1}H Shift	Δ(δ)
C1	50.15	3.14	47.51	2.6	2.84	0.3	52.39	2.2	3.74	0.6
C2	67.20	n/a	56.16	11.0	n/a	n/a	70.70	3.5	n/a	n/a
C3	45.84	3.98	51.47	5.6	3.80	0.2	46.71	0.9	3.59	0.4
C4	46.35	3.35	40.21	6.1	3.15	0.2	47.01	0.7	3.68	0.3
C5	144.44	n/a	131.39	13.1	n/a	n/a	145.41	1.0	n/a	n/a
C6	37.39	2.63, 2.93	38.88	1.5	2.47, 2.54	0.2, 0.4	35.51	1.9	1.96, 2.59	0.7, 0.3
C7	48.86	2.79	43.89	5.0	2.64	0.2	49.44	0.6	2.66	0.1
C8	45.69	2.72	48.64	3.0	2.92	0.2	46.40	0.7	2.59	0.1
C9	40.87	3.05	41.20	0.3	2.66	0.4	40.23	0.6	2.44	0.6
C10	38.37	1.09, 1.28	33.66	4.7	1.62, 1.70	0.5, 0.4	41.42	3.1	1.57, 1.67	0.5, 0.4
C11	197.61	n/a	199.59	2.0	n/a	n/a	198.45	0.8	n/a	n/a
C12	135.95	n/a	138.99	3.0	n/a	n/a	132.09	3.9	n/a	n/a
			average Δ(δ):	**4.8**		**0.29**		**1.7**		**0.41**

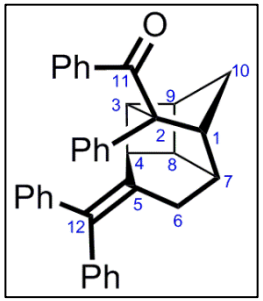

3C. Best-Fit* Assignments for **5a**: (all values in ppm)

	Assigned ^{13}C Shift	Assigned ^{1}H Shift(s)	MestReNova Estimates (Mnova Best) ^{13}C Shift	Δ(δ)	^{1}H Shift	Δ(δ)	DFT Estimates (B3LYP/6-31G*) ^{13}C Shift	Δ(δ)	^{1}H Shift	Δ(δ)
C1	50.15	3.14	41.14	9.0	2.63	0.5	49.34	0.8	2.88	0.3
C2	67.20	n/a	57.02	10.2	n/a	n/a	69.25	2.1	n/a	n/a
C3	45.84	3.98	45.87	0.0	2.68	1.3	43.05	2.8	3.86	0.1
C4	46.35	3.35	44.90	1.5	2.95	0.4	59.60	13.3	2.65	0.7
C5	144.44	n/a	132.28	12.2	n/a	n/a	149.61	5.2	n/a	n/a
C6	37.39	2.63, 2.93	43.63	6.2	2.06, 2.09	0.6, 0.8	40.26	2.9	2.81, 2.89	0.2, 0.0
C7	48.86	2.79	44.23	4.6	2.05	0.7	49.10	0.2	2.81	0.0
C8	45.69	2.72	47.28	1.6	2.89	0.2	44.62	1.1	2.80	0.1
C9	40.87	3.05	42.07	1.2	2.22	0.8	38.09	2.8	2.58	0.5
C10	38.37	1.09, 1.28	37.74	0.6	1.47, 1.59	0.4, 0.3	42.38	4.0	1.54, 1.60	0.5, 0.3
C11	197.61	n/a	200.63	3.0	n/a	n/a	205.40	7.8	n/a	n/a
C12	135.95	n/a	123.53	12.4	n/a	n/a	140.61	4.7	n/a	n/a
			average Δ(δ):	**5.2**		**0.61**		**4.0**		**0.26**

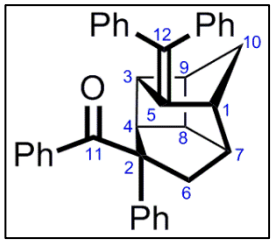

3D. Best-Fit* Assignments for **5b**: (all values in ppm)

	Assigned ^{13}C Shift	Assigned ^{1}H Shift(s)	MestReNova Estimates (Mnova Best) ^{13}C Shift	Δ(δ)	^{1}H Shift	Δ(δ)	DFT Estimates (B3LYP/6-31G*) ^{13}C Shift	Δ(δ)	^{1}H Shift	Δ(δ)
C1	50.15	3.14	41.14	9.0	2.63	0.5	49.03	1.1	3.20	0.1
C2	67.20	n/a	57.02	10.2	n/a	n/a	68.82	1.6	n/a	n/a
C3	45.84	3.98	45.87	0.0	2.68	1.3	42.41	3.4	3.15	0.8
C4	46.35	3.35	44.90	1.5	2.95	0.4	54.45	8.1	3.90	0.6
C5	144.44	n/a	132.28	12.2	n/a	n/a	143.41	1.0	n/a	n/a
C6	37.39	2.63, 2.93	43.63	6.2	2.06, 2.09	0.6, 0.8	37.53	0.1	2.59, 3.40	0.0, 0.5
C7	48.86	2.79	44.23	4.6	2.05	0.7	50.50	1.6	2.73	0.1
C8	45.69	2.72	47.28	1.6	2.89	0.2	47.79	2.1	2.84	0.1
C9	40.87	3.05	42.07	1.2	2.22	0.8	39.00	1.9	2.70	0.4
C10	38.37	1.09, 1.28	37.74	0.6	1.47, 1.59	0.4, 0.3	42.95	4.6	1.50, 1.64	0.4, 0.4
C11	197.61	n/a	200.63	3.0	n/a	n/a	191.55	6.1	n/a	n/a
C12	135.95	n/a	123.53	12.4	n/a	n/a	133.14	2.8	n/a	n/a
			average Δ(δ):	**5.2**		**0.61**		**2.9**		**0.33**

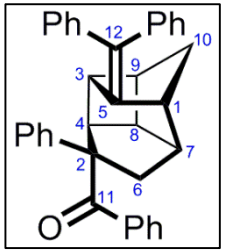

*Best fit assignments are not supported by correlations in the 2D NMR but are included here for comparative purposes.

Table S4. Comparison of Regioisomer and Diastereomer Ground State Energies.

	4a	4b	5a	5b	
ΔH_f (PM3): [a]	506.029	499.296	484.578	486.297	kJ/mol
$\Delta[\Delta H_f]$: [a]	+21.45	+14.72	+0.00	+1.72	kJ/mol
ΔH_f (B3LYP): [b]	-1465.067503	-1465.061453	-1465.071036	-1465.068730	Hartrees
$\Delta[\Delta H_f]$: [b]	+2.22	+6.01	+0.00	+1.45	kJ/mol

[a] Semi-empirical geometry optimization using a PM3 parameter set.

[b] DFT geometry optimization using a B3LYP functional and a 6-31G* basis set.

Table S5. Comparison of Putative Cationic Intermediate Energies.

	intermediate D	intermediate E	
ΔH_f (PM3): [a]	1275.589	1246.767	kJ/mol
$\Delta[\Delta H_f]$: [a]	+28.82	+0.00	kJ/mol
ΔH_f (B3LYP): [b]	-1465.440452	-1465.436185	Hartrees
$\Delta[\Delta H_f]$: [b]	+0.00	+2.68	kJ/mol

[a] Semi-empirical geometry optimization using a PM3 parameter set.

[b] DFT geometry optimization using a B3LYP functional and a 6-31G* basis set.

Experimental Details:

General Considerations

Unless otherwise stated, all reactions were performed in flame-dried glassware equipped with rubber septa under a positive pressure of argon. Organic solutions were concentrated at 35-40 °C by rotary evaporation. THF was freshly distilled over sodium and benzophenone. Anhydrous 2-MeTHF was purchased from Aldrich and used as received. Solvents and air-sensitive solutions were transferred via stainless steel cannula or via plastic syringe equipped with a stainless-steel needle. Analytical thin layer chromatography (TLC) was performed on MACHEREY-NAGEL pre-coated ALUGRAM® SILG/UV_{254} TLC plates (0.20 mm silica gel 60 with 254 nm fluorescent indicator). TLC plates were visualized under UV light (254 nm) and developed by staining and heating with $KMnO_4$, p-anisaldehyde, ceric ammonium nitrate (CAM), phosphomolybdic acid (PMA), or iodine. Flash column chromatography was performed on silica gel (60 Å, 40-63 µm, Silicycle SiliaFlash® F60).

All NMR spectra were recorded at ambient temperature (298-300 K). ^{1}H and ^{13}C NMR spectra were recorded at 500.27 and 125.81 MHz, respectively, on a Bruker AVANCE NEO 500 spectrometer equipped with a BBF probe. The ^{1}H and ^{13}C NMR spectra for compound **7** were recorded at 300.27 and 75.50 MHz, respectively, on a Bruker AVANCE 300 spectrometer equipped with a 5mm PABBO BB-1H/D Z-GRD probe. ^{1}H chemical shifts (δ) are reported in parts-per-million (ppm) relative to tetramethylsilane and referenced to the solvent peak ($CDCl_3$, δ 7.26; CD_2Cl_2, δ 5.32). NMR data is presented as follows: chemical shift, multiplicity (s = singlet, d = doublet, dd = doublet of doublets, t = triplet, q = quartet, p = pentet, m = multiplet, ddt = doublet of doublet of triplets, dtd = doublet of triplet of doublets, bs = broad singlet, app = apparent), coupling constants (*J*, reported in Hz), integration. All ^{13}C NMR spectra are proton-decoupled ($^{13}C\{^{1}H\}$). ^{13}C chemical shifts (δ) are reported in parts-per-million (ppm) relative to tetramethylsilane and referenced to the solvent peak ($CDCl_3$, δ 77.16; CD_2Cl_2, δ 53.84). Prior to recording NOESY spectra, samples were sparged by bubbling argon through the NMR tube for several minutes.

Infrared spectra were obtained using a Perkin-Elmer ATR spectrometer. IR wavenumbers (ν) are reported in cm^{-1}. Accurate masses were obtained by electrospray ionization (positive mode) high resolution mass spectrometry (HRMS) using a Thermo Scientific™ Exactive™ Plus Orbitrap Ultimate 3000 LC-MS system. Melting points were measured using a Gallenkamp melting point apparatus, and are uncorrected.

Improved Synthesis of Thiele Acid

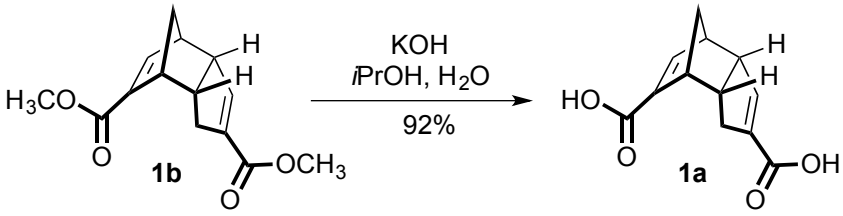

Our previous reported route to Thiele acid[2] was improved by a simple modification of the work-up procedure. 10% aqueous KOH solution (16 mL, 27 mmol, 6.7 eq.) was added dropwise to a solution of Thiele's ester (1.0002 g, 4.03 mmol) in *i*PrOH (16 mL). After stirring at room temperature for 5 hours, *i*PrOH was removed *in vacuo*. The mixture was acidified with 10% aqueous HCl solution (until pH = 1) and cooled to 0 °C. The white precipitate was filtered and washed successively with hexanes (2 x 10 mL), cold EtOAc (5 mL) and cold Et_2O (5 mL) to give pure **1a** as a white solid (0.82 g, 92%).

Synthesis of Bis-Adamantyl Thiele Ester (1d)

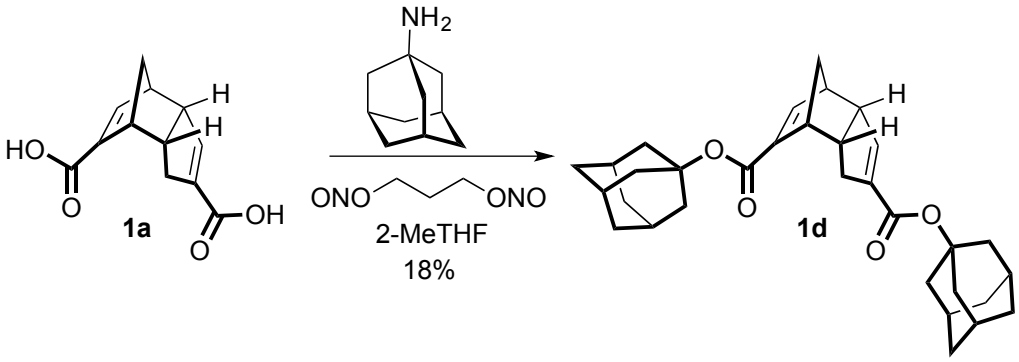

Compound **1d** was prepared using Lebel's esterification protocol.[3] To an oven-dried, 100 mL, two-necked round-bottom flask was added 1.0 g of Thiele's acid (4.5 mmol) and anhydrous 2-MeTHF (45.5 mL, 0.1 M). To a separate oven-dried, 50 mL round-bottom flask was added 1-Adamantylamine (2.718 g, 18 mmol, 4 equiv) and 5.0 mL anhydrous 2-MeTHF. Both flasks were stirred at room temperature until a suspension was observed. 1,3-Propanedinitrite (1.68 mL, 14.4 mmol, 3.2 equiv) was added to the flask containing the acid, which was followed by drop-wise cannula transfer of the amine solution. The reaction mixture was stirred vigorously and heated to reflux at 80 °C overnight, which resulted in a clear orange solution. After the removal of solvent *in vacuo*, saturated aq. NH_4Cl solution (30 mL) was added to quench the excess

[2] J. Chen, B. Kilpatrick, A. G. Oliver and J. E. Wulff, *J. Org. Chem.*, 2015, **80**, 8979.
[3] C. Audubert and H. Lebel, *Org. Lett.*, 2017, **19**, 4407.

amine. The aqueous solution was then extracted with EtOAc (3 x 15 mL). The combined organic layers were washed with brine (25 mL), dried over $MgSO_4$, and concentrated to give a brownish orange solid. Flash column chromatography on silica gel (dry loading with silica, 20:1 hexanes/EtOAc) afforded 0.40 g (18%) of compound **1d** as a pale yellow solid. R_f = 0.19 (20:1 hexanes/EtOAc). **m.p.** = 168 – 171 °C. **^{1}H NMR** (500.27 MHz, $CDCl_3$) δ 6.71 (d, *J* = 3.2 Hz, 1H), 6.40 (d, *J* = 2.3 Hz, 1H), 3.40-3.46 (m, 1H), 3.26-3.30 (m, 1H), 3.06-3.10 (m, 1H), 2.84-2.91 (m, 1H), 2.38 (ddt, *J* = 18.0, 10.4, 2.1 Hz, 1H), 2.10-2.20 (m, 12H), 2.06-2.10 (m, 7H), 1.60-1.72 (m, 13H), 1.34 (d, *J* = 8.5 Hz, 1H); **^{13}C NMR** (125.81 MHz, $CDCl_3$) δ 164.7, 164.3, 146.4, 141.9, 140.4, 140.2, 80.2, 80.1, 54.2, 50.2, 47.4, 46.7, 41.6, 41.5, 41.2, 36.5, 33.2, 30.84, 30.80; **IR** (film) 2909, 1706, 1694, 1632, 1265, 1152 cm^{-1}; **HRMS (ESI+)** *m/z* [M + Na] calcd for $C_{32}H_{40}O_4Na^+$ 511.28187, found: 511.28201.

General Procedure A: Photochemical Synthesis of Thiele Cages

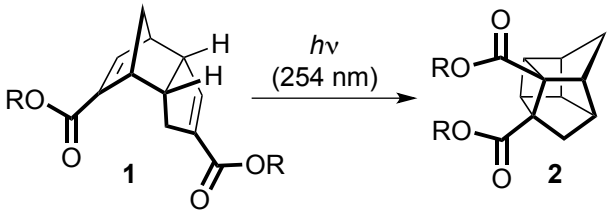

In a flame-dried, 100 mL quartz round-bottom flask, the corresponding Thiele ester (or acid) was dissolved in spectro-grade acetone. The flask was the sealed with a rubber septum and equipped with an argon balloon. The solution was irradiated at 254nm in a photochemical chamber reactor (model RMR-600 Rayonet) and monitored by TLC until completion.

N.B. We found that rigorous degassing of the acetone (by the freeze-pump-thaw method) was unnecessary. When degassed acetone was used for the synthesis of **2b**, the conversion and purity profile was essentially unaltered. The reaction could also be carried out in 2-MeTHF instead of acetone.

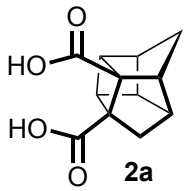

Compound **2a** was prepared via general procedure A with the use of Thiele's acid (0.48 g, 2.20 mmol) and 40 mL (0.055 M) of acetone. Once the starting material had been completely

consumed, the crude reaction mixture was concentrated *in vacuo*. To this mixture, 1 mL of saturated aq. $NaHCO_3$ solution was added, which was followed by 15 mL of deionized water. The solution was washed with Et_2O (2 x 3 mL) and then acidified with 6N aq. H_2SO_4 (10mL). The aqueous solution was extracted with Et_2O (4 x 30 mL). The combined organic layers were dried over $MgSO_4$ and concentrated to give a foamy oily residue. Flash column chromatography on silica gel (dry loading with silica, 1:4 Et_2O/DCM with 2% v/v AcOH) afforded 0.36 g (74%) of compound **2a** as white foamy solid. An alternative way to purify the compound is to recrystallize it from Et_2O/Pentane which gives white microcrystalline solid. R_f = 0.32 (1:4 Et_2O/DCM with 2% v/v AcOH). **m.p.** = 187 – 190 °C. **^{1}H NMR** (500.27 MHz, $CDCl_3$) δ 3.15-3.20 (m, 1H), 2.92-2.97 (m, 2H), 2.78-2.86 (m, 2H), 2.56-2.60 (m, 1H), 2.19 (d, *J* = 11.5 Hz, 1H), 1.73 (d, *J* = 11.4 Hz, 1H), 1.66 (d, *J* = 11.4 Hz, 1H), 1.52 (d, *J* = 11.4 Hz, 1H); **^{13}C NMR** (125.81 MHz, $CDCl_3$) δ 180.7, 180.4, 61.9, 59.4, 54.9, 47.7, 44.1, 43.7, 41.4, 41.0, 38.8, 37.5; **IR** (film) 3099, 2984, 1710, 1259, 644 cm^{-1}; **HRMS (ESI+)** *m/z* [M + Na] calcd for $C_{12}H_{12}O_4Na$+ 243.06277, found: 243.06268.

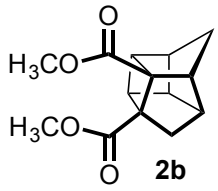

2b

Compound **2b** was prepared via general procedure A with the use of Thiele's ester (1.38 g, 5.56 mmol) and 30 mL (0.2 M) of acetone. Once the starting material had been completely consumed, the product mixture was concentrated in vacuo to give 1.75 g of yellow oil. Flash column chromatography on silica gel (dry loading with Celite™ 545, 93:7 hexanes/EtOAc) afforded 0.75 g (55 %) of compound **2b** as colourless oil. R_f ≈ 0.27 (93:7 hexanes/EtOAc). Compound **2b** is not detectable by UV (254 nm) or with conventional TLC stains ($KMnO_4$, CAM, PMA, I_2, p-anisaldehyde). **^{1}H NMR** (500.27 MHz, $CDCl_3$) δ 3.68 (s, 3H), 3.65 (s, 3H), 3.11-3.15 (m, 1H), 2.89-2.93 (m, 1H), 2.84-2.87 (m, 1H), 2.75-2.81 (m, 1H), 2.52-2.57 (m, 1H), 2.16 (d, *J* = 11.5 Hz, 1H), 1.72 (d, *J* = 11.3 Hz, 1H), 1.64 (d, *J* = 11.3 Hz, 1H), 1.50 (d, *J* = 11.4 Hz, 1H); **^{13}C NMR** (125.81 MHz, $CDCl_3$) δ 173.8, 173.6, 61.1, 59.4, 54.3, 51.9, 51.8, 47.5, 44.4, 43.8, 41.3, 40.9, 39.7, 37.8; **IR** (film) 2953, 1728, 1435, 1256, 1097 cm^{-1}; **HRMS (ESI+)** *m/z* [M + Na] calcd for $C_{14}H_{16}O_4Na$+ 271.09407, found: 271.09371.

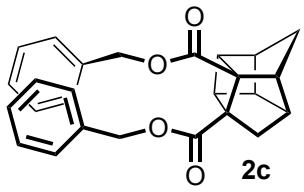

2c

Compound **2c** was prepared via general procedure A with the use of dibenzyl Thiele's ester (0.33 g, 0.82 mmol) and 6.3 mL (0.13 M) of acetone. Once the starting material had been completely consumed, the product mixture was concentrated *in vacuo* to give 0.35 g of yellow oil. Flash column chromatography on silica gel (dry loading with silica, 10:1 hexanes/EtOAc) afforded 0.11 g (33%) of compound **2c** as colourless oil. R_f = 0.44 (6:1 hexane/EtOAc). **^{1}H NMR** (500.27 MHz, $CDCl_3$) δ 7.23-7.28 (m, 10H), 5.02 (d, *J* = 12.6 Hz, 1H), 4.97 (d, *J* = 12.6 Hz, 1H), 4.93 (d, *J* = 12.6 Hz, 1H), 4.93 (d, *J* = 12.6 Hz, 1H), 3.17-3.22 (m, 1H), 2.90-2.94 (m, 1H), 2.86-2.90 (m, 1H), 2.75-2.82 (m, 2H), 2.53-2.59 (m, 1H), 2.22 (d, *J* = 11.5 Hz, 1H), 1.76 (d, *J* = 11.4 Hz, 1H), 1.64 (d, *J* = 11.4 Hz, 1H), 1.52 (d, *J* = 11.4 Hz, 1H); **^{13}C NMR** (125.81 MHz, $CDCl_3$) δ 173.1, 172.9, 136.4, 136.3, 128.62, 128.60, 128.14, 128.08, 128.02, 66.2, 66.1, 61.3, 59.3, 54.6, 47.5, 44.5, 43.8, 41.4, 41.1, 39.5, 37.7; **IR** (film) 2964, 1724, 1254, 1095, 734, 695 cm^{-1}; **HRMS (ESI+)** *m/z* [M + Na] calcd for $C_{26}H_{24}O_4Na^+$ 423.15667, found: 423.15635.

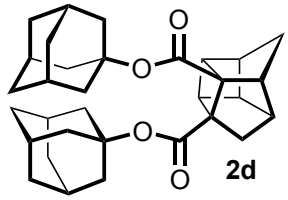

2d

Compound **2d** was prepared via general procedure A with the use of compound **1** (0.50 g, 1.02 mmol) and 40 mL (0.03 M) of acetone. Once the starting material had been completely consumed, the product mixture was concentrated *in vacuo* to give pale yellow foamy solid. Flash column chromatography on silica gel (dry loading with silica, eluent 20:1 hexanes/EtOAc) afforded 0.17 g (34%) of compound **2d** as a white solid. R_f = 0.44 (9:1 hexanes/EtOAc). **m.p.** = 193 – 197 °C. **^{1}H NMR** (500.27 MHz, $CDCl_3$) δ 3.00-3.05 (m, 1H), 2.84-2.89 (m, 1H), 2.64-2.75 (m, 3H), 2.44-2.48 (m, 1H), 2.03-2.19 (m, 19H), 1.60-1.71 (m, 13H), 1.57 (d, *J* = 11.1 Hz, 1H), 1.47 (d, *J* = 11.1 Hz, 1H); **^{13}C NMR** (125.81 MHz, $CDCl_3$) δ 172.64, 172.43, 80.10, 80.03, 61.97, 59.44, 55.16, 47.08, 44.26, 43.52, 41.62, 41.55, 41.32, 41.24, 38.88, 37.40, 36.45, 36.41, 30.95; **IR** (film) 2906, 1718, 1262, 1199, 1057 cm^{-1}; **HRMS (ESI+)** *m/z* [M + Na] calcd for $C_{32}H_{40}O_4Na^+$ 511.28187, found: 511.28208.

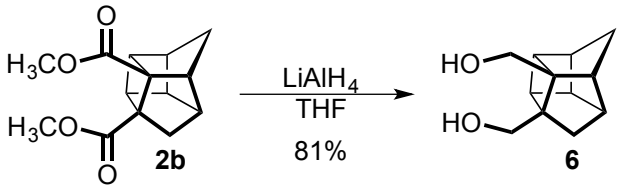

$LiAlH_4$ (104.9 mg, 2.764 mmol) was suspended in dry THF (2 mL) and cooled to 0 °C. Under argon in a 20-mL vial, Thiele cage **2b** (151.9 mg, 0.6118 mmol) was dissolved in dry THF (2 mL). The solution of **2b** was added to the $LiAlH_4$ suspension via cannula. The 20-mL vial and cannula were subsequently rinsed with THF (2 x 1 mL) and the reaction was left to warm to room temperature over 22 hours. The reaction was cooled to 0 °C, quenched with EtOAc (12 mL), then decanted into an flask containing 20 mL of Rochelle's salt solution (0.5 M). The mixture was stirred vigorously for 14 hours. The two phases were separated, and the aqueous phase was then extracted with EtOAc (3 x 15 mL). The combined organic phases were washed with brine (1 x 40 mL), dried over Na_2SO_4, then concentrated *in vacuo* to afford 127 mg of a white solid. The crude solid was re-dissolved in EtOAc, adsorbed onto Celite™ 545, and loaded onto a SiO_2 column. The column was flushed with several column volumes of hexanes followed by hexanes/EtOAc (1:1 v/v) to afford 95.2 mg (81 %) of **6** as a powdery white solid. **N.B.** Compound **6** is UV inactive, but can be visualized by TLC upon staining with *p*-anisaldehyde. $\boldsymbol{R_f}$ = 0.32 (1:1 hexanes/EtOAc). **m.p.** = 133-135 °C. **^{1}H NMR** (500.27 MHz, $CDCl_3$) δ 4.06 (d, *J* = 11.4 Hz, 1H), 3.85 (d, *J* = 11.4 Hz, 1H), 3.66 (d, *J* = 11.8 Hz, 1H), 3.44 (d, *J* = 11.8 Hz, 1H), 3.04 (br, 1H), 2.77-2.82 (m, 1H), 2.63-2.75 (br, m, 2H), 2.56-2.60 (m, 1H), 2.46-2.51 (m, 1H), 2.28-2.37 (m, 2H), 1.91 (d, *J* = 10.7 Hz, 1H), 1.59 (d, *J* = 11.2 Hz, 1H), 1.28 (d, *J* = 11.2 Hz, 1H), 1,18 (d, *J* = 10.7 Hz, 1H); **^{13}C NMR** (125.81 MHz, $CDCl_3$) δ 62.81, 62.79, 57.0, 56.2, 50.3, 46.8, 43.9, 41.1, 40.8, 39.7, 39.1, 37.7); **IR** (film) 3274, 2956, 1239, 1033, 1005 cm^{-1}; **HRMS (ESI+)** *m/z* [M + H] calcd for $C_{12}H_{17}O_2$+ 193.12233, found: 193.12240.

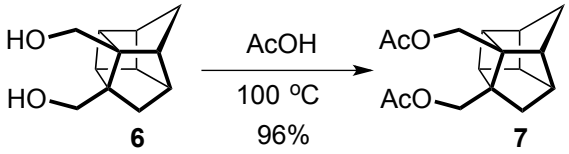

To a 10-mL round bottom flask was added 42.6 mg of diol **6** (0.222 mmol) and acetic acid (3 mL). The flask was equipped with a reflux condenser and placed in a pre-heated oil bath (100 °C). The reaction was stirred open to air for 18 hours. The crude reaction mixture was concentrated *in vacuo* to afford 70.4 mg of a crude brown oil. The crude oil was dissolved in several mL of Et_2O then filtered through a short plug of silica. Concentration of the filtrate afforded 59.0 mg (96 %) of bis-acetate **7** as a clear, pale yellow oil. **N.B.** Compound **7** is UV

inactive, but can be visualized by TLC upon staining with *p*-anisaldehyde. R_f = 0.68 (1:1 hexanes/EtOAc). **^{1}H NMR** (300.27 MHz, $CDCl_3$) δ 4.47 (d, *J* = 11.6 Hz, 1H), 4.32 (d, *J* = 11.6 Hz, 1H), 4.09 (d, *J* = 11.7 Hz, 1H), 4.02 (d, *J* = 11.7 Hz, 1H), 2.84-2.80 (m, 1H), 2.71 (app p, *J* = 5.7 Hz, 1H), 2.52-2.41 (m, 4H), 2.03 (s, 3H), 2.03 (s, 3H), 1.74 (d, *J* = 10.8 Hz, 1H), 1.61 (d, *J* = 11.6 Hz, 1H), 1.32 (app t, *J* = 10.0 Hz, 2H). **^{13}C NMR** (75.51 MHz, $CDCl_3$) δ 171.40, 171.33, 64.91, 64.20, 54.17, 53.51, 51.37, 47.18, 43.70, 41.50, 41.18, 39.98, 39.14, 37.68, 21.11, 21.08. **IR** (film) 2948, 2857, 1736, 1225, 1027 cm^{-1}; **HRMS (ESI+)** *m/z* [M + H] calcd for $C_{16}H_{21}O_4$+ 277.14346, found: 277.14356.

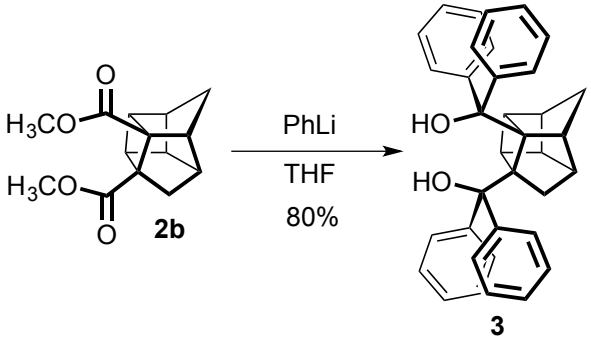

In a 50-mL round bottom flask, **2b** (108 mg, 0.43 mmol) was dissolved in dry THF (25 mL) and cooled to 0 °C to give a clear, colourless solution. Commercial (Aldrich) PhLi solution (1.8 M in Bu_2O, 1.5 mL, 2.7 mmol) was added dropwise by syringe over 8.5 minutes to give a clear, bright yellow solution. The reaction was gradually warmed to room temperature over 17.5 hours, then quenched at 0 °C with the addition of sat. NH_4Cl (5 mL). The mixture was diluted with water (5 mL) and Et_2O (10 mL). The two phases were separated, and the aqueous phase was then extracted with Et_2O (3 x 7 mL). The combined organic phases were washed with brine (1 x 12 mL), dried over Na_2SO_4, then concentrated *in vacuo* to afford 292.2 mg of a foamy off-white (slightly pale yellow) solid. Flash column chromatography on silica gel (dry loading with Celite™ 545, 10:1 hexanes/EtOAc) afforded 171.3 mg (80 %) of compound **3** as a white foamy solid. White crystals could be obtained by recrystallizing the column-purified solid in Et_2O/Pentane. Slow evaporation of crystalline **3** from Et_2O afforded an X-ray quality crystal. R_f = 0.20 (10:1 hexanes/EtOAc), **m.p.** = 175-178 °C. **^{1}H NMR** (500.27 MHz, $CDCl_3$) δ 7.35-7.41 (m, 2H), 6.95-7.28 (m, 15H), 6.77-6.87 (m, 3H), 4.62 (s, 1H), 4.17 (s, 1H), 3.45-3.50 (m, 1H), 3.12 (t, *J* = 6.4 Hz, 1H), 3.04-3.07 (m, 1H), 2.64-2.74 (m, 2H), 2.53-2.58 (m, 1H), 2.43-2.47 (m, 1H), 2.07 (d, *J* = 11.7 Hz, 1H), 0.96 (d, *J* = 11.3 Hz, 1H), –0.65 (d, *J* = 11.3 Hz, 1H); **^{13}C NMR** (125.81 MHz, $CDCl_3$) δ 147.6, 147.2, 146.8, 145.8, 128.18, 128.15, 128.01, 127.97, 127.66, 127.32, 127.06, 127.05, 127.01, 126.87, 126.75, 126.26, 80.4, 80.3, 70.3, 68.8, 54.1, 47.2, 44.5, 42.7, 42.3, 40.9, 39.0, 38.4; **IR** (film) 3197, 2985, 1444, 1172, 703, 696 cm^{-1}; **HRMS (ESI+)** *m/z* [M + Na] calcd for $C_{36}H_{32}O_2Na$+ 519.22944, found: 519.22954.

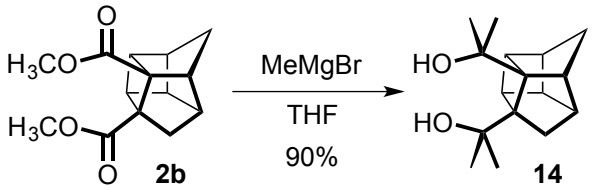

To a flame-dried 25-mL round bottom flask under argon, was added Thiele cage **2b** (100 mg, 0.403 mmol) as a solution in dry THF (4 mL). The solution was cooled to 0 °C, then MeMgBr (3.0 M in Et_2O) was added dropwise over 3.5 minutes. The reaction was gradually warmed to room temperature over 14 hours. The reaction was quenched at 0 °C with saturated aqueous NH_4Cl (5 mL) and diluted with Et_2O (10 mL). The phases were separated. The aqueous phase was extracted with Et_2O (3 x 7 mL). The combined organic phases were washed with brine (1 x 15 mL), dried over Na_2SO_4, then concentrated *in vacuo* to afford a clear, colourless oil (150 mg). The crude oil was adsorbed onto Celite™ 545 and loaded onto a SiO_2 column. Gradient elution (5:1→4:1→3:1 hexanes/ EtOAc) afforded tetramethyldiol **14** as a white oily solid (90 mg, 90 %). R_f = 0.11 (3:1 hexanes/ EtOAc). **m.p.** 107-108 °C. **^{1}H NMR** (500.27 MHz, $CDCl_3$) δ 3.98 (bs, 2H), 2.79-2.75 (m, 1H), 2.73 (q, *J* = 4.7 Hz, 1H), 2.66-2.58 (m, 2H), 2.43 (m, 1H), 2.39 (m, 1H), 1.68 (d, *J* = 10.8 Hz, 1H), 1.51-1.44 (m, 2H), 1.48 (s, 3H), 1.42 (s, 3H), 1.30 (dd, *J* = 10.8, 1.9 Hz, 1H), 1.13 (s, 3H), 1.00 (s, 3H); **^{13}C NMR** (125.81 MHz, $CDCl_3$) δ 72.86, 72.16, 68.36, 66.18, 53.37, 47.28, 43.45, 41.37, 41.12, 40.73, 39.32, 39.06, 29.66, 29.55, 29.20, 28.00; **IR** (film) 3233, 2964, 2940, 2857, 1173 cm^{-1}.

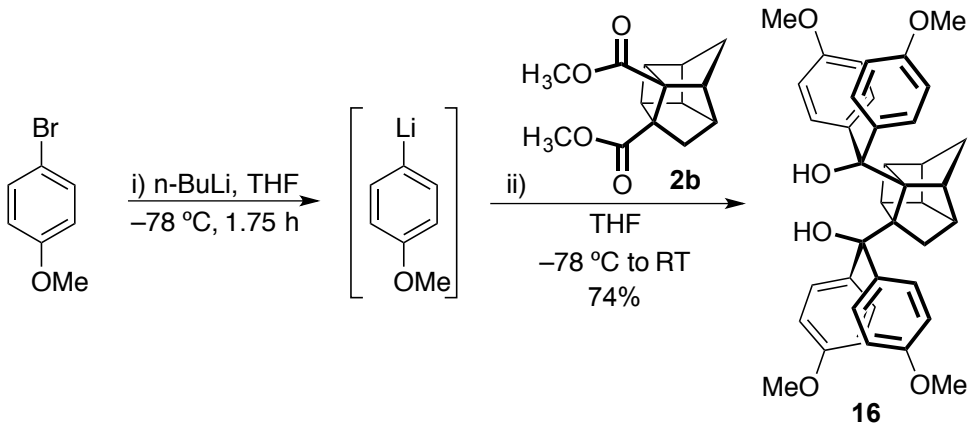

To a flame-dried 25-mL round bottom flask was added 4-bromoanisole (448 mg, 2.40 mmol) followed by anhydrous THF (2 mL). The solution was cooled to –78 °C then n-BuLi (0.96 mL, 2.40 mmol; 2.5 M in hexanes) was added dropwise by syringe over 4.5 minutes affording a clear, colourless solution. The reaction was stirred at –78 °C for 1.75 h then Thiele cage **2b** (100 mg, 0.403 mmol) was added as a solution in THF (4 mL) dropwise over 5 minutes at –78 °C. The reaction turned slightly pale yellow. The reaction was gradually warmed to room temperature over 9 hours. The reaction was cooled to 0 °C then quenched with saturated aqueous NH_4Cl (5 mL) then diluted with Et_2O (10 mL). The two phases were separated, and the aqueous phase was then extracted with Et_2O (3 x 10 mL). The combined organic phases were washed with brine (1 x 50 mL), dried over Na_2SO_4, then concentrated *in vacuo* to afford 361 mg of a clear, pale yellow oil. The crude oil was re-dissolved in Et_2O, adsorbed onto Celite™ 545, and loaded onto a SiO_2 column packed with hexanes. Gradient elution (20:1→14:1→4:1→3:1→1:1 hexanes/ EtOAc) afforded compound **16** (185 mg, 74 %) as a white solid. $\boldsymbol{R_f}$ = 0.31 (1:1 hexanes/ EtOAc), **m.p.** = 108-112 °C. **^{1}H NMR** (500.27 MHz, $CDCl_3$) δ 7.20 (d, *J* = 8.9 Hz, 2H), 7.08-7.00 (m, 2H), 7.03 (d, *J* = 8.9 Hz, 2H), 6.99-6.80 (m, 2H), 6.72 (d, *J* = 9.0 Hz, 2H), 6.64 (d, *J* = 9.3 Hz, 2H), 6.45 (d, *J* = 8.3 Hz, 2H), 6.32 (d, *J* = 8.9 Hz, 2H), 3.77 (s, 3H), 3.73 (s, 3H), 3.71 (s, 3H), 3.67 (s, 3H), 3.42 (q, *J* = 5.1 Hz, 1H), 3.11 (app t, *J* = 6.4 Hz, 1H), 2.95 (bs, 1H), 2.77 (app p, *J* = 5.6 Hz, 1H), 2.62-2.54 (m, 2H), 2.49-2.44 (m, 1H), 2.22-2.13 (m, 1H), 0.98 (d, *J* = 11.2 Hz, 1H), –0.56 (d, *J* = 11.3 Hz, 1H); **^{13}C NMR** (125.81 MHz, $CDCl_3$) δ 158.23, 157.99, 157.44, 157.33, 140.23, 139.81, 139.78, 138.34, 129.50, 129.27, 129.01, 128.15, 112.98, 112.47, 112.01, 80.14, 79.62, 70.07, 69.01, 55.22, 55.20, 54.85, 54.71, 53.69, 47.39, 44.52, 42.34, 42.24, 40.94, 39.00, 38.40; **IR** (film) 3314, 2963, 2835, 1607, 1507, 1248, 823 cm^{-1}; **LRMS (ESI+)** *m/z* [M + Na] calcd for $C_{40}H_{41}O_6Na$+ 639.27, found: 639.37.

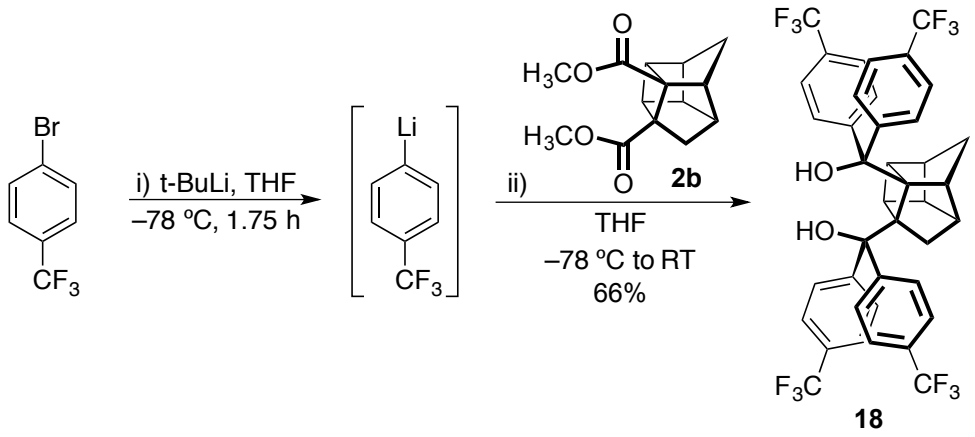

18

To a flame-dried 25-mL round bottom flask was added t-BuLi (2.84 mL, 4.84 mmol; 1.7 M in pentane). The solution was cooled to –78 °C then 4-bromobenzotrifluoride (544 mg, 2.42 mmol) was added dropwise over 30 minutes as a solution in THF (2 mL) affording a cloudy greenish-yellow suspension. The reaction was stirred at –78 °C for 1.75 h then Thiele cage **2b** (50 mg, 0.201 mmol) was added as a solution in THF (2 mL) dropwise over 12 minutes at –78 °C. The reaction was gradually warmed to room temperature over 19 hours to afford a clear, dark orange solution. The reaction was cooled to 0 °C then quenched with saturated aqueous NH_4Cl (4 mL) then diluted with Et_2O (10 mL). The two phases were separated, and the aqueous phase was then extracted with Et_2O (3 x 7 mL). The combined organic phases were washed with brine (1 x 20 mL), dried over Na_2SO_4, then concentrated *in vacuo* to afford 310 mg of a clear, dark orange oil. The crude oil was dissolved in a minimal amount of toluene, loaded onto a plug of SiO_2, then flushed with 10:1 hexanes/ EtOAc to eliminate orange impurities. The clear, slightly pale yellow filtrate was concentrated, then adsorbed onto Celite™ 545. The adsorbed crude was loaded onto a SiO_2 column packed with petroleum ether (b.p. 35-60 °C). Gradient elution (9:1→4:1→1:1 petroleum ether: Et_2O) afforded compound **18** (102 mg, 66 %) as an off-white solid. R_f = 0.16 (4:1 petroleum ether: Et_2O), **m.p.** = 210-213 °C. **^{1}H NMR** (500.27 MHz, $CDCl_3$) δ 7.47 (d, *J* = 8.4 Hz, 2H), 7.40 (d, *J* = 8.4 Hz, 2H), 7.35 (d, *J* = 8.4 Hz, 2H), 7.31-7.22 (m, 4H), 7.19 (d, *J* = 8.4 Hz, 2H), 7.15-7.00 (m, 2H), 7.04 (d, *J* = 8.3 Hz, 2H), 5.90 (s, 1H), 4.78 (s, 1H), 3.47 (app dd, *J* = 6.3, 3.9 Hz, 1H), 3.12-3.01 (m, 2H), 2.80 (app p, *J* = 5.7 Hz, 1H), 2.73 (m, 1H), 2.66 (d, *J* = 11.8 Hz, 1H), 2.54 (m, 1H), 2.28 (d, *J* = 11.7 Hz, 1H), 1.06 (d, *J* = 11.6 Hz, 1H), –0.69 (d, *J* = 11.6 Hz, 1H); **^{13}C NMR** (125.81 MHz, $CDCl_3$) δ 150.78, 149.92, 149.53, 148.82, 128.43, 128.33, 128.11, 127.28, 125.04, 125.01, 124.61, 124.58, 124.55, 124.44, 124.09, 124.06, 80.61, 80.02, 69.50, 68.35, 53.38, 47.90, 43.94, 42.61, 42.41, 40.94, 39.02, 38.52; **^{19}F NMR** (470.68 MHz, $CDCl_3$) δ –62.48 (s), –62.79 (s), –62.91 (app t, *J* = 5.2 Hz), –62.95 (app t, *J* = 5.2 Hz); **IR** (film) 3292, 2977, 1617, 1323, 1112, 1069, 826 cm^{-1}.

General Procedure B: The Extended Pinacol Rearrangement

To a 20-mL scintillation vial open to air at room temperature, was added the diol substrate (1.0 equiv.), followed by MeOH (c ≈ 0.03 M), and then by concentrated H_2SO_4 (2.5 equiv.) via micropipette. The reaction vial was placed in a pre-heated oil bath (~40 °C) and stirred overnight with the vial loosely capped. The crude reaction mixture was removed from heating and then quenched with saturated aqueous $NaHCO_3$. MeOH was removed *in vacuo* and the resultant crude was diluted with water and partitioned with EtOAc. Upon separation of the phases, the aqueous phase was extracted three times with EtOAc. The combined EtOAc phases were dried over Na_2SO_4 then concentrated to give a crude residue, which was purified by column chromatography on SiO_2.

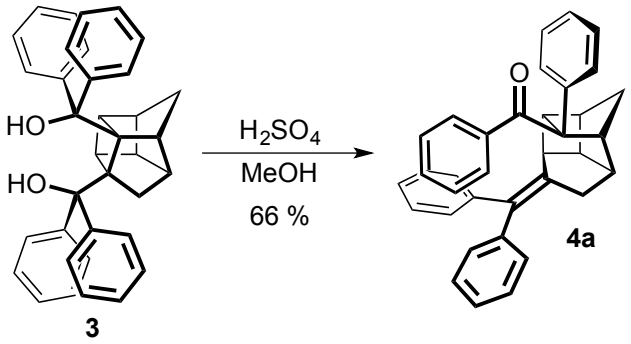

Compound **4a** was prepared via general procedure B using tetraphenyldiol **3** (51.9 mg, 0.105 mmol), MeOH (3.0 mL), and concentrated H_2SO_4 (13.9 µL, 0.261 mmol). The addition of H_2SO_4 resulted in the formation of a bright yellow oil that dissipated upon stirring. The walls of the vial were rinsed with MeOH (2 x 0.4 mL), and the reaction was subsequently heated to 43 °C. Upon initial heating, the reaction mixture was clear and colourless. The reaction was stirred at 43 °C for 24 hours, which afforded a white precipitate. The crude reaction mixture was removed from heating, and then quenched with saturated aqueous $NaHCO_3$ (2 mL). The MeOH was removed *in vacuo* and the resultant crude was diluted with water and partitioned with EtOAc. The phases were separated, and the aqueous phase was extracted with EtOAc (3 x ~5 mL). The combined EtOAc phases were dried over Na_2SO_4 then concentrated to give a yellow oily residue, that upon exposure to high-vacuum, resulted in the formation of a foamy off-white solid. The crude residue was re-dissolved in EtOAc and adsorbed onto Celite™ 545 (~276 mg). The adsorbed crude was loaded onto a SiO_2 column packed with petroleum ether (b.p. 35-60 °C). The column was flushed with several column volumes of petroleum ether. Gradient elution (100:1→50:1→20:1→10:1→3:7 petroleum ether: Et_2O) afforded compound **4a** (32.9 mg, 66 %) as a white solid. R_f = 0.47 (9:1 petroleum ether: Et_2O), **m.p.** = 185-187 °C. **^{1}H NMR** (500.27 MHz,

$CDCl_3$) δ 7.74 (d, *J* = 8.2 Hz, 2H), 7.34-7.15 (m, 11H), 7.10 (d, *J* = 8.2 Hz, 2H), 7.01 (m, 1H), 6.94 (m, 2H), 6.19 (d, *J* = 8.1 Hz, 2H), 3.94 (app dtd, *J* = 6.6, 4.5, 1.8 Hz, 1H), 3.36 (t, *J* = 6.8 Hz, 1H), 3.17 (dt, *J* = 3.6, 1.7 Hz, 1H), 3.03 (d, *J* = 17.9 Hz, 1H), 3.02 (m, 1H), 2.81-2.78 (m, 1H), 2.73-2.69 (m, 1H), 2.65 (dd, *J* = 18.1, 7.1 Hz, 1H), 1.27 (app dt, *J* = 11.2, 1.6 Hz, 1H), 1.12 (app dt, *J* = 11.1, 1.8 Hz, 1H); **^{1}H NMR** (500.27 MHz, CD_2Cl_2) δ 7.76 (d, *J* = 8.2 Hz, 2H), 7.37-7.19 (m, 11H), 7.08 (d, *J* = 7.6 Hz, 2H), 7.03-6.94 (m, 3H), 6.20 (d, *J* = 7.4 Hz, 2H), 3.98 (app dtd, *J* = 6.6, 4.5, 1.8 Hz, 1H), 3.35 (t, *J* = 6.8 Hz, 1H), 3.14 (bs, 1H), 3.05 (app t, *J* = 4.9 Hz, 1H), 2.93 (d, *J* = 18.0 Hz, 1H), 2.82-2.78 (m, 1H), 2.75-2.70 (m, 1H), 2.63 (dd, *J* = 18.0, 7.0 Hz, 1H), 1.28 (app dt, *J* = 10.9, 1.6 Hz, 1H), 1.10 (app dt, *J* = 10.9, 1.9 Hz, 1H); **^{13}C NMR** (125.81 MHz, $CDCl_3$) δ 197.74, 143.87, 142.80, 142.79, 142.39, 138.06, 135.72, 131.72, 130.14, 129.34, 129.32, 128.72, 128.41, 128.09, 127.90, 127.43, 127.20, 126.83, 126.45, 126.30, 125.78, 66.73, 49.63, 48.44, 46.01, 45.48, 45.17, 40.41, 38.13, 36.98; **^{13}C NMR** (125.81 MHz, CD_2Cl_2) δ 197.61, 144.44, 143.39, 143.18, 142.96, 138.28, 135.95, 132.23, 130.56, 129.68, 129.56, 129.07, 128.93, 128.51, 128.36, 127.68, 127.64, 127.22, 127.02, 126.73, 126.23, 67.20, 46.35, 45.84, 45.69, 40.87, 38.37, 37.39; **IR** (film) 3056, 2973, 1661, 1244, 953 cm^{-1}; **HRMS (ESI+)** *m/z* [M + H] calcd for $C_{36}H_{31}O^+$, 479.23697 found: 479.23723.

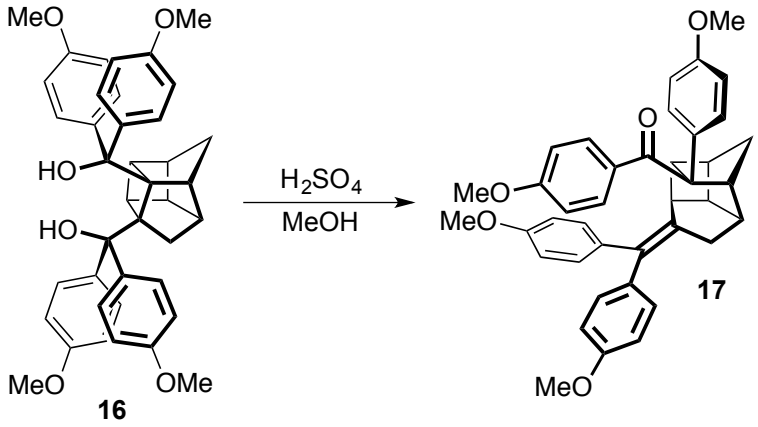

Compound **17** was prepared via general procedure B with the use of diol **16** (71.5 mg, 0.116 mmol), MeOH (3.0 mL), and concentrated H_2SO_4 (16.2 µL, 0.298 mmol). The addition of H_2SO_4 caused the reaction to turn yellowish-orange and resulted in the instant formation of a white precipitate. The reaction was stirred at 40 °C for 20.5 hours, to afford a greenish-brown mixture. The crude reaction mixture was removed from heating and quenched with saturated aqueous $NaHCO_3$ (1.4 mL) resulting in the formation of a white solid. The MeOH was removed *in vacuo* and the resultant crude was partitioned with EtOAc (7 mL). The phases were separated, and then the aqueous phase was extracted with EtOAc (3 x 4 mL). The combined EtOAc phases were dried over Na_2SO_4 then concentrated to give a brown oily solid. The crude was adsorbed onto Celite™ 545 and loaded onto a SiO_2 column packed with petroleum ether

(b.p. 35-60 °C). Gradient elution (5:1→4:1→3:1→2:1→1:1 petroleum ether: Et_2O) afforded compound **17** together with an unidentified impurity (total mass = 59.4 mg). Quantification with an internal standard indicated that the mixture contained 57% by mass of the target compound (34.0 mg), for a final overall yield of 49%. A small subsample was subjected to further purification by column chromatography on SiO_2 (PhMe → 50 % DCM/ PhMe → 70 % DCM/ PhMe → 80 % DCM/ PhMe) to provide an analytical sample for analysis. R_f = 0.62 (1:1 hexanes/ EtOAc), **m.p.** = 89-92 °C. **^{1}H NMR** (500.27 MHz, $CDCl_3$) δ 7.69 (d, *J* = 8.9 Hz, 2H), 7.18 (d, *J* = 9.0 Hz, 2H), 7.03 (d, *J* = 8.7 Hz, 2H), 6.86-6.82 (m, 1H), 6.82 (d, *J* = 8.7 Hz, 2H), 6.76 (app dd, *J* = 9.3, 2.7 Hz, 1H), 6.63 (d, *J* = 8.9 Hz, 2H), 6.50 (d, *J* = 8.7 Hz, 2H), 6.18 (d, *J* = 8.7 Hz, 2H), 3.86-3.83 (m, 1H), 3.81 (s, 3H), 3.74 (s, 3H), 3.72 (s, 3H), 3.70 (s, 3H), 3.36 (t, *J* = 6.7 Hz, 1H), 3.11 (bs, 1H), 3.04 (d, *J* = 17.9 Hz, 1H), 2.97 (app t, *J* = 4.4 Hz, 1H), 2.79-2.73 (m, 1H), 2.71-2.65 (m, 1H), 2.55 (dd, *J* = 17.9, 7.1 Hz, 1H), 1.24 (d, *J* = 11.0 Hz, 1H), 1.12 (dt, *J* = 11.0, 1.7 Hz, 1H); **^{13}C NMR** (125.81 MHz, $CDCl_3$) δ 196.53, 162.10, 158.26, 157.79, 157.56, 142.50, 135.91, 135.77, 134.73, 134.60, 132.09, 131.28, 130.48, 129.98, 128.48, 127.37, 114.42, 113.87, 113.21, 113.19, 112.48, 65.86, 55.42, 55.32, 55.28, 55.23, 49.64, 48.37, 45.80, 45.74, 45.11, 40.27, 38.01, 36.99; **IR** (film) 2933, 2835, 1657, 1600, 1507, 1242, 830, 730 cm^{-1}; **LRMS (ESI+)** *m/z* [M + H] calcd for $C_{40}H_{39}O_5$+ 599.28, found: 599.27. **LRMS (ESI+)** *m/z* [M + Na] calcd for $C_{40}H_{38}O_5Na$+ 621.26, found: 621.37.

General Procedure C: Screening of Cage-Opening Reactions

Thermal

To a 20-mL scintillation vial was added 8.0 mg of the corresponding Thiele cage, followed by a magnetic stir bead, and 2.0 mL of solvent (toluene, xylene, chloroform, ethyl acetate, ethanol, acetic acid or dimethyl sulfoxide). The vial was sealed with a rubber septum and Teflon tape, then equipped with an argon balloon. The reaction mixture was heated overnight at either 50 °C or 100 °C then concentrated *in vacuo*. The percent conversion was estimated by analysis the crude ^{1}H NMR.

Photochemical

To a quartz cuvette (10 mm, 3.5 mL) was added 3.0 mg of the corresponding Thiele cage and 1 mL of deuterated solvent (benzene-d6 or methanol-d4). The cuvette was sealed with a septum and Teflon tape. The solution was irradiated with light of certain wavelength (254 nm, 300 nm or 350 nm) overnight. The percent conversion was estimated by analysis of the crude ^{1}H NMR.

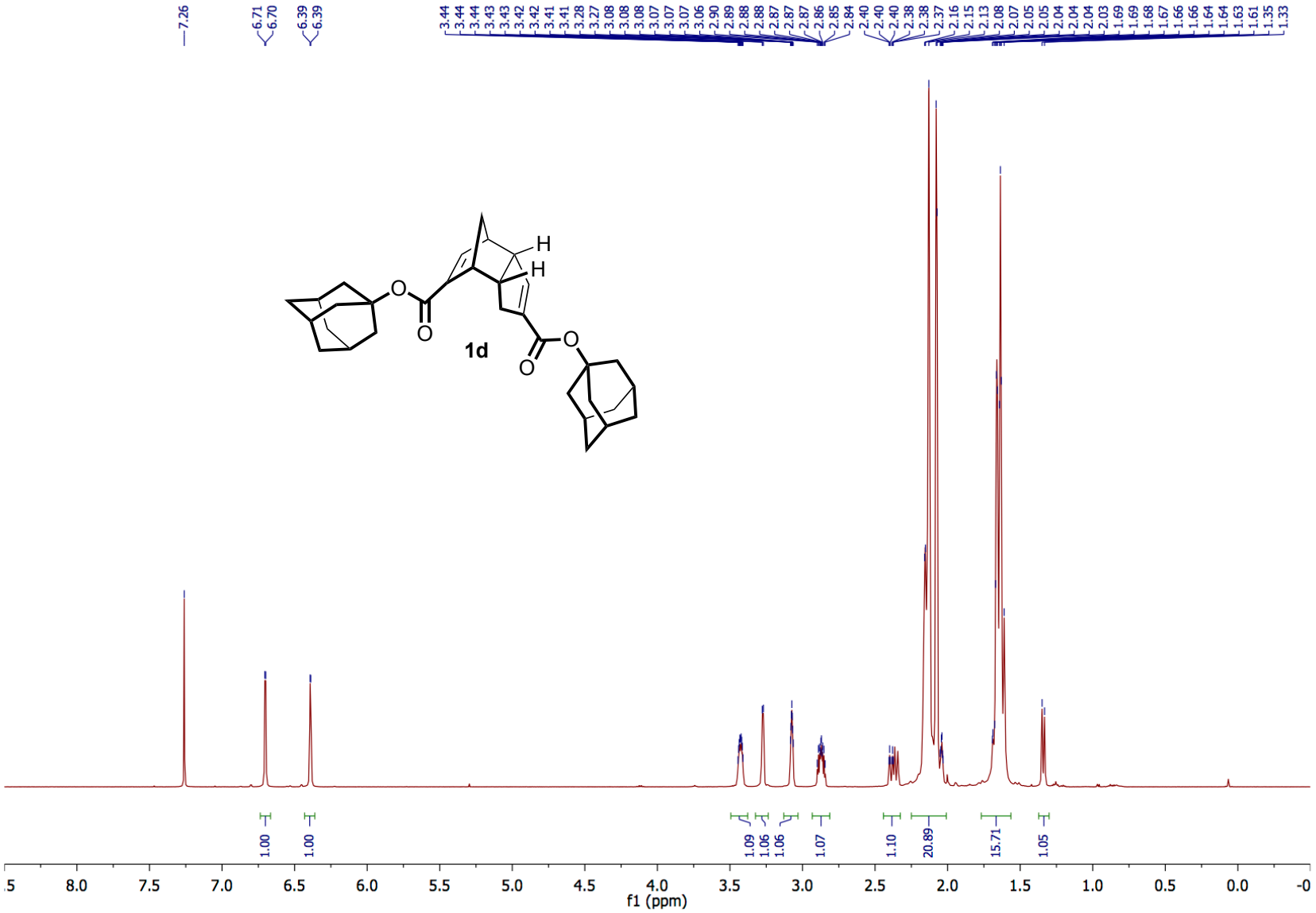

Figure S3. ^{1}H NMR of compound **1d** (500.27 MHz, $CDCl_3$).

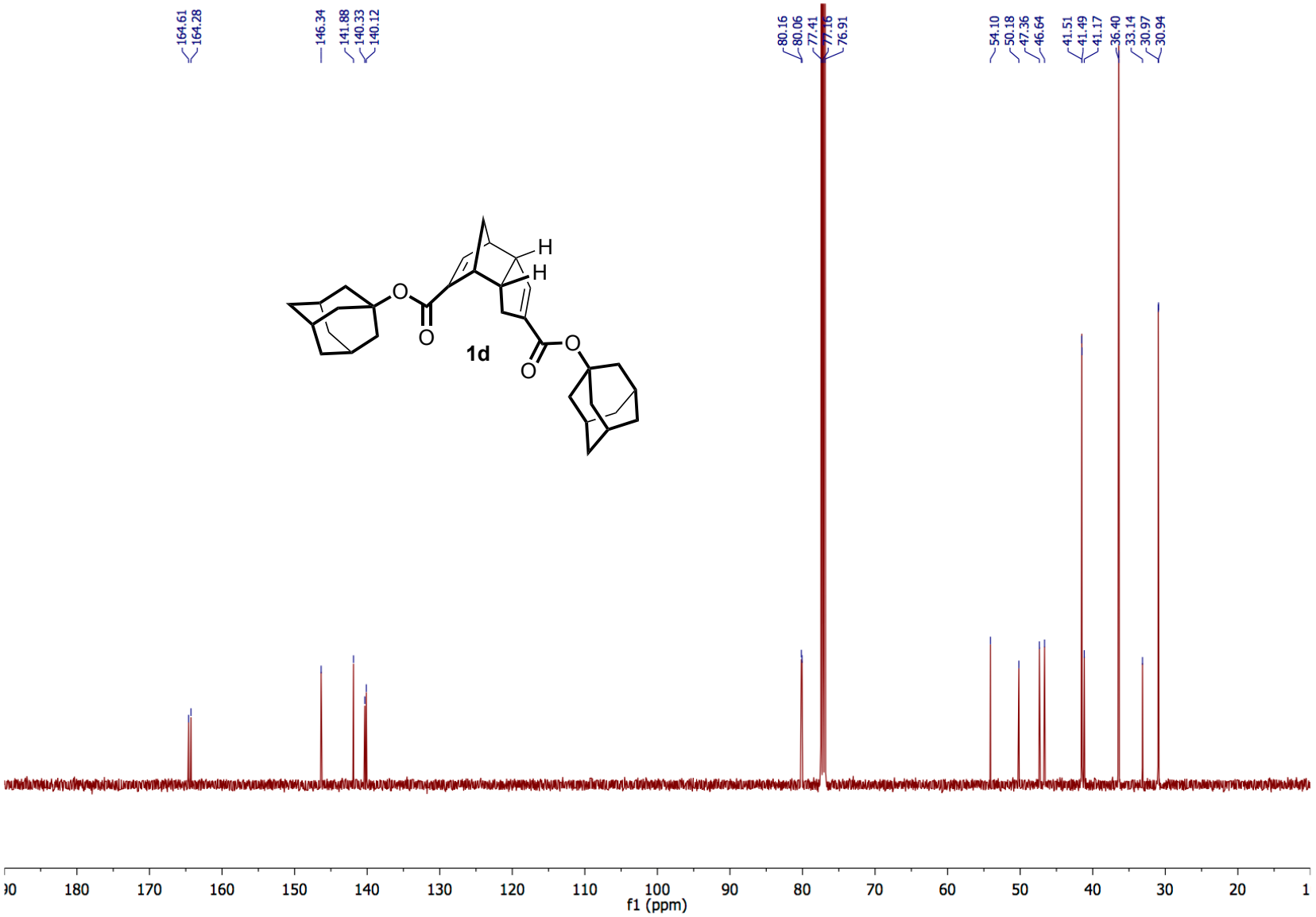

Figure S4. ^{13}C NMR of compound **1d** (125.81 MHz, $CDCl_3$).

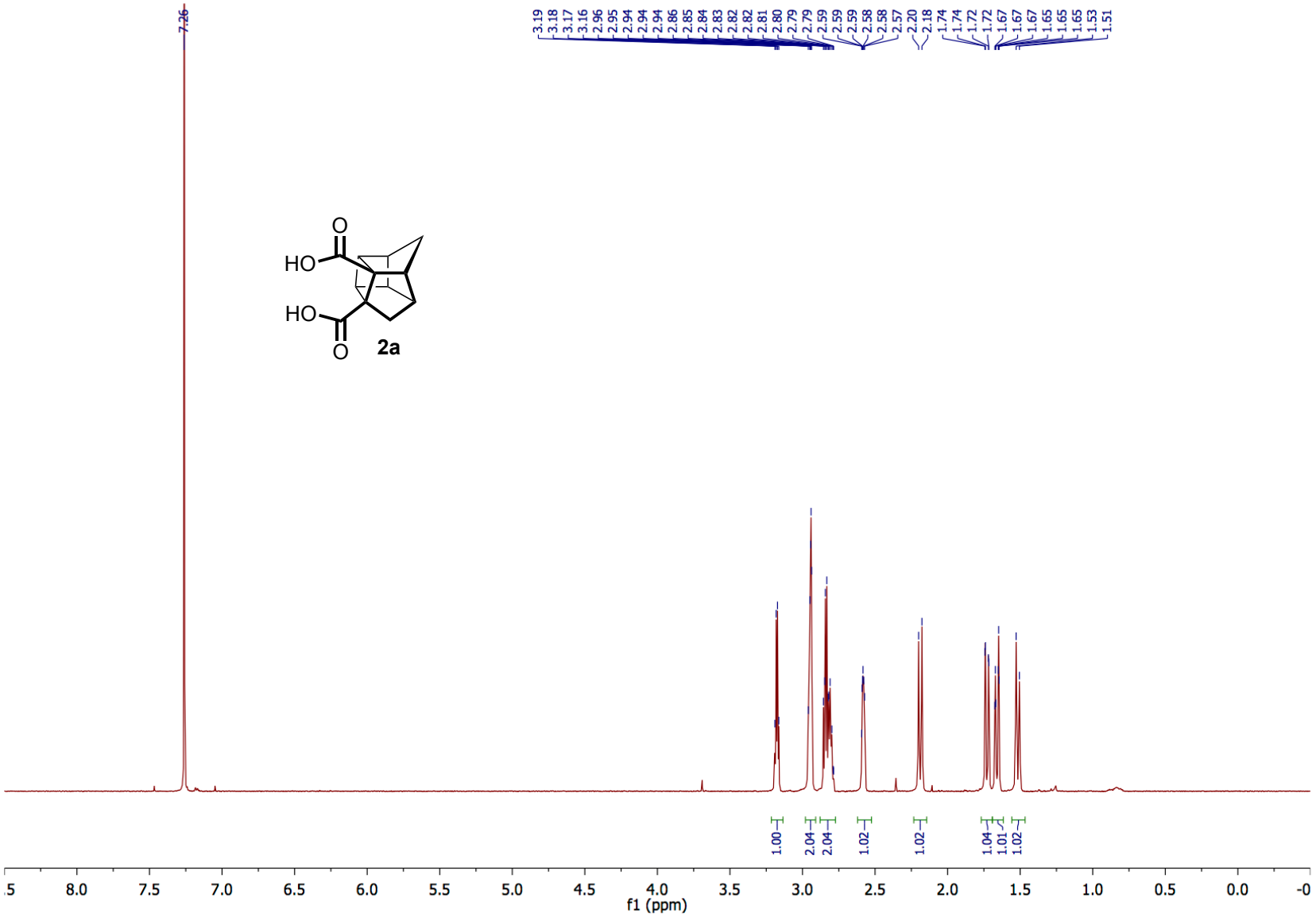

Figure S5. ^{1}H NMR of compound **2a** (500.27 MHz, $CDCl_3$).

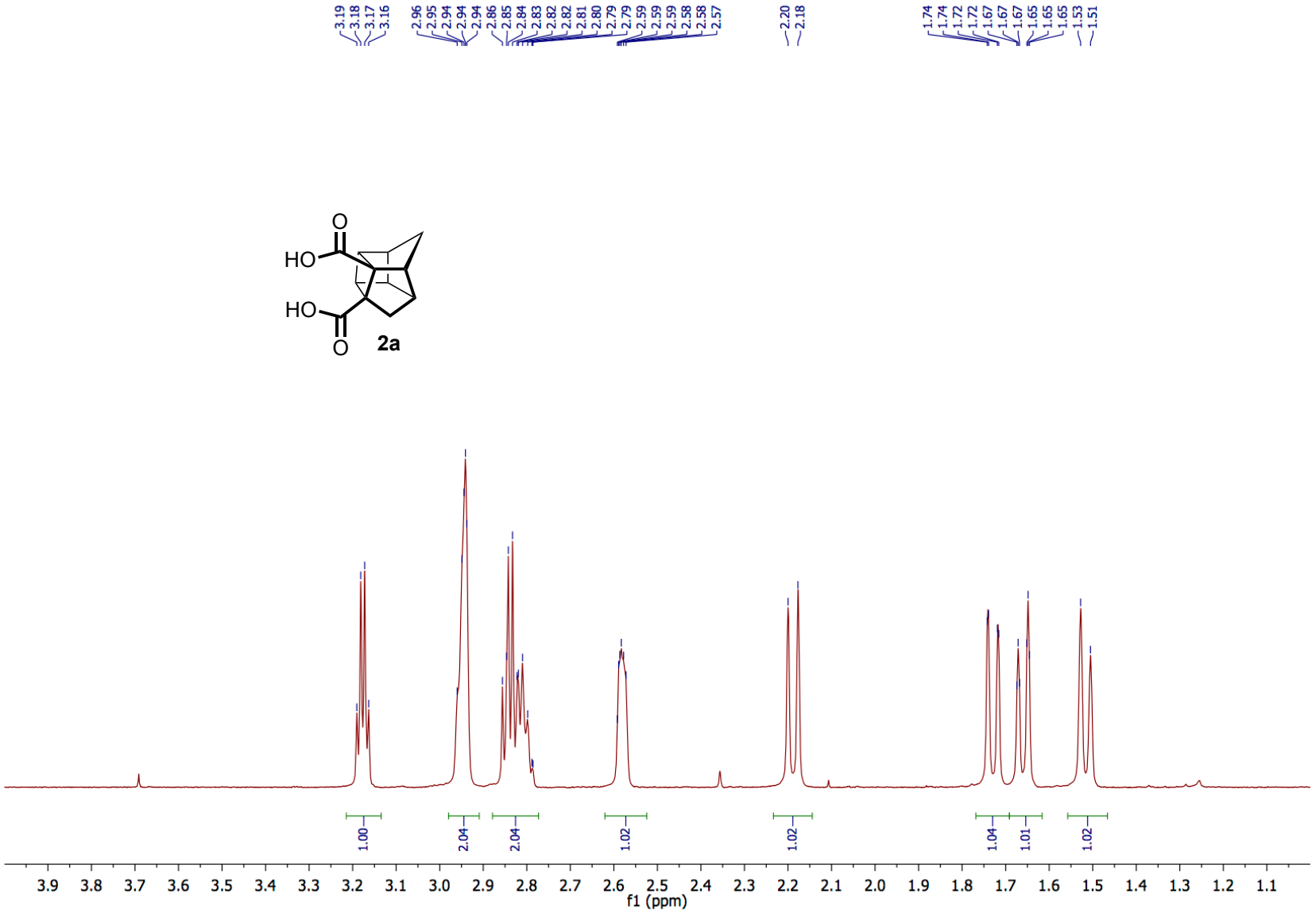

Figure S6. Upfield region (4.0-1.0 ppm) of the ^{1}H NMR of compound **2a** (500.27 MHz, $CDCl_3$).

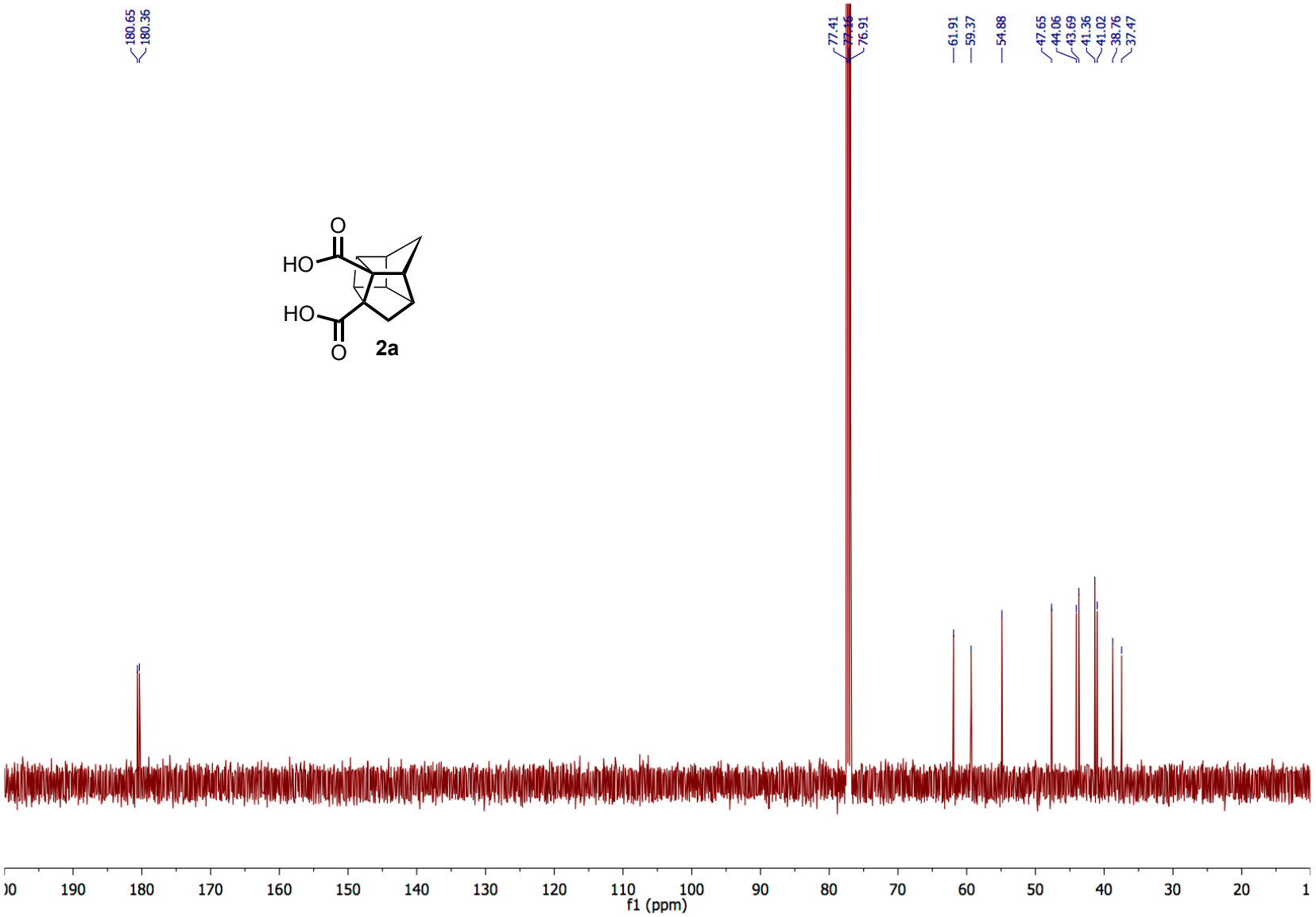

Figure S7. ^{13}C NMR of compound **2a** ($CDCl_3$, 125.81 MHz).

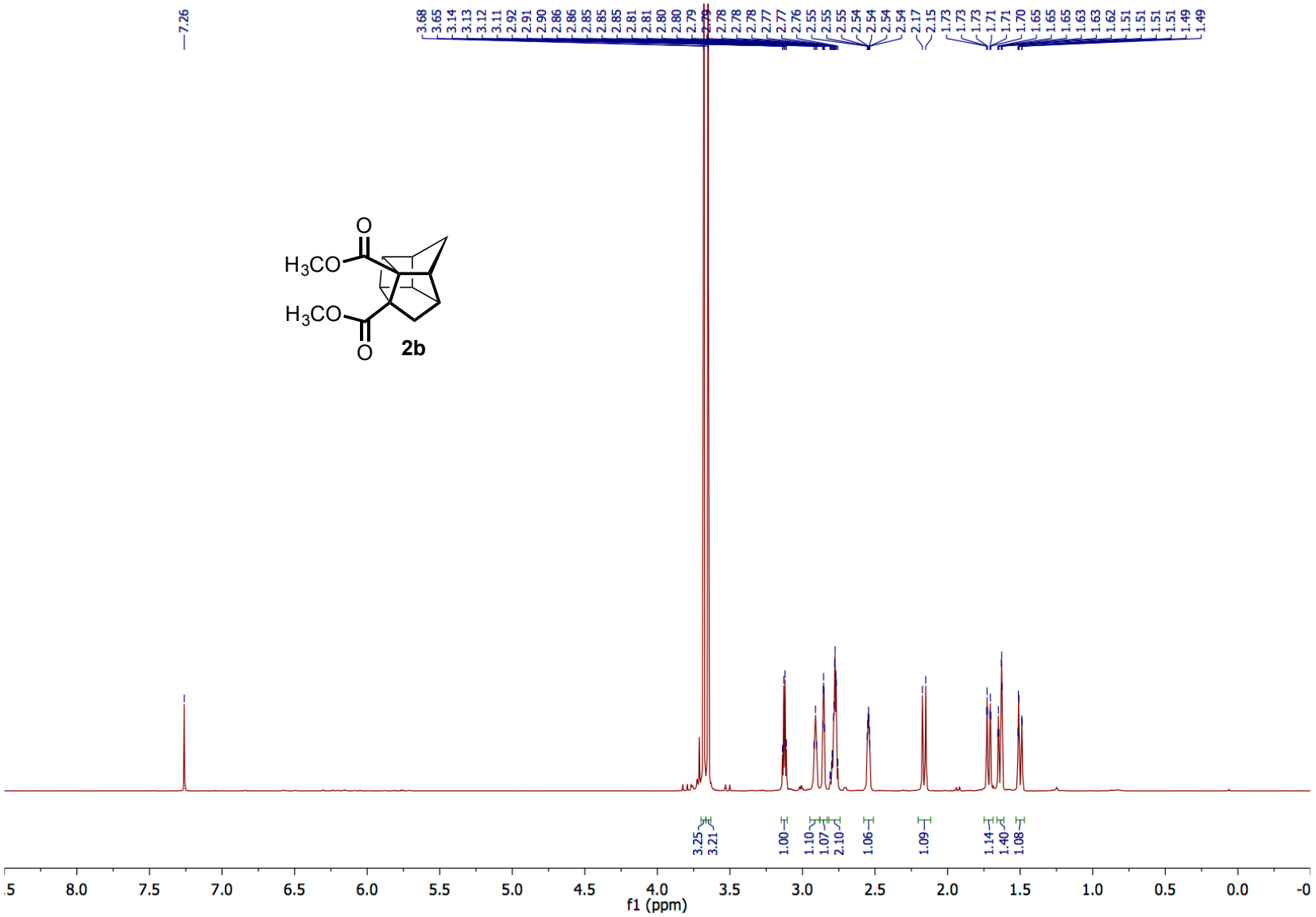

Figure S8. ^{1}H NMR of compound **2b** (500.27 MHz, $CDCl_3$).

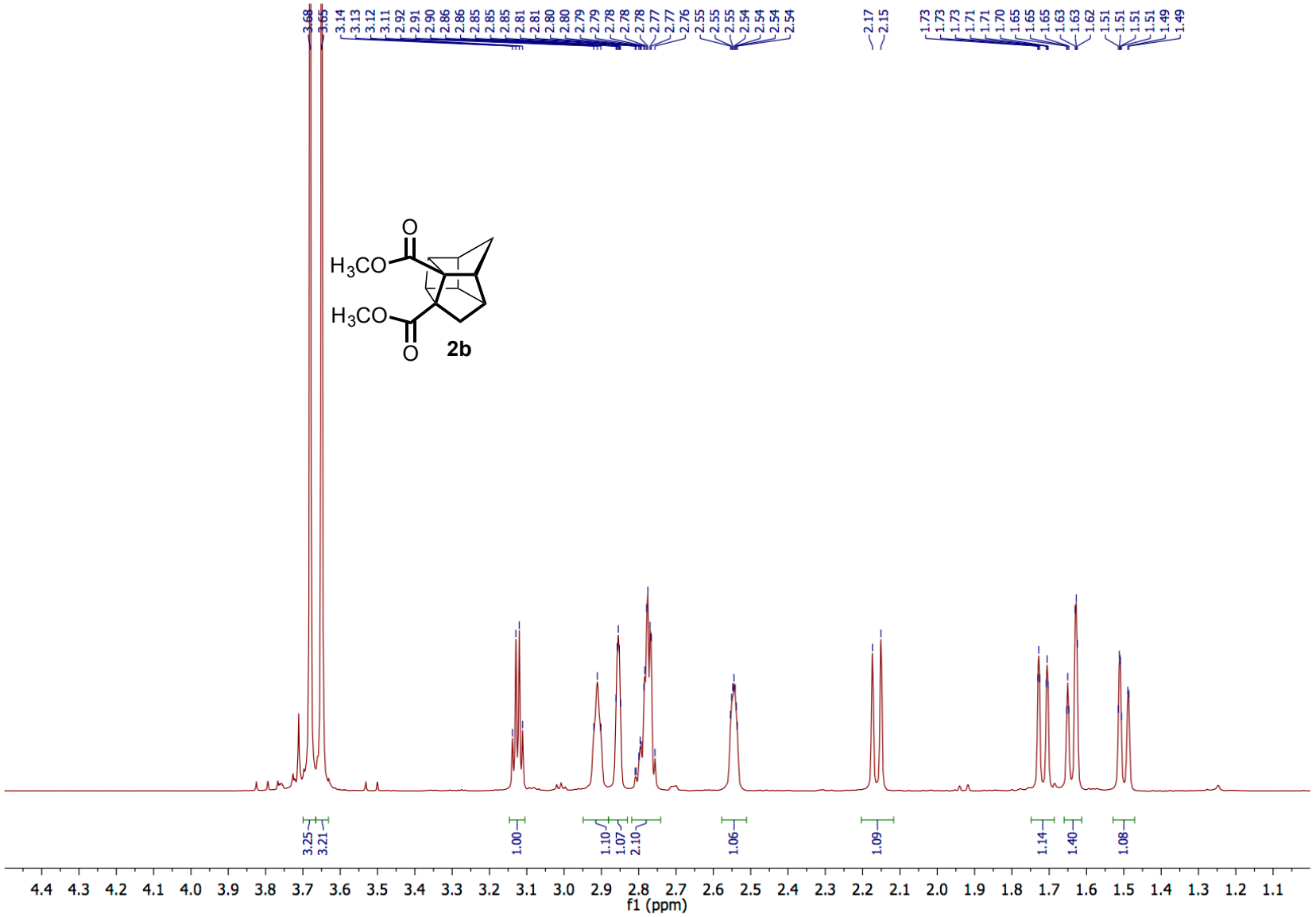

Figure S9. Upfield region (4.5-1.0 ppm) of the ^{1}H NMR of compound **2b** (500.27 MHz, $CDCl_3$).

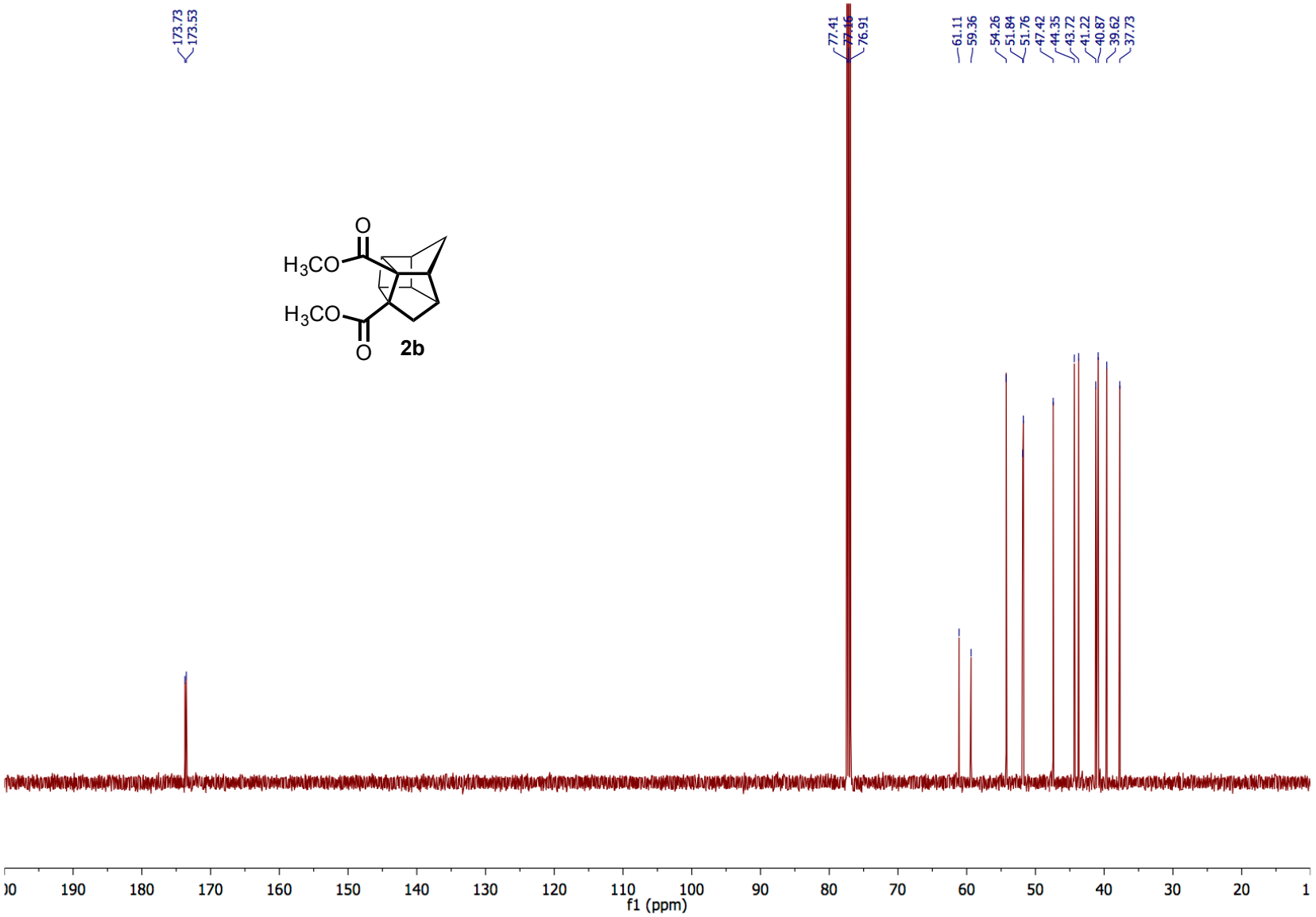

Figure S10. ^{13}C NMR of compound **2b** (125.81 MHz, $CDCl_3$).

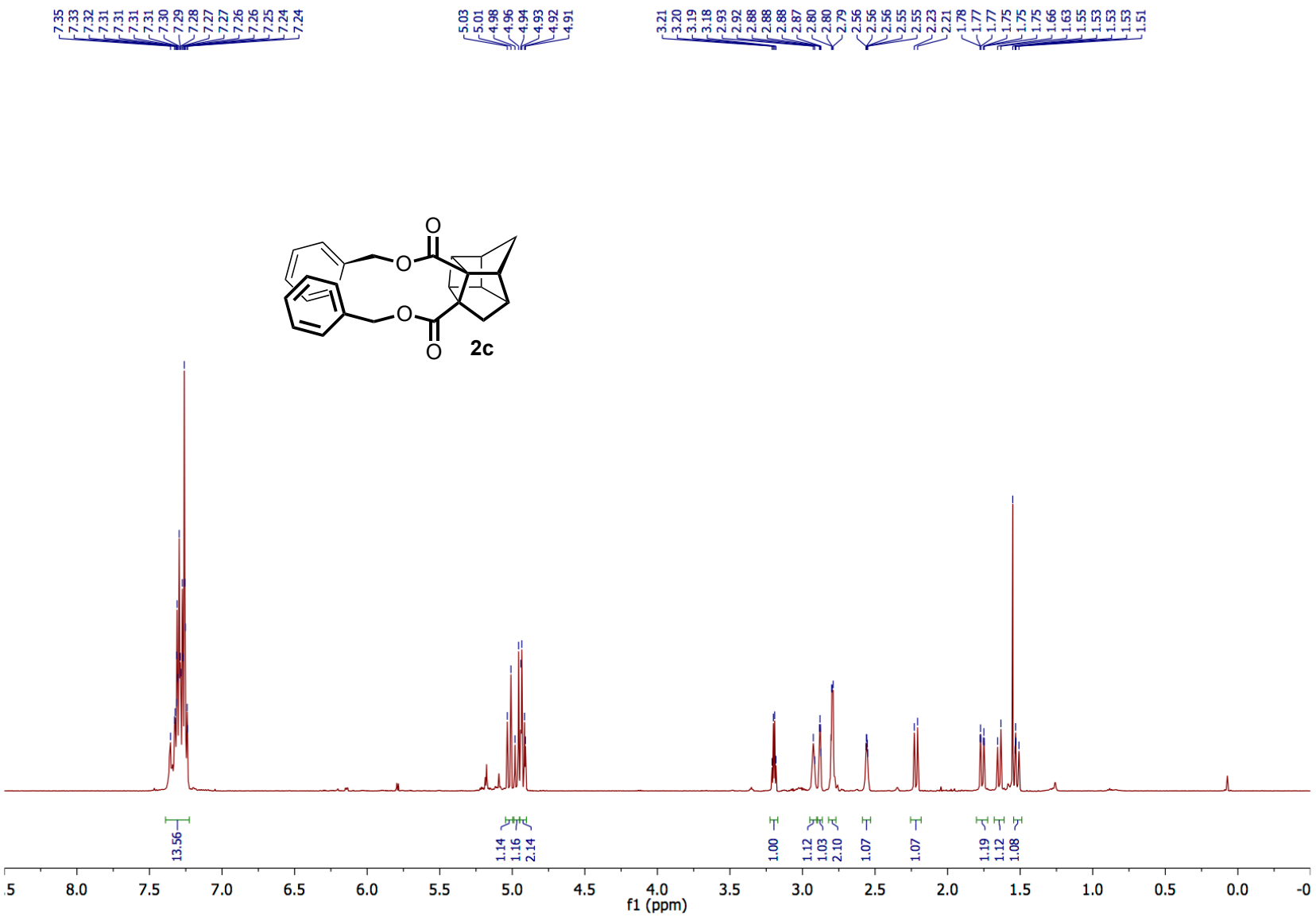

Figure S11. ^{1}H NMR of compound **2c** (500.27 MHz, $CDCl_3$).

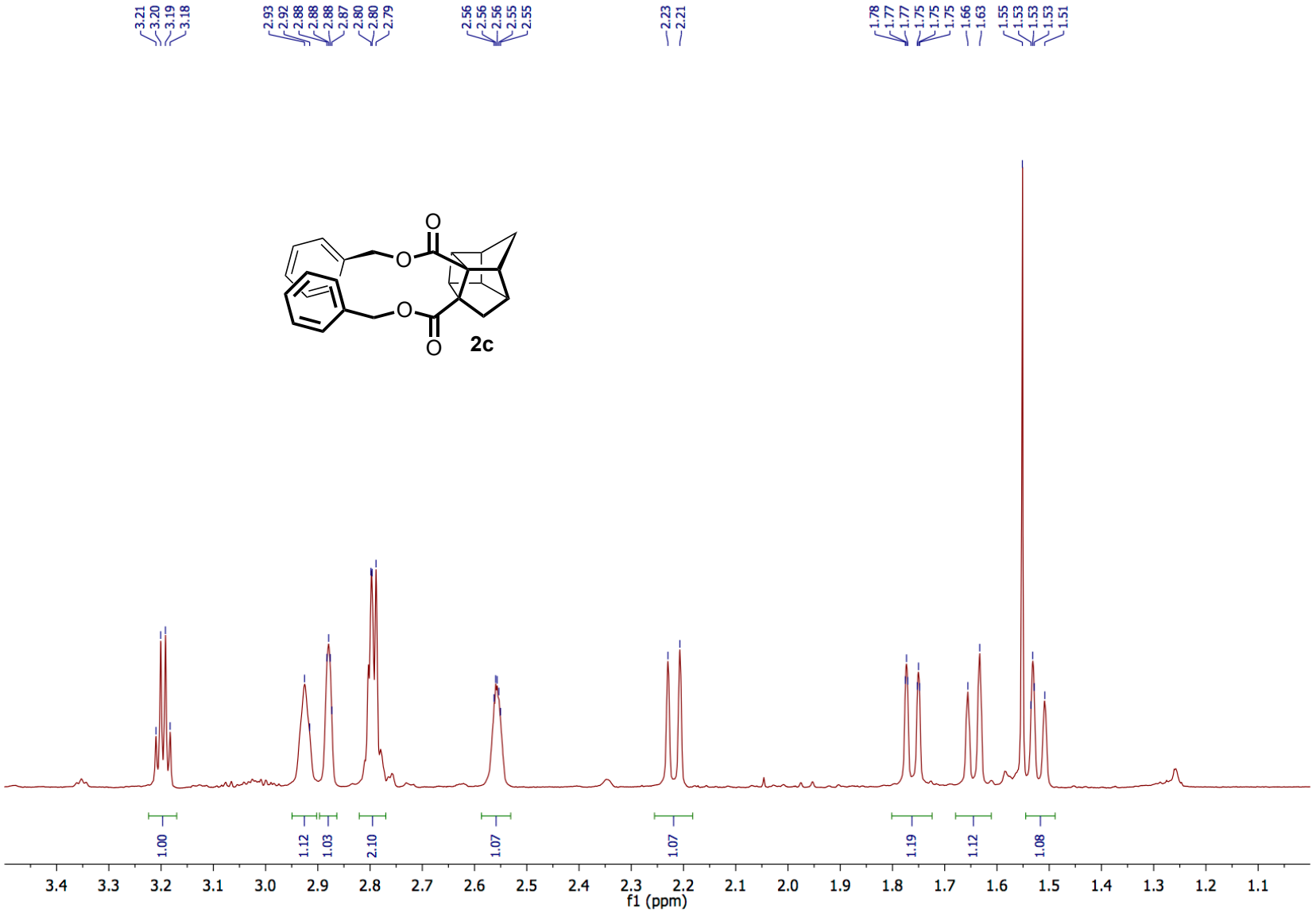

Figure S12. Upfield region (3.5-1.0 ppm) of the ^{1}H NMR of compound **2c** (500.27 MHz, $CDCl_3$).

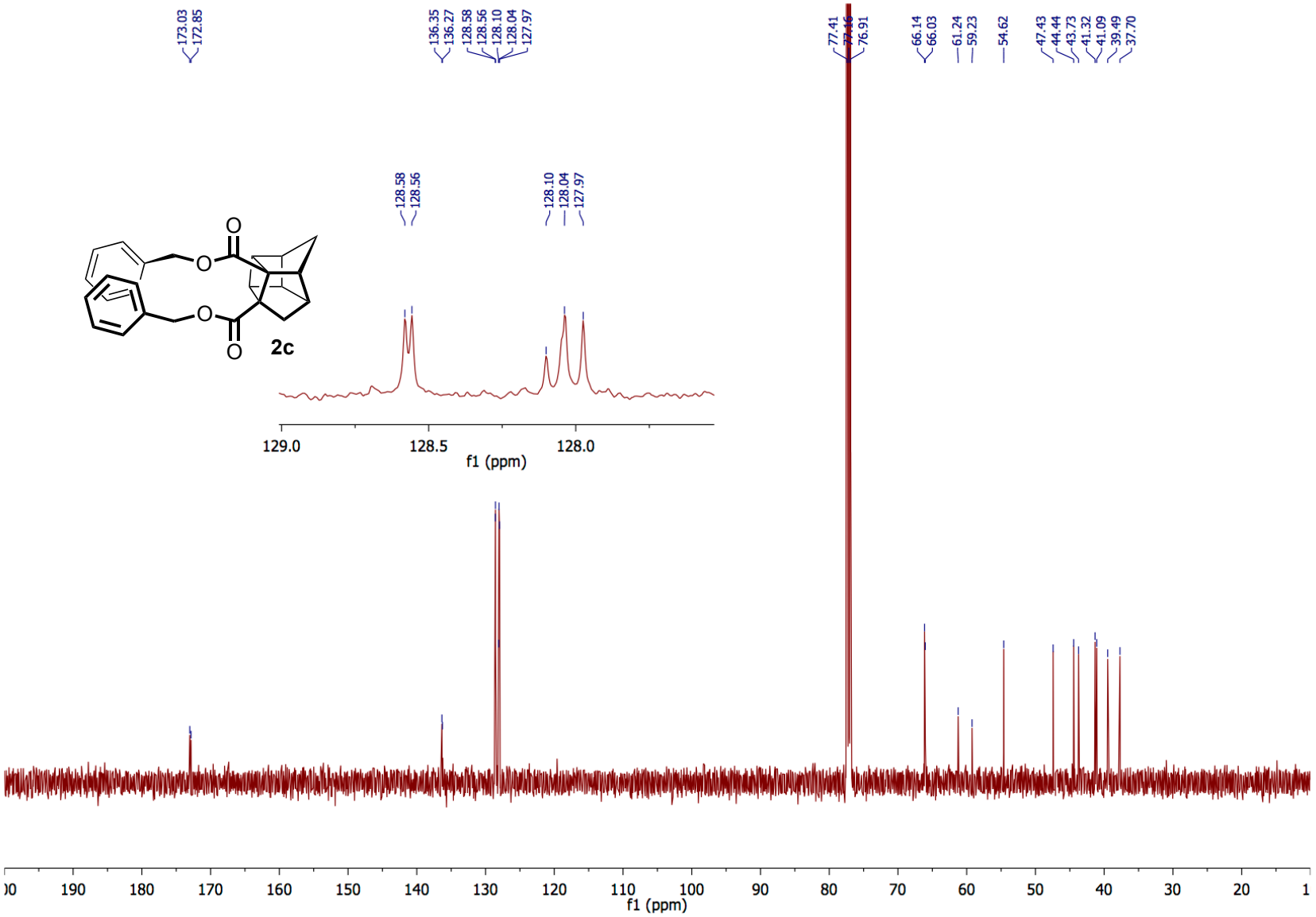

Figure S13. ^{13}C NMR of compound **2c** (125.81 MHz, $CDCl_3$).

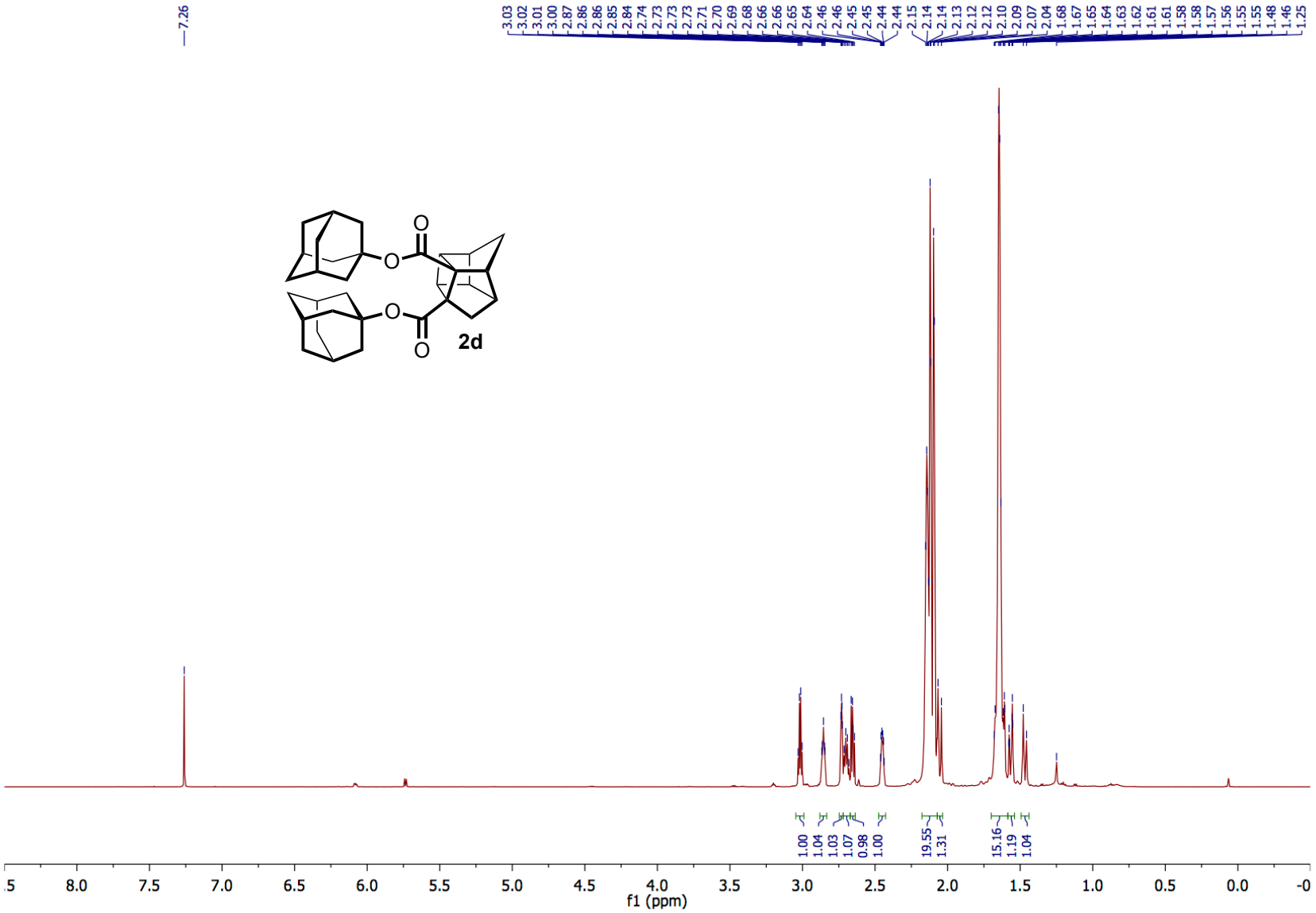

Figure S14. ^{1}H NMR of compound **2d** (500.27 MHz, $CDCl_3$).

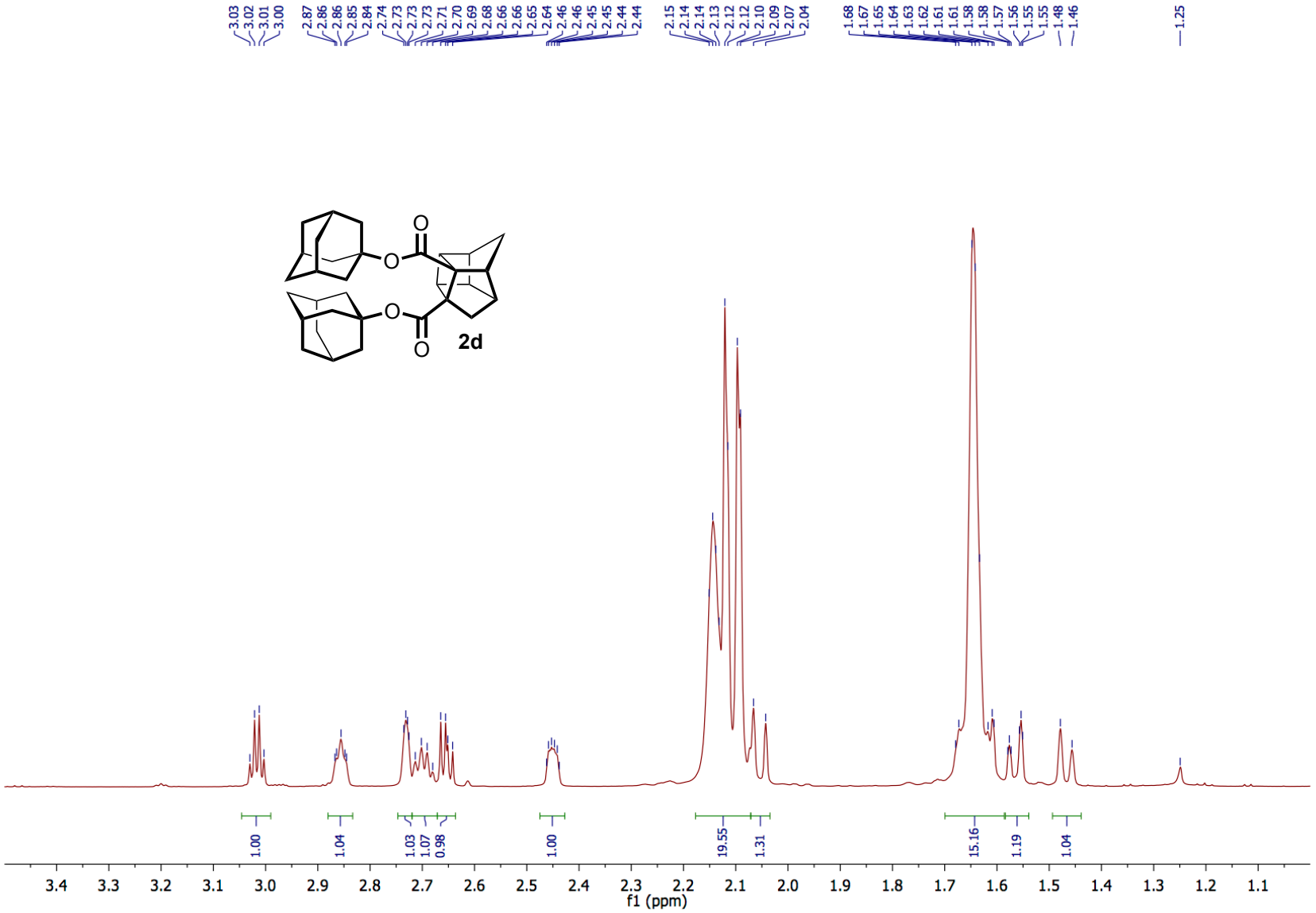

Figure S15. Upfield region (3.5-1.0 ppm) of the ^{1}H NMR of compound **2d** (500.27 MHz, $CDCl_3$).

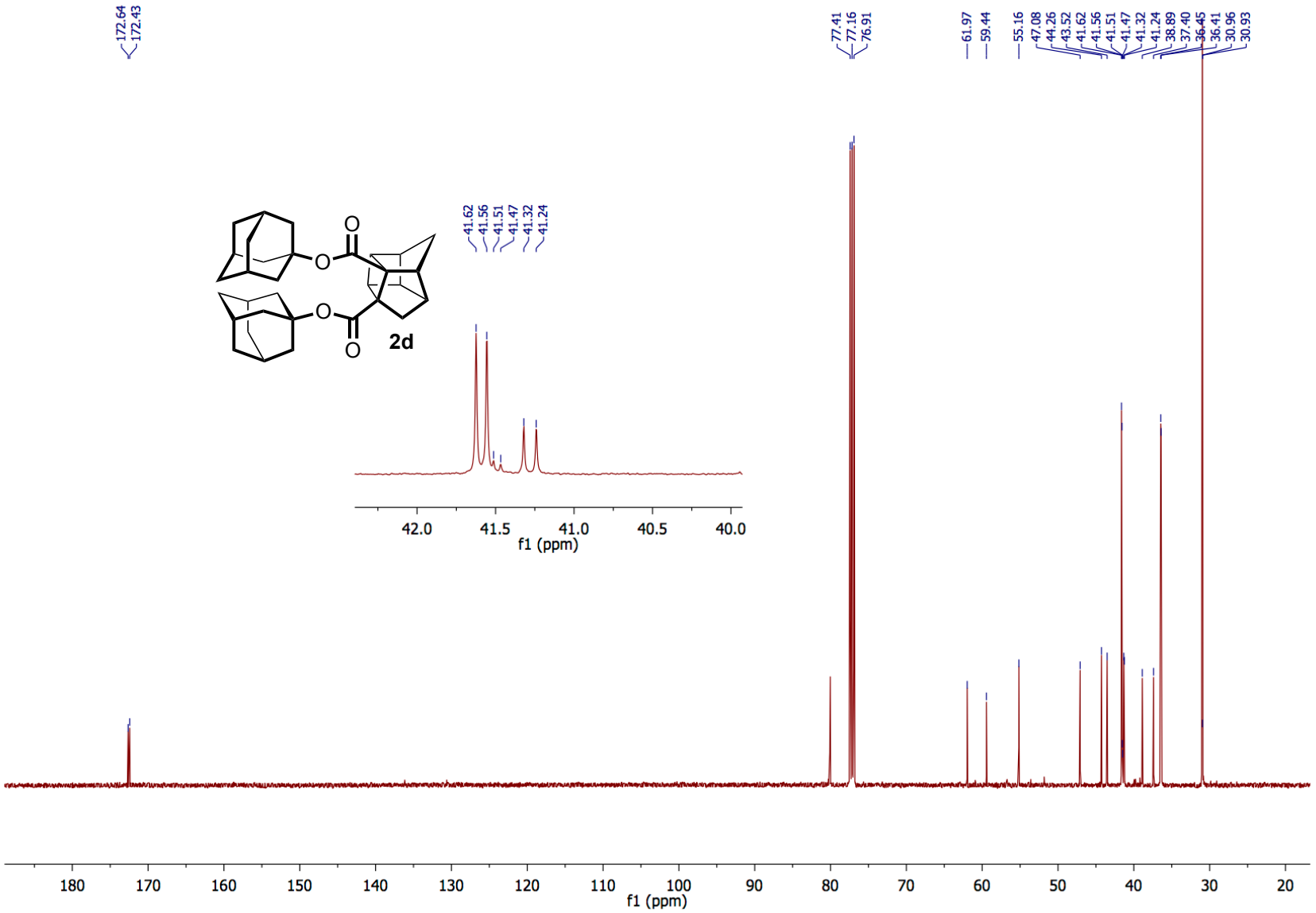

Figure S16. ^{13}C NMR of compound **2d** (125.81 MHz, $CDCl_3$).

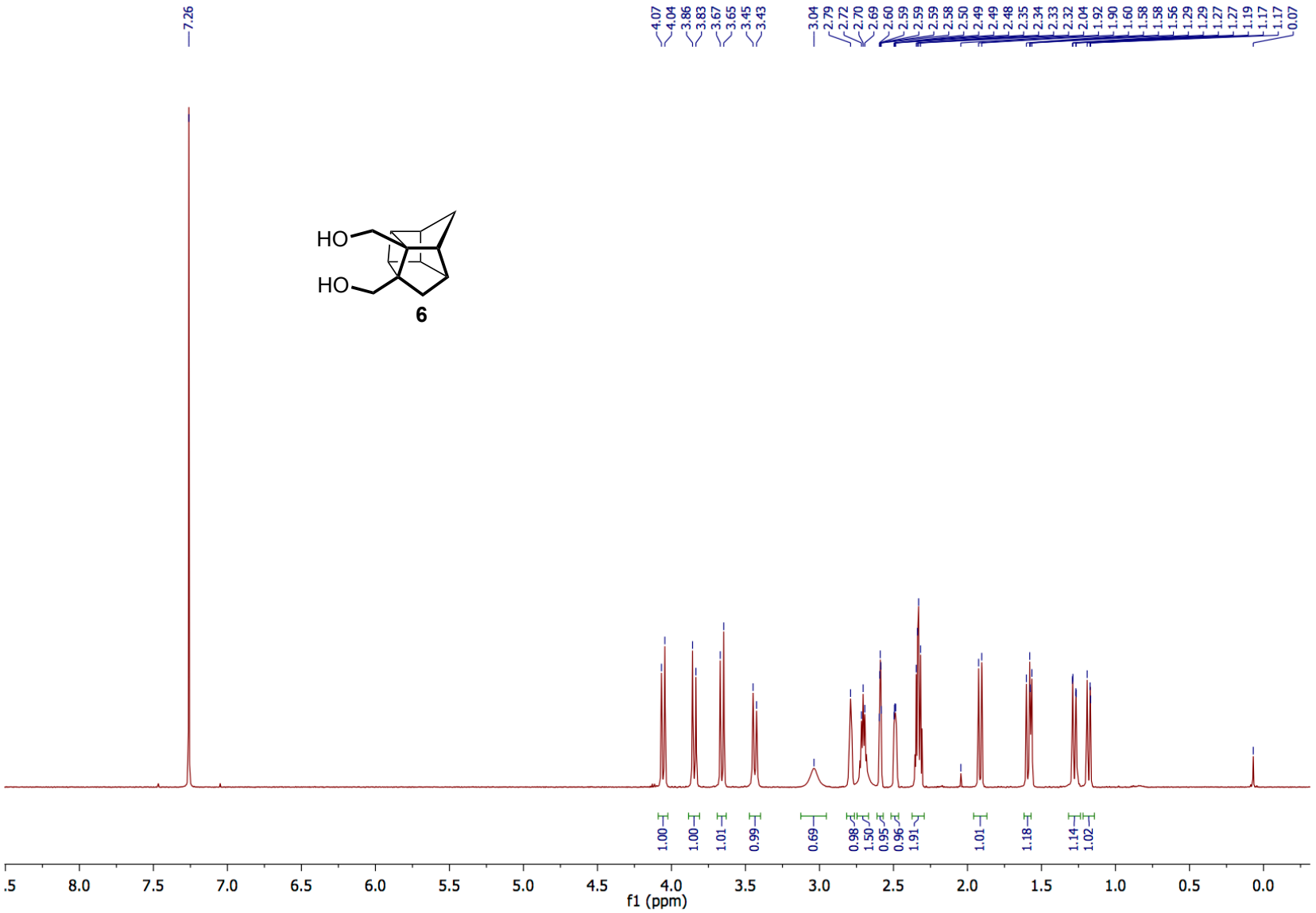

Figure S17. ^{1}H NMR of compound **6** (500.27 MHz, $CDCl_3$).

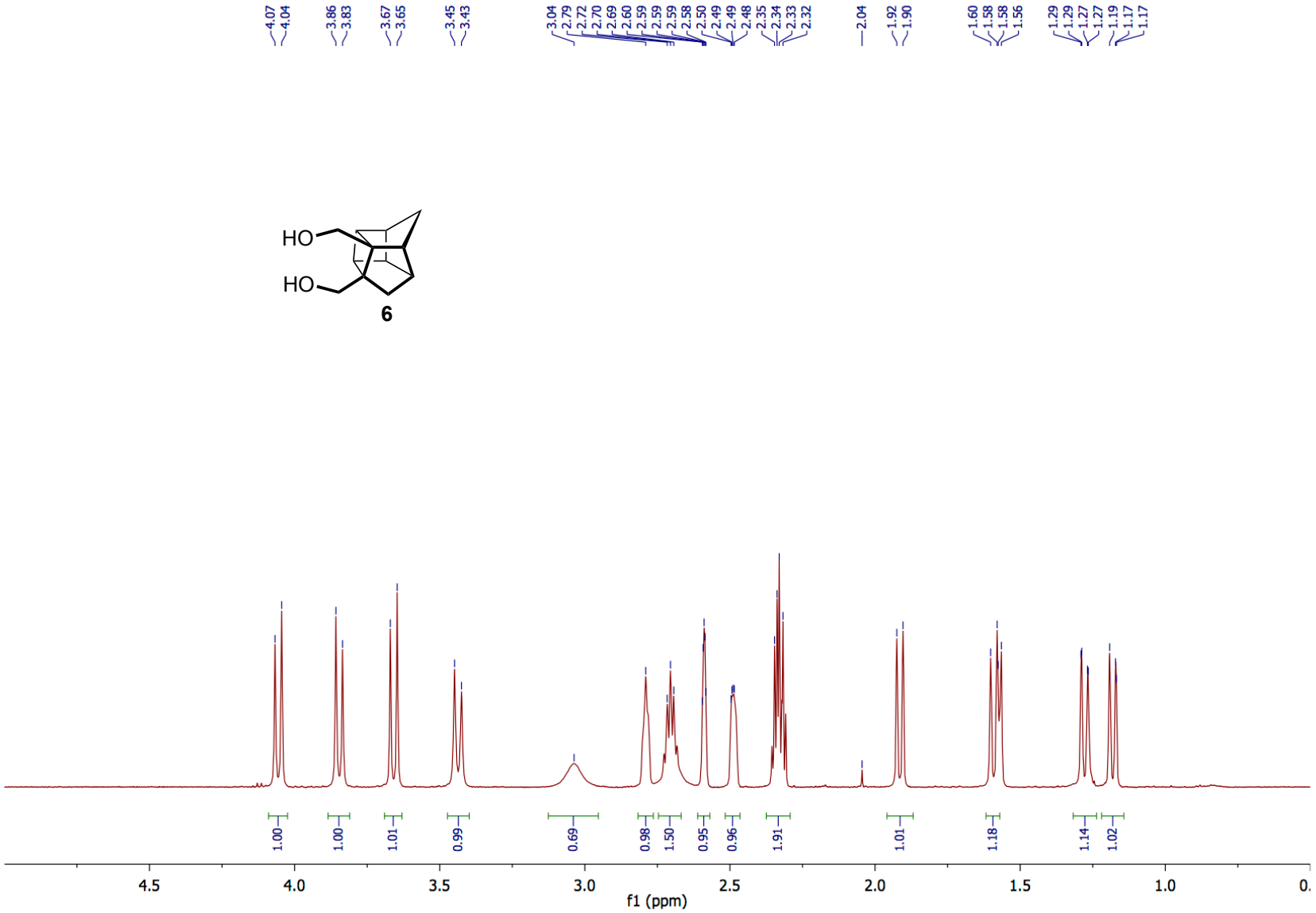

Figure S18. Upfield region (5.0-0.0 ppm) of the ^{1}H NMR of compound **6** (500.27 MHz, $CDCl_3$).

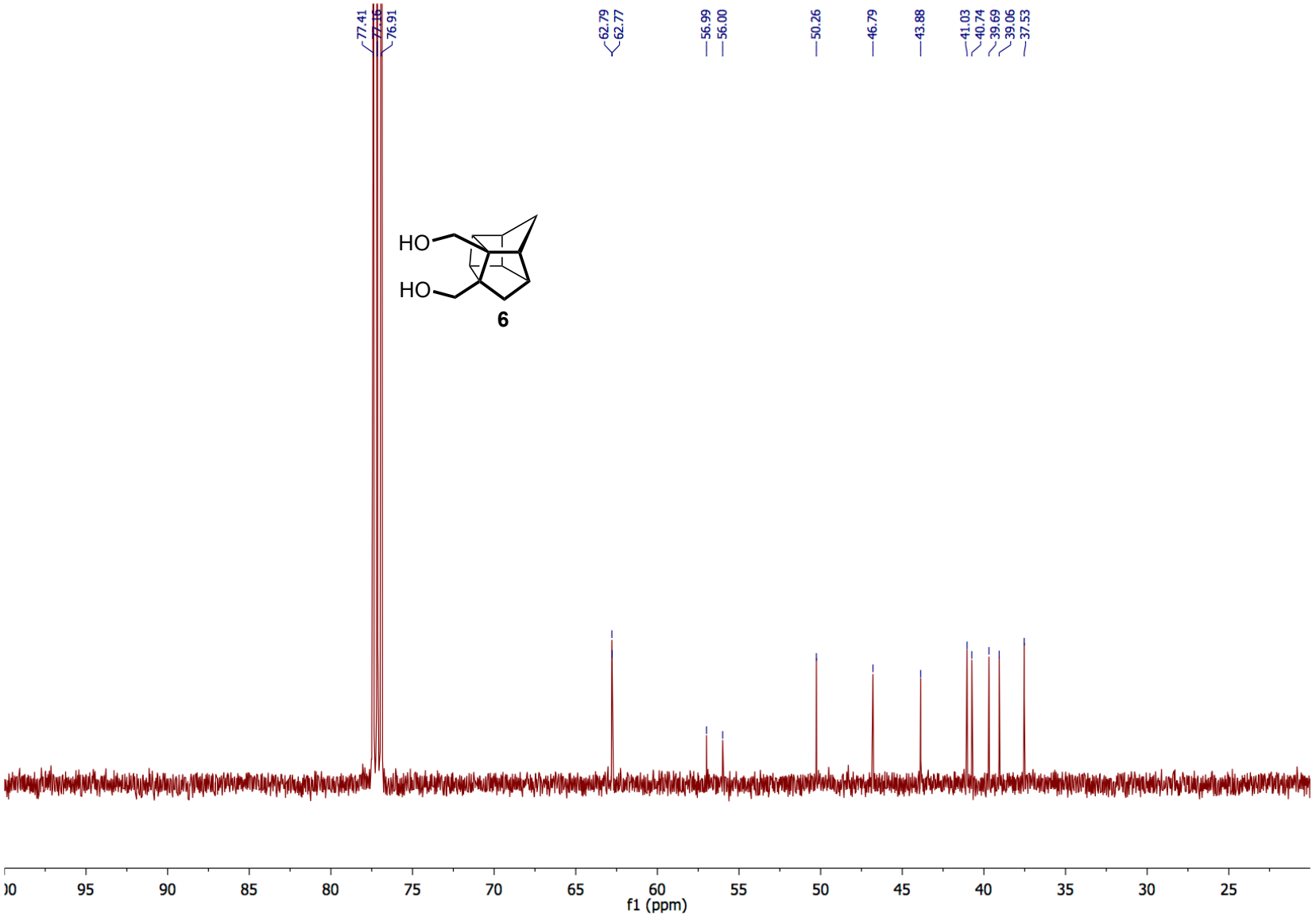

Figure S19. ^{13}C NMR of compound **6** (125.81 MHz, $CDCl_3$).

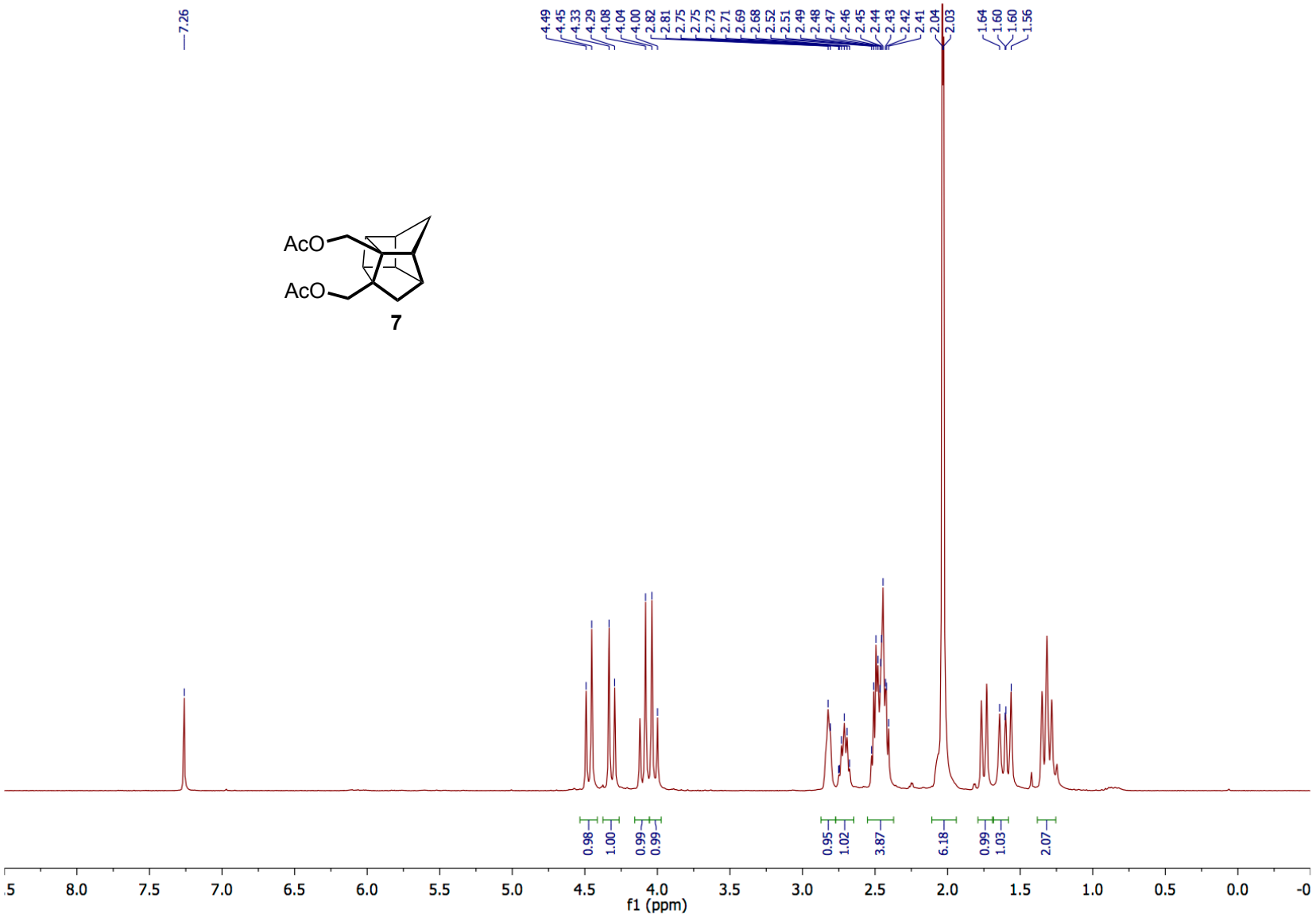

Figure S20. ^{1}H NMR of compound **7** (300.27 MHz, $CDCl_3$).

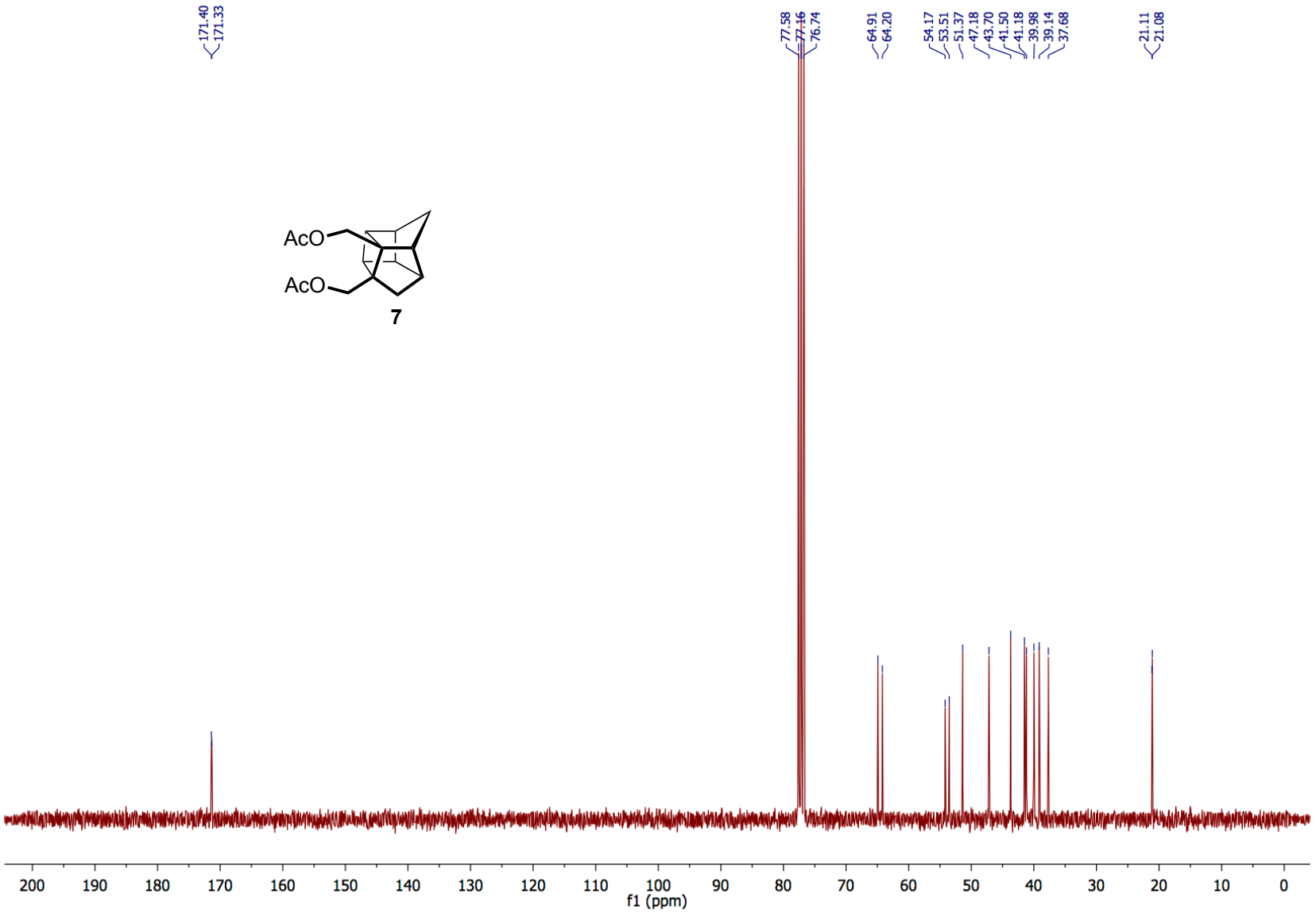

Figure S21. ^{13}C NMR of compound **7** (75.70 MHz, $CDCl_3$).

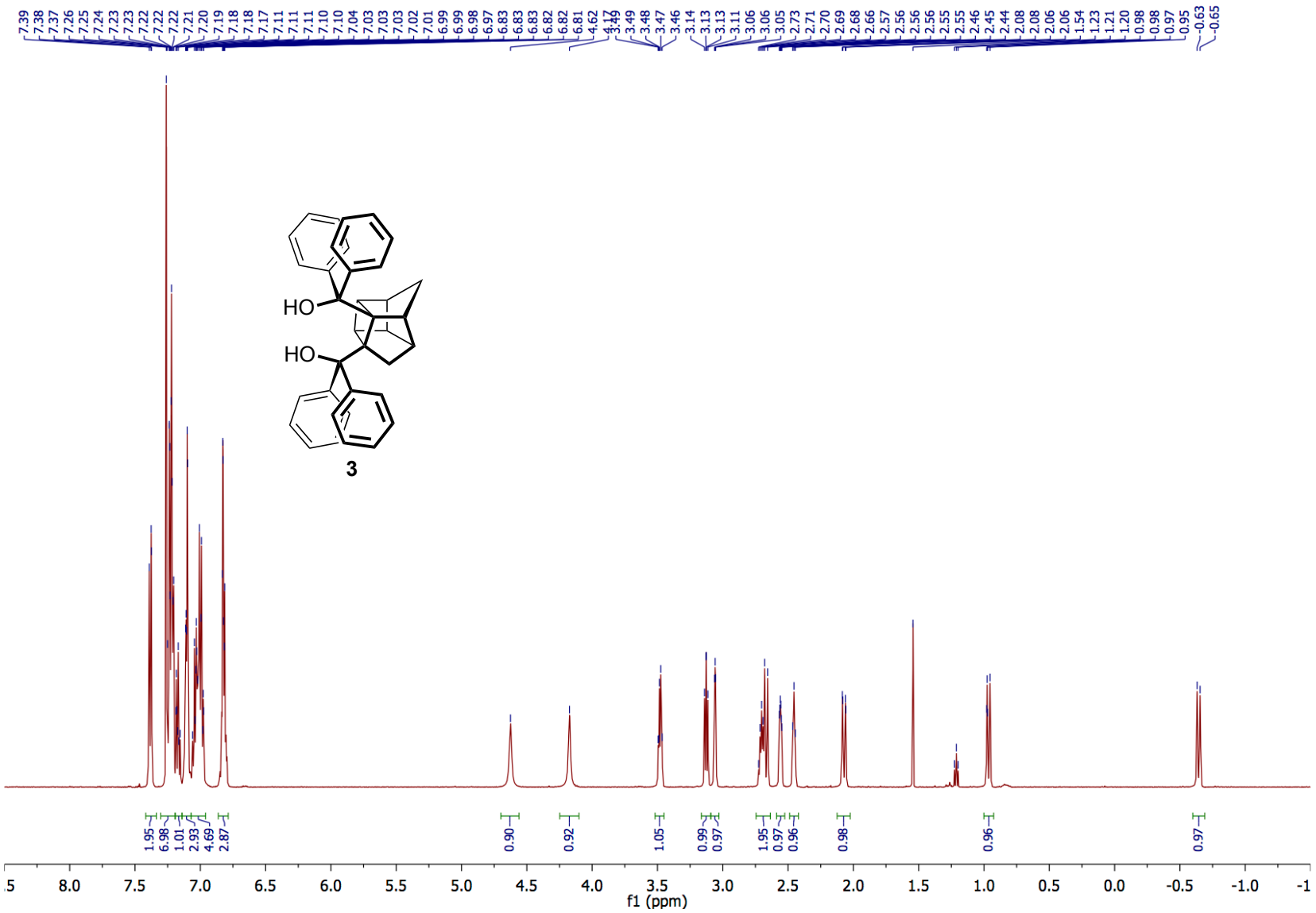

Figure S22. ^{1}H NMR of compound **3** (500.27 MHz, $CDCl_3$).

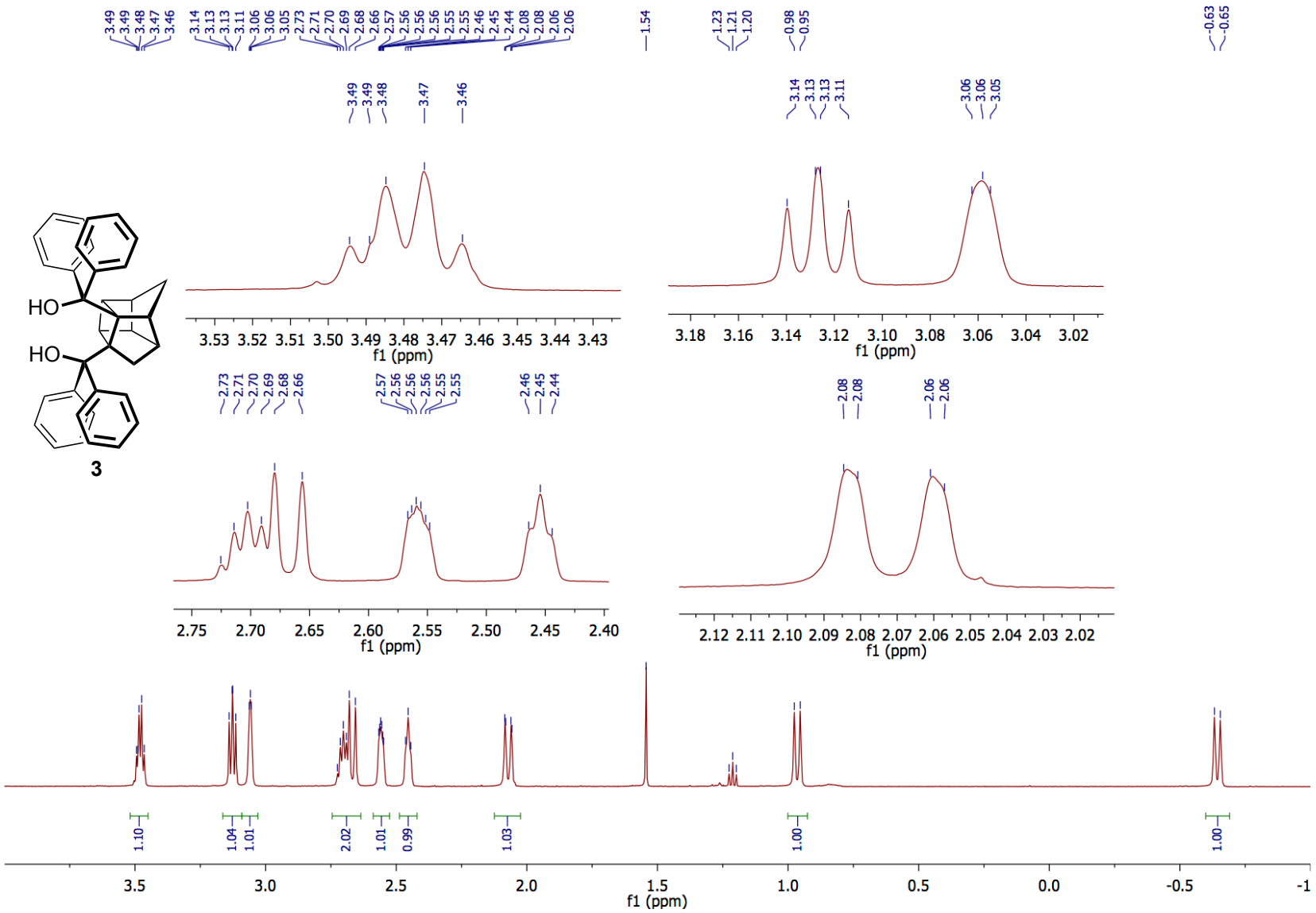

Figure S23. Upfield region of the ^{1}H NMR of compound **3** (500.27 MHz, $CDCl_3$).

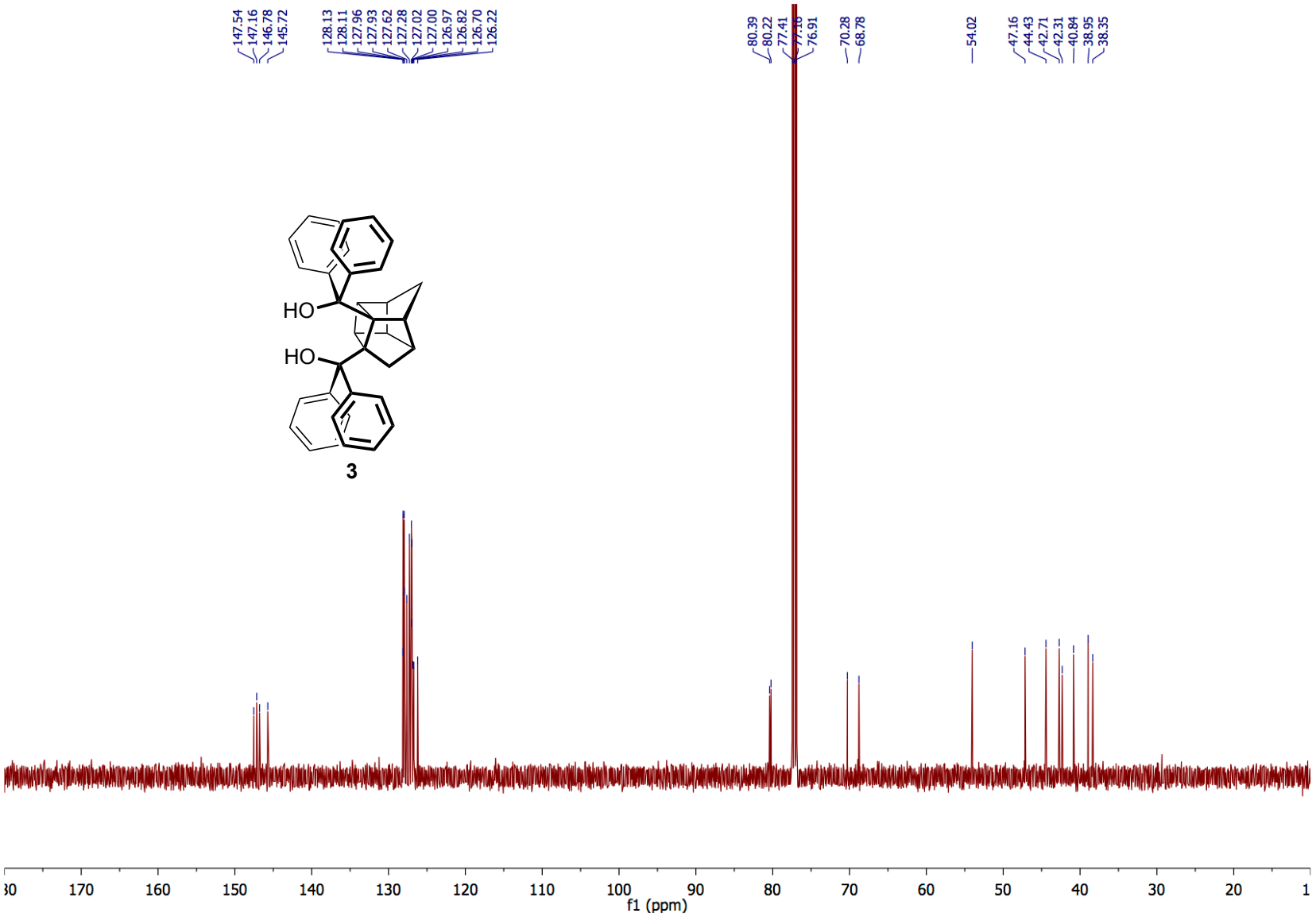

Figure S24. ^{13}C NMR of compound **3** (125.81 MHz, $CDCl_3$).

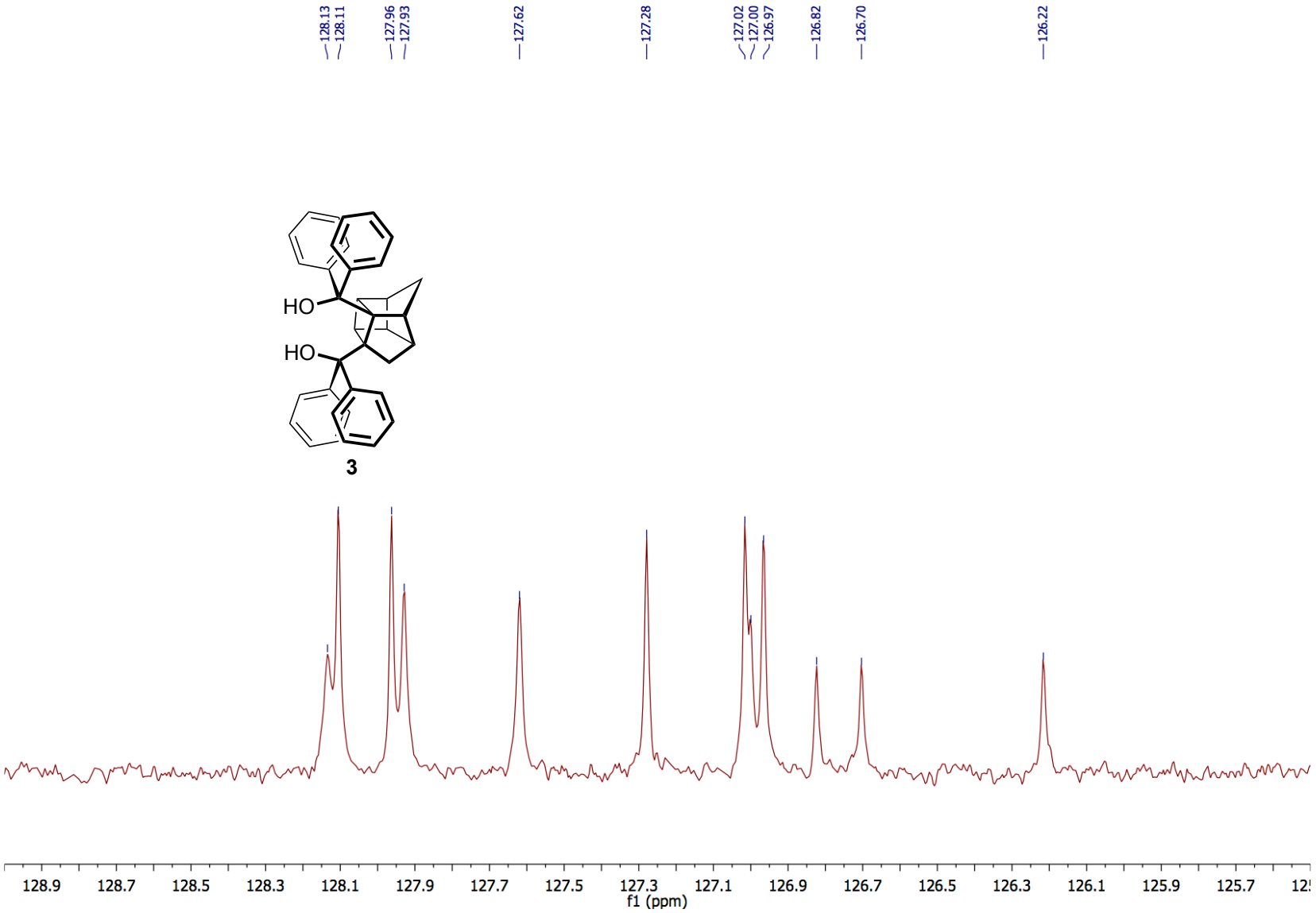

Figure S25. Aromatic region of the ^{13}C NMR of compound **3** (125.81 MHz, $CDCl_3$).

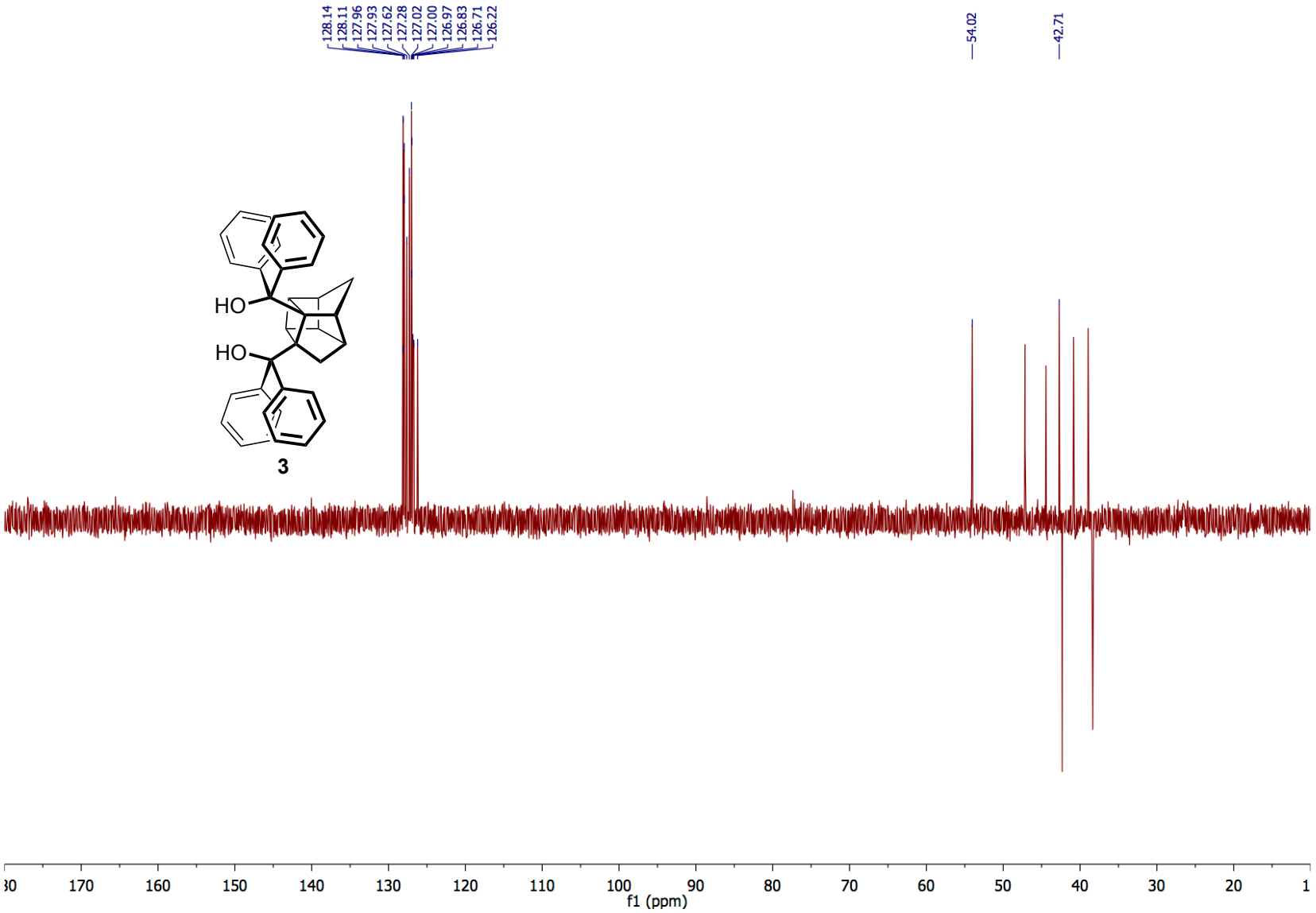

Figure S26. ^{13}C DEPT-135 spectrum of compound **3** (125.81 MHz, $CDCl_3$).

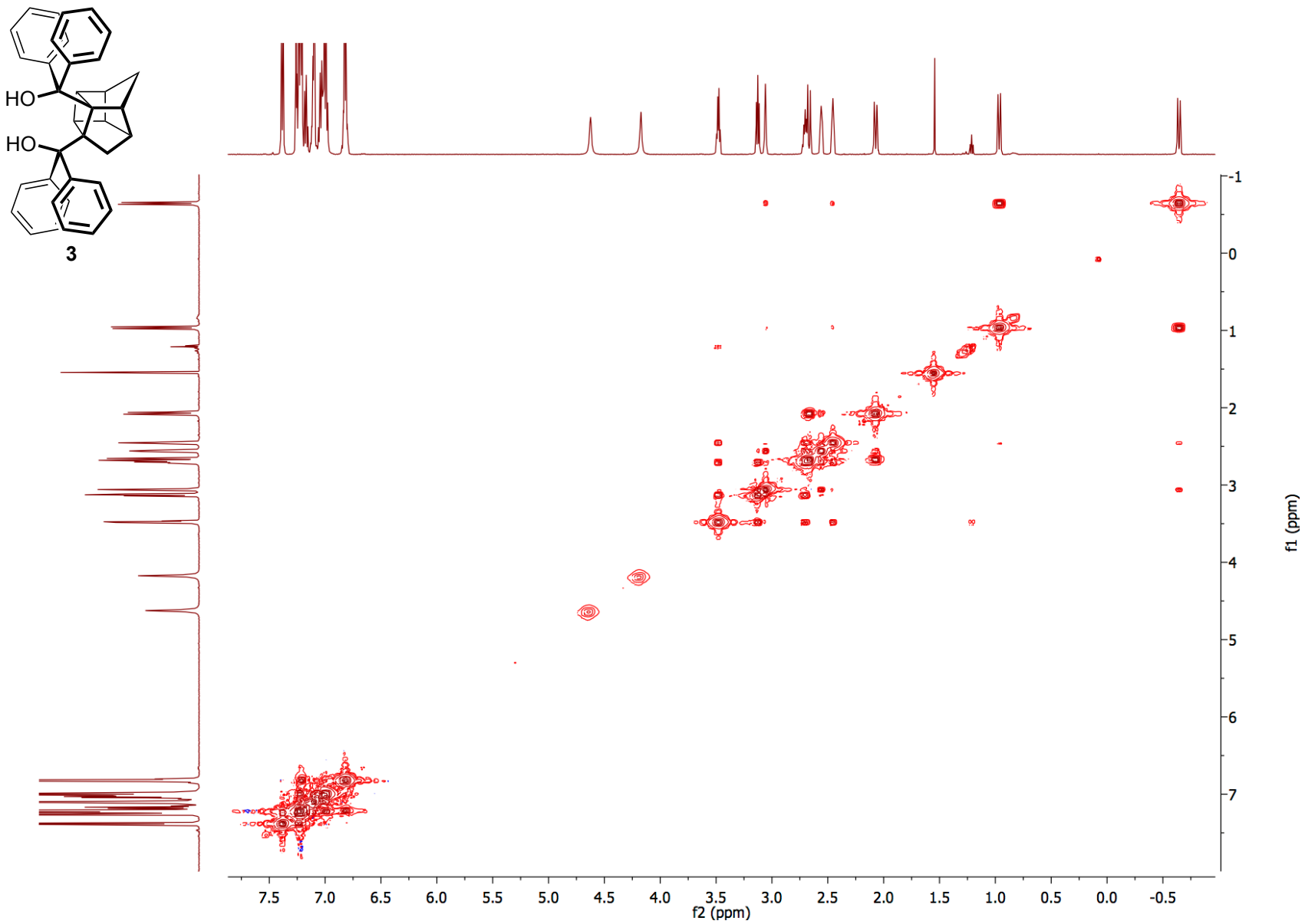

Figure S27. Gradient COSY spectrum of compound **3** (500.27 MHz, $CDCl_3$).

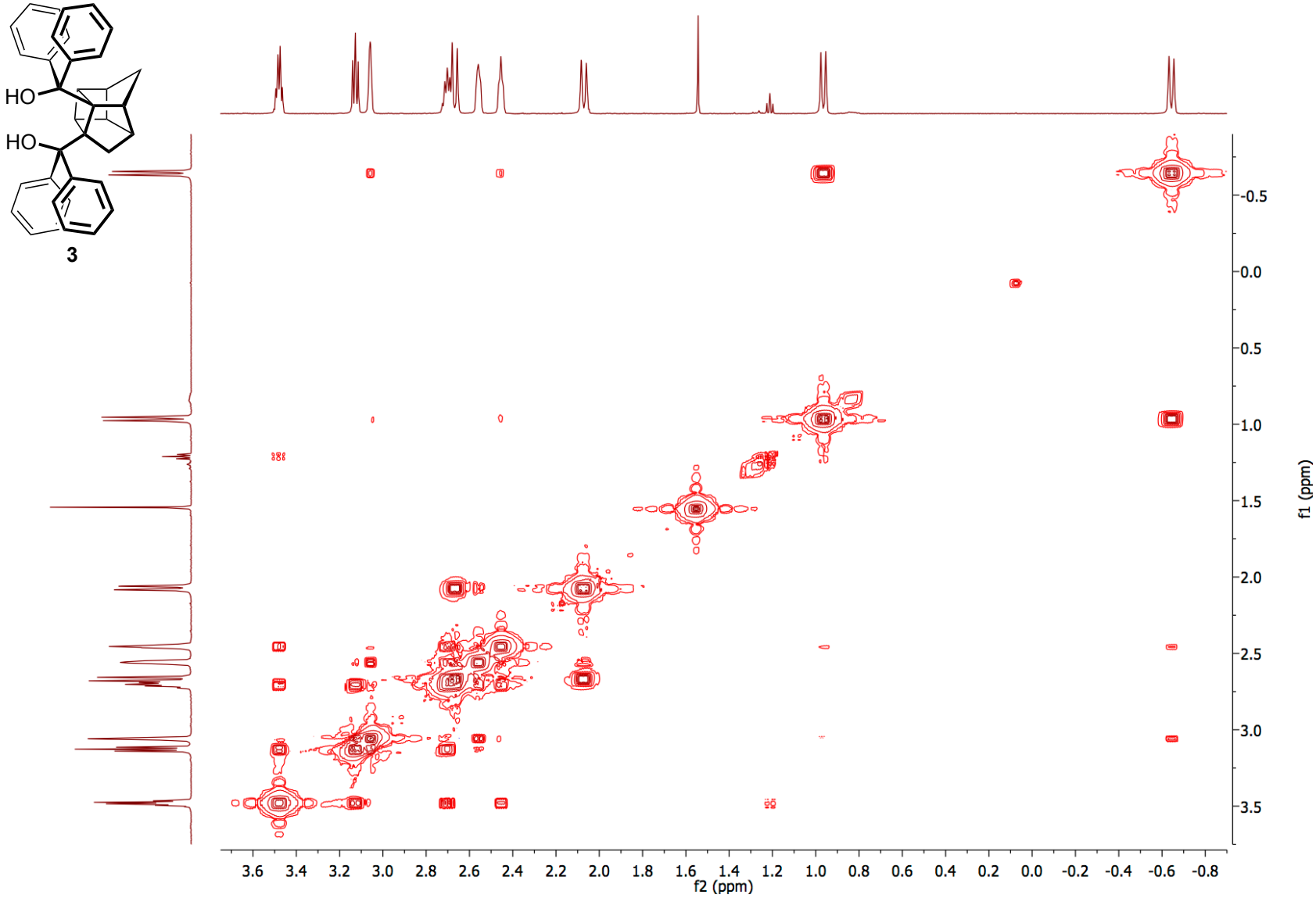

Figure S28. Upfield region of the gradient COSY spectrum of compound **3** (500.27 MHz, $CDCl_3$).

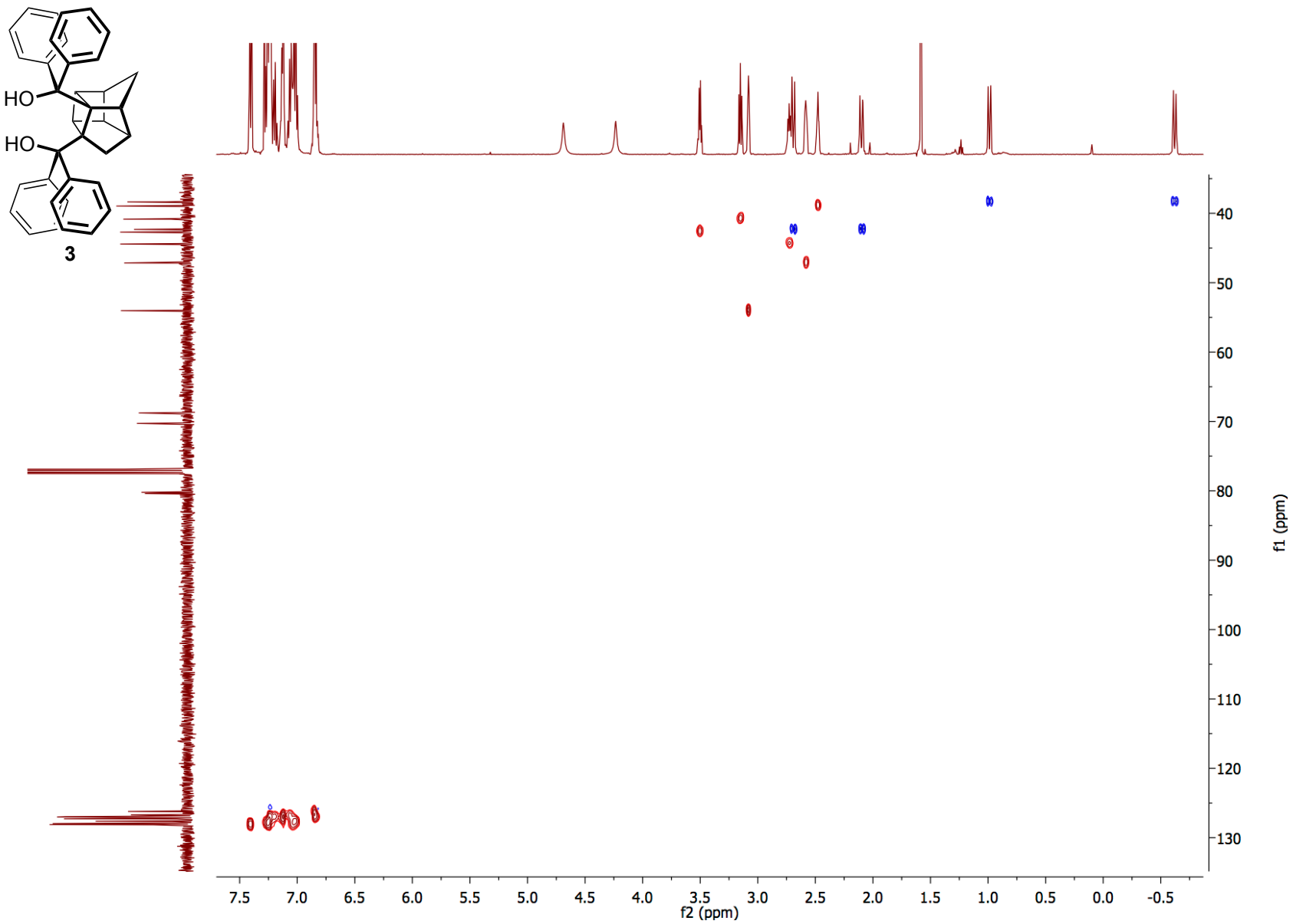

Figure S29. Gradient HSQC spectrum of compound **3** (500.27, 125.81 MHz, $CDCl_3$).

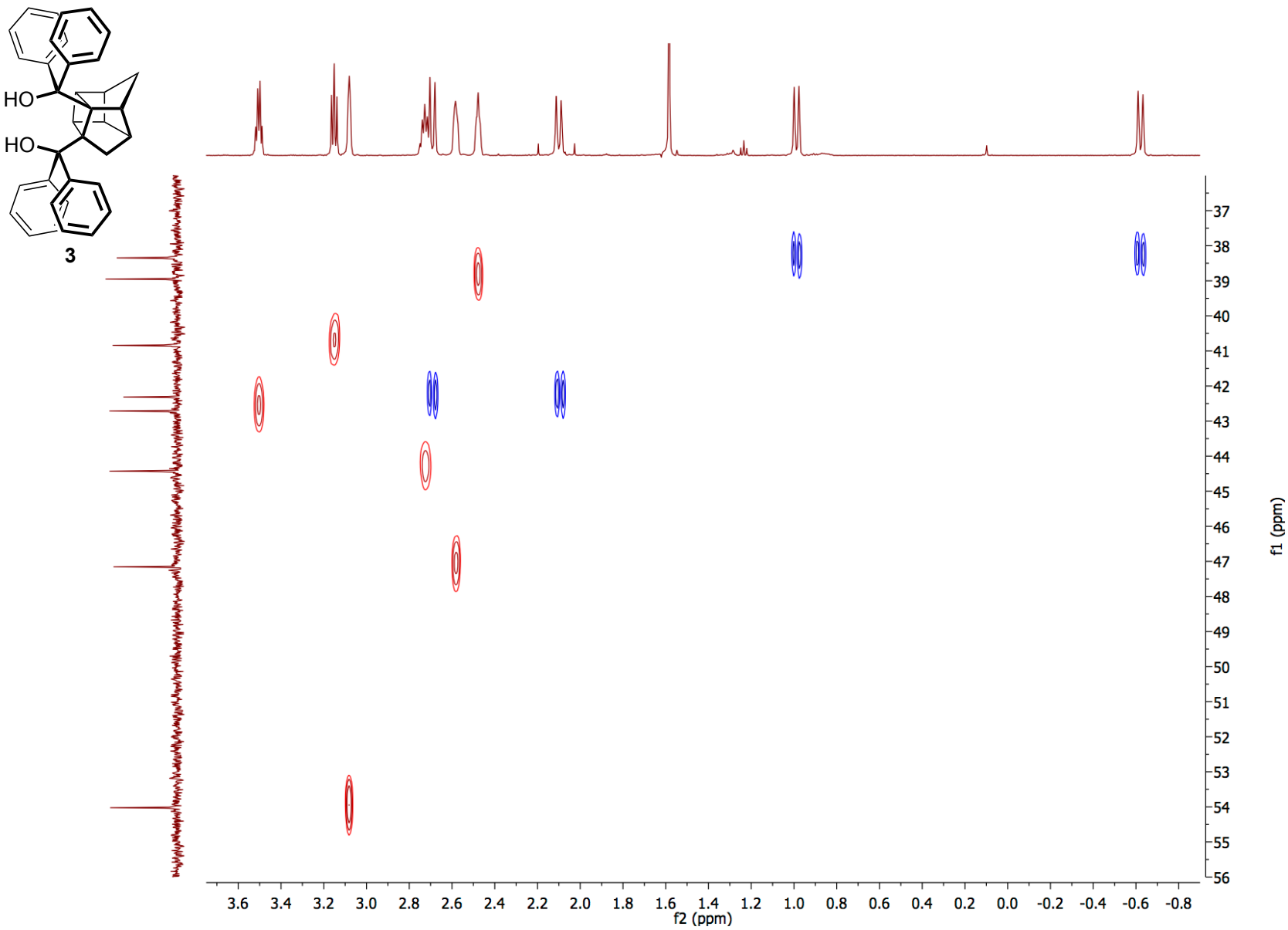

Figure S30. Gradient HSQC spectrum of compound **3** (500.27, 125.81 MHz, $CDCl_3$).

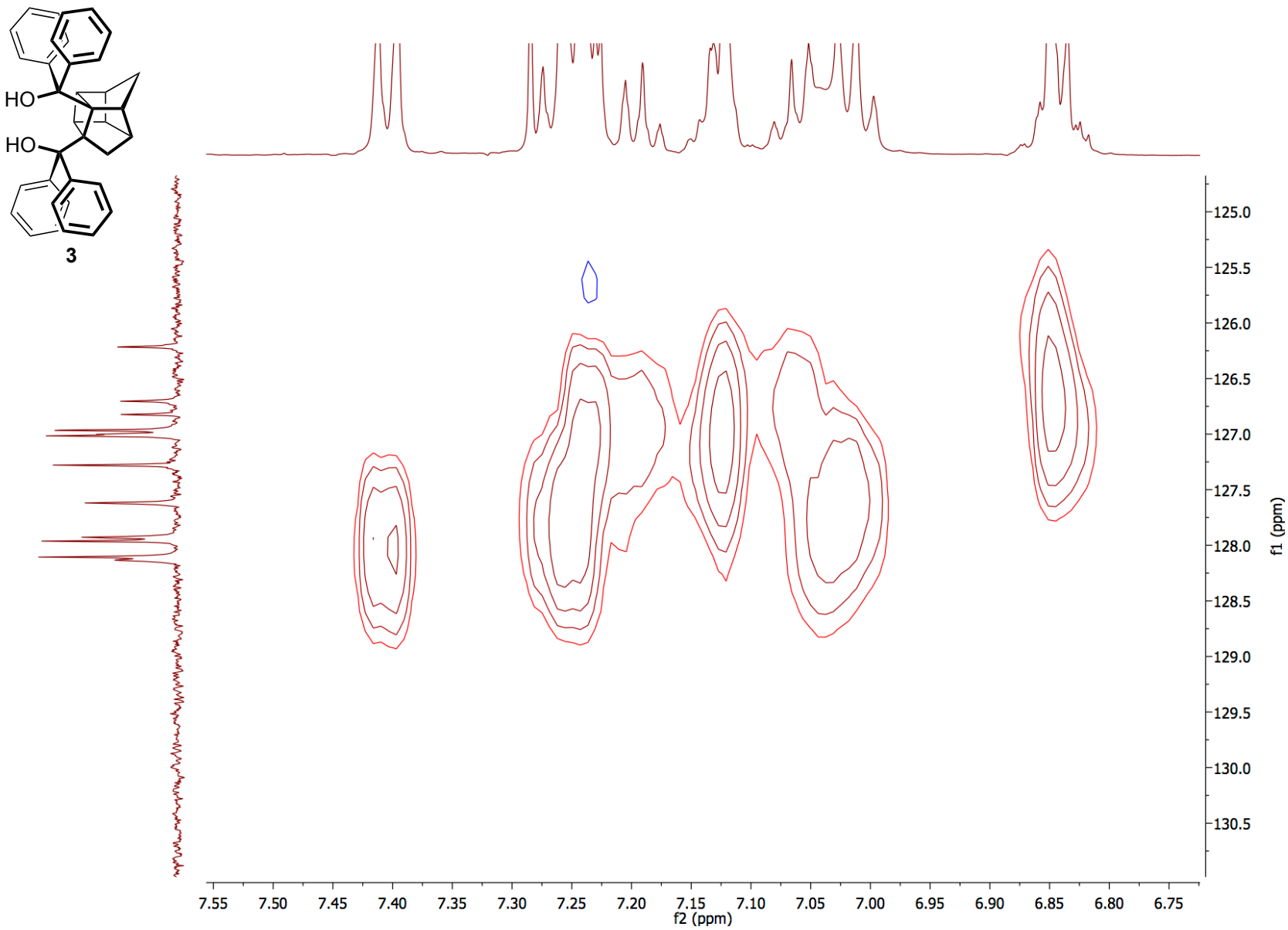

Figure S31. Gradient HSQC spectrum of compound **3** (500.27, 125.81 MHz, $CDCl_3$).

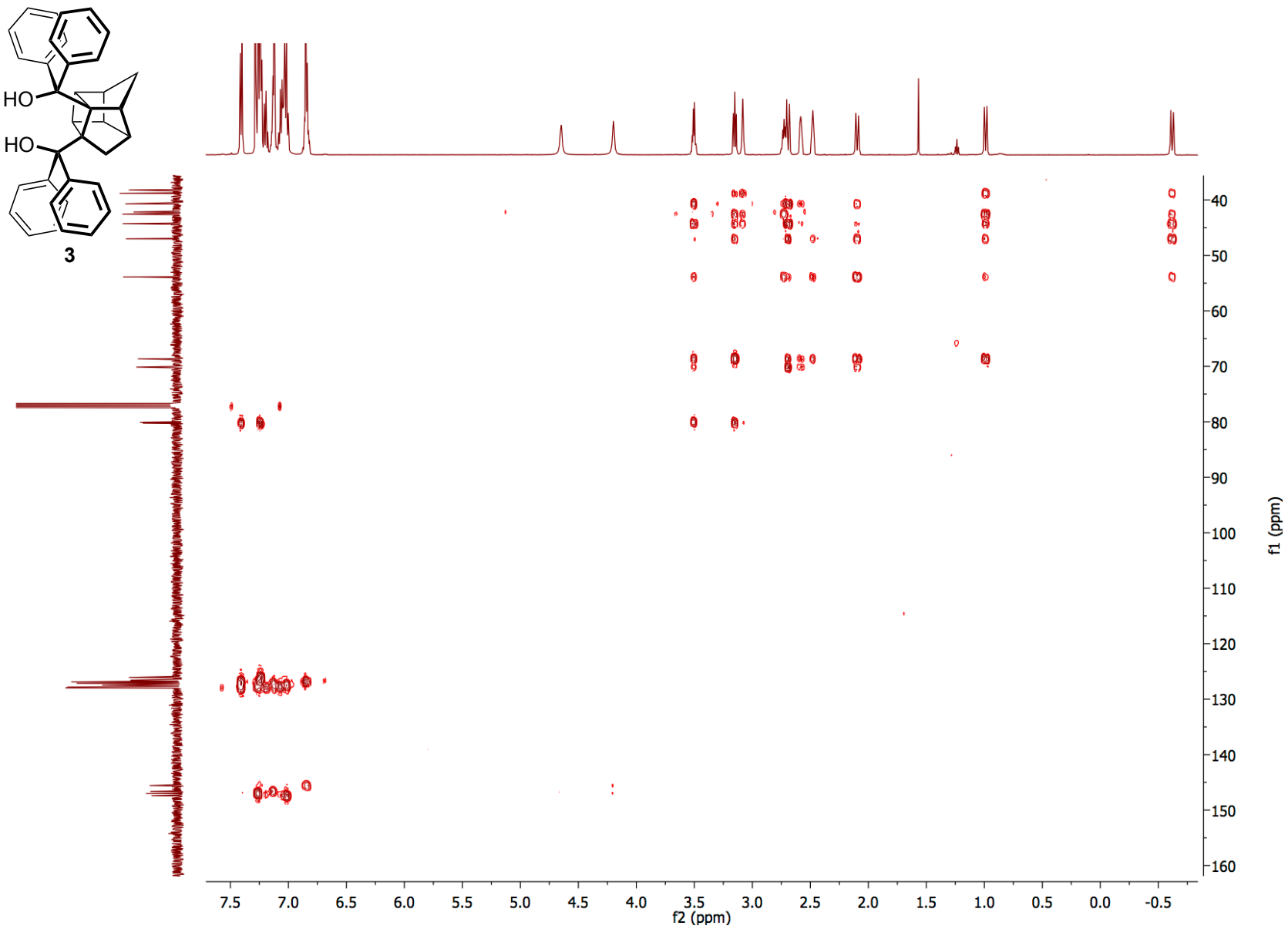

Figure S32. Gradient HMBC spectrum of compound **3** (500.27, 125.81 MHz, $CDCl_3$).

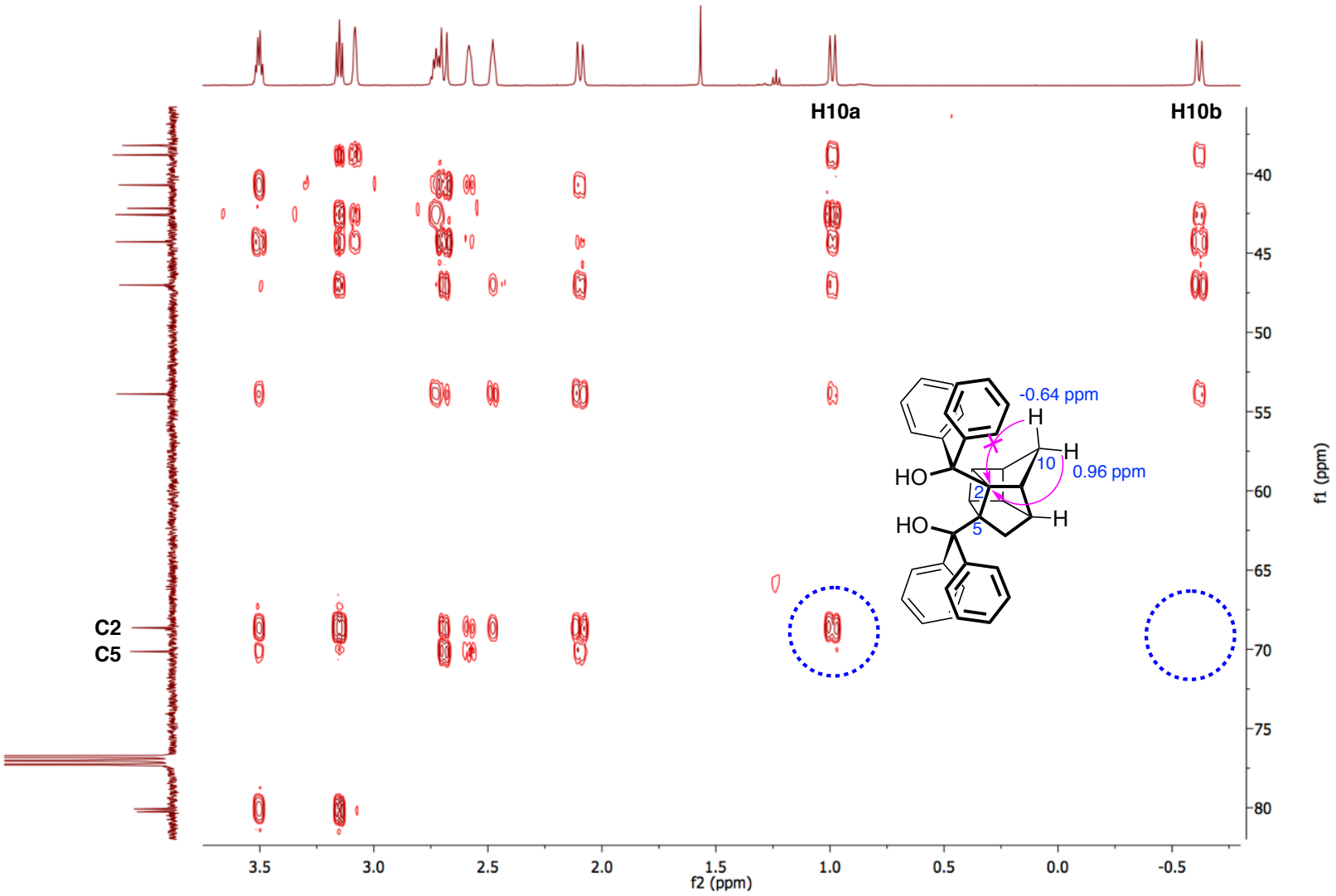

Figure S33. Gradient HMBC spectrum of compound **3** (500.27, 125.81 MHz, $CDCl_3$) highlighting the observed ^3J H10α/C2 correlation and the absence of a ^3J H10β/C2 correlation due to poor orbital alignment.

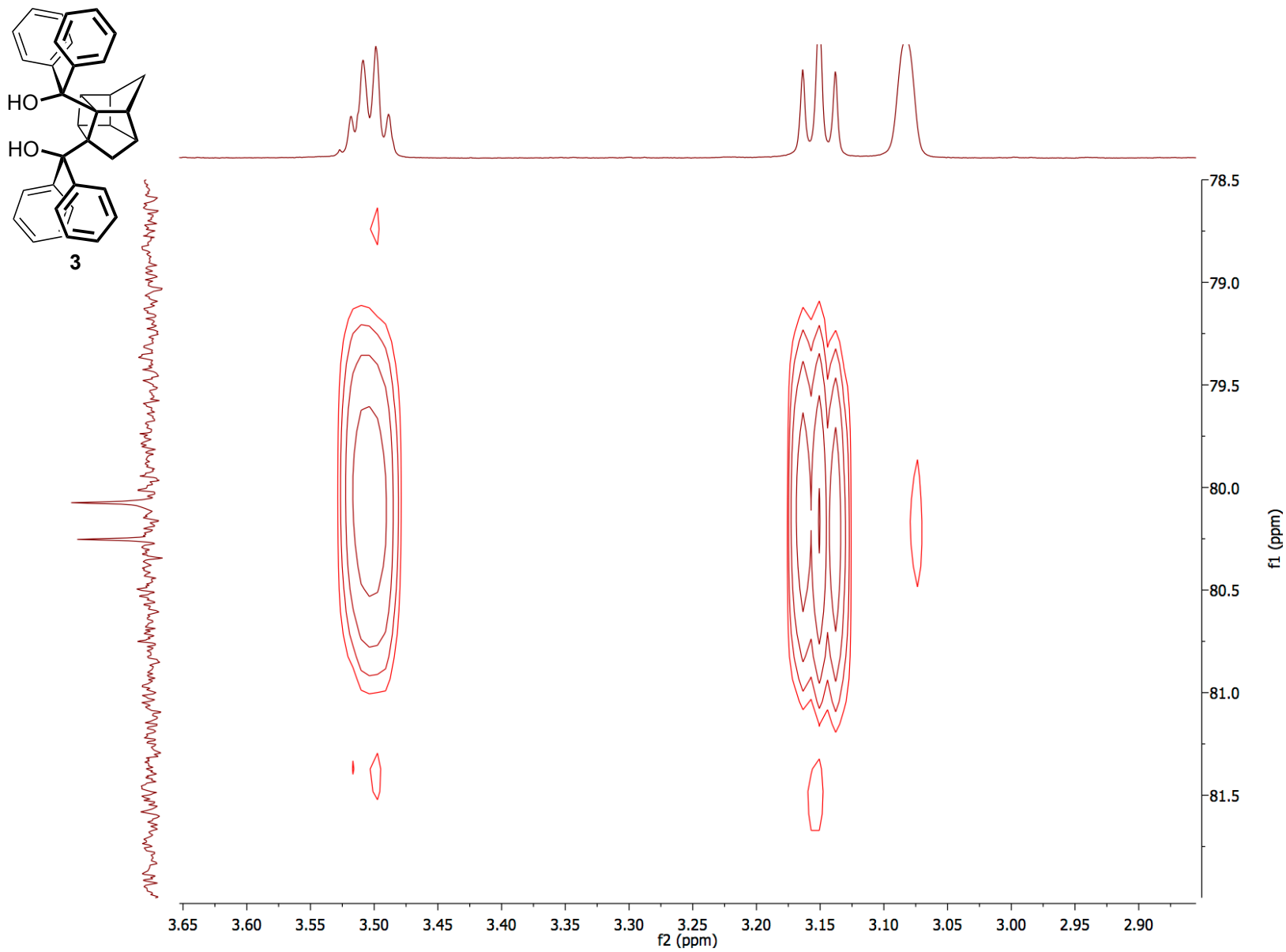

Figure S34. Gradient HMBC spectrum of compound **3** (500.27, 125.81 MHz, $CDCl_3$).

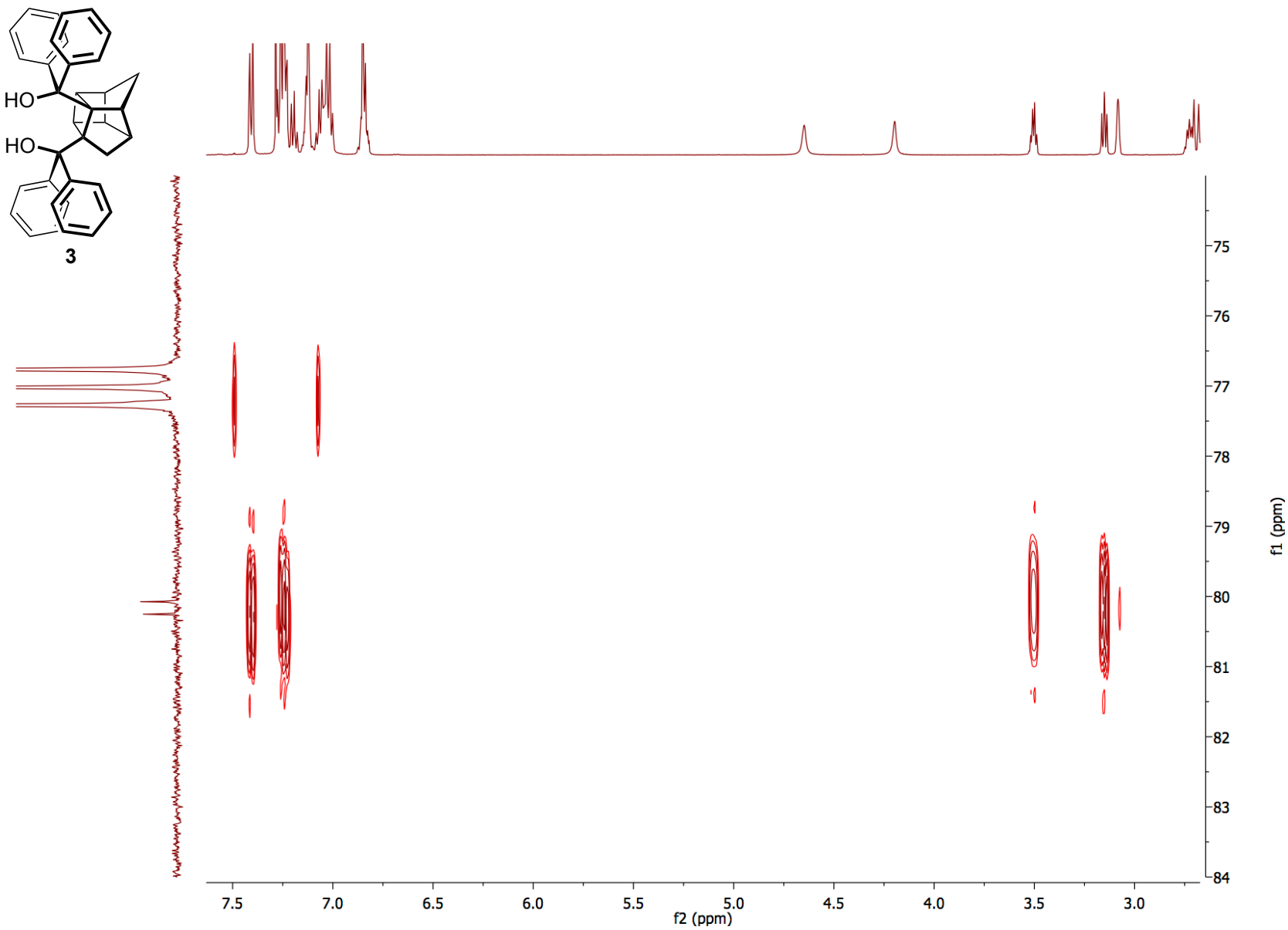

Figure S35. Gradient HMBC spectrum of compound **3** (500.27, 125.81 MHz, $CDCl_3$).

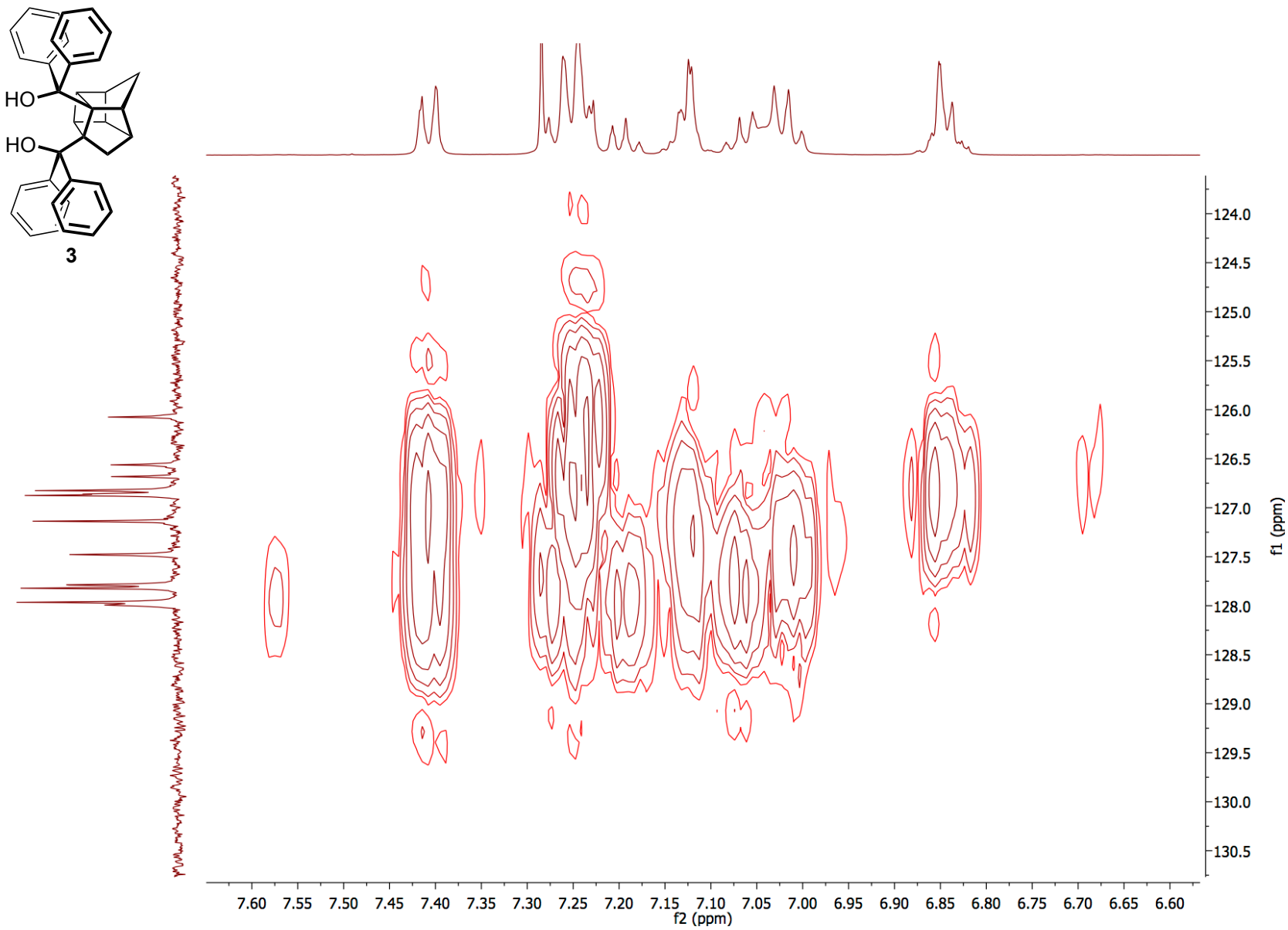

Figure S36. Gradient HMBC spectrum of compound **3** (500.27, 125.81 MHz, $CDCl_3$).

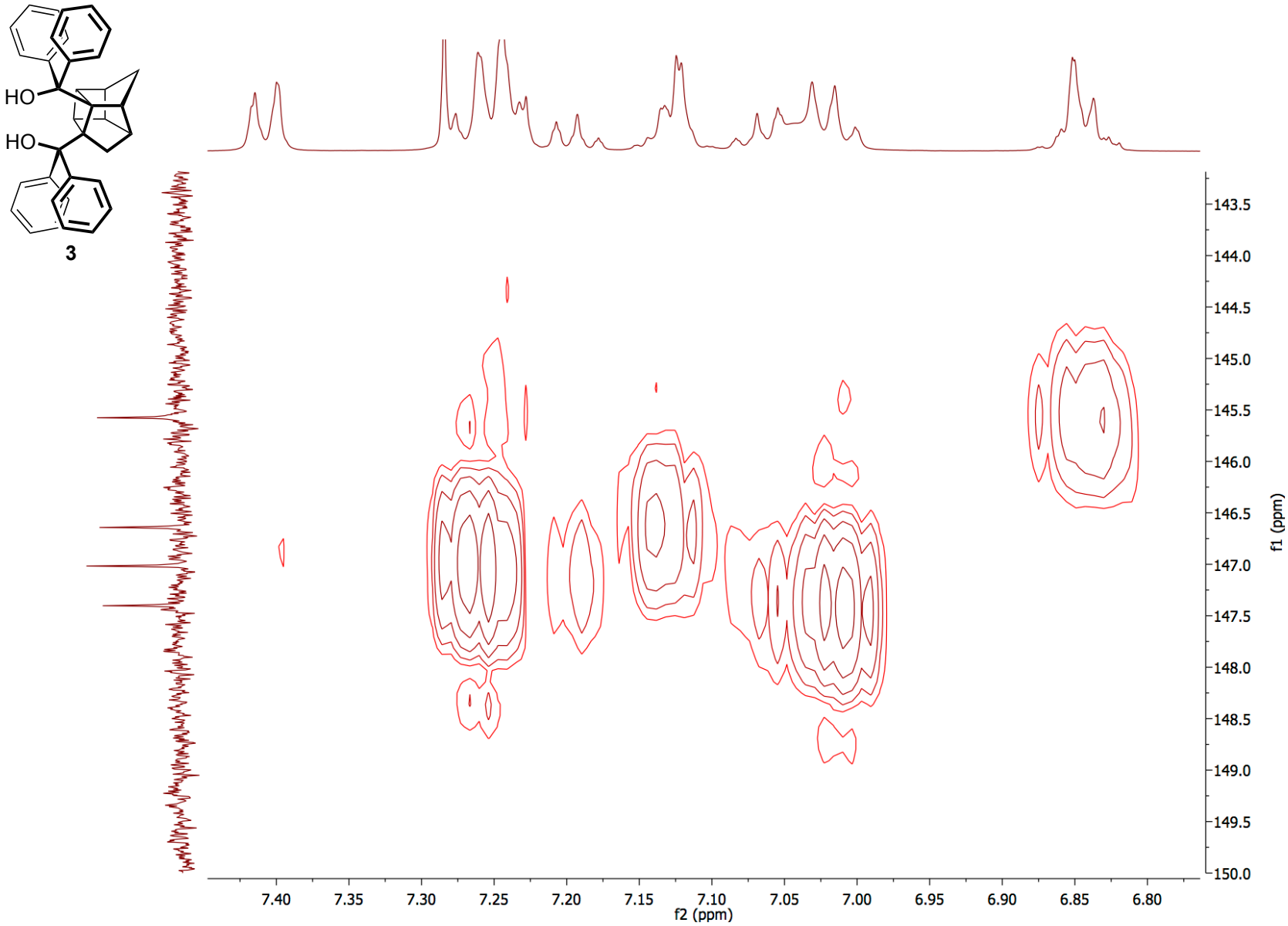

Figure S37. Gradient HMBC spectrum of compound **3** (500.27, 125.81 MHz, $CDCl_3$).

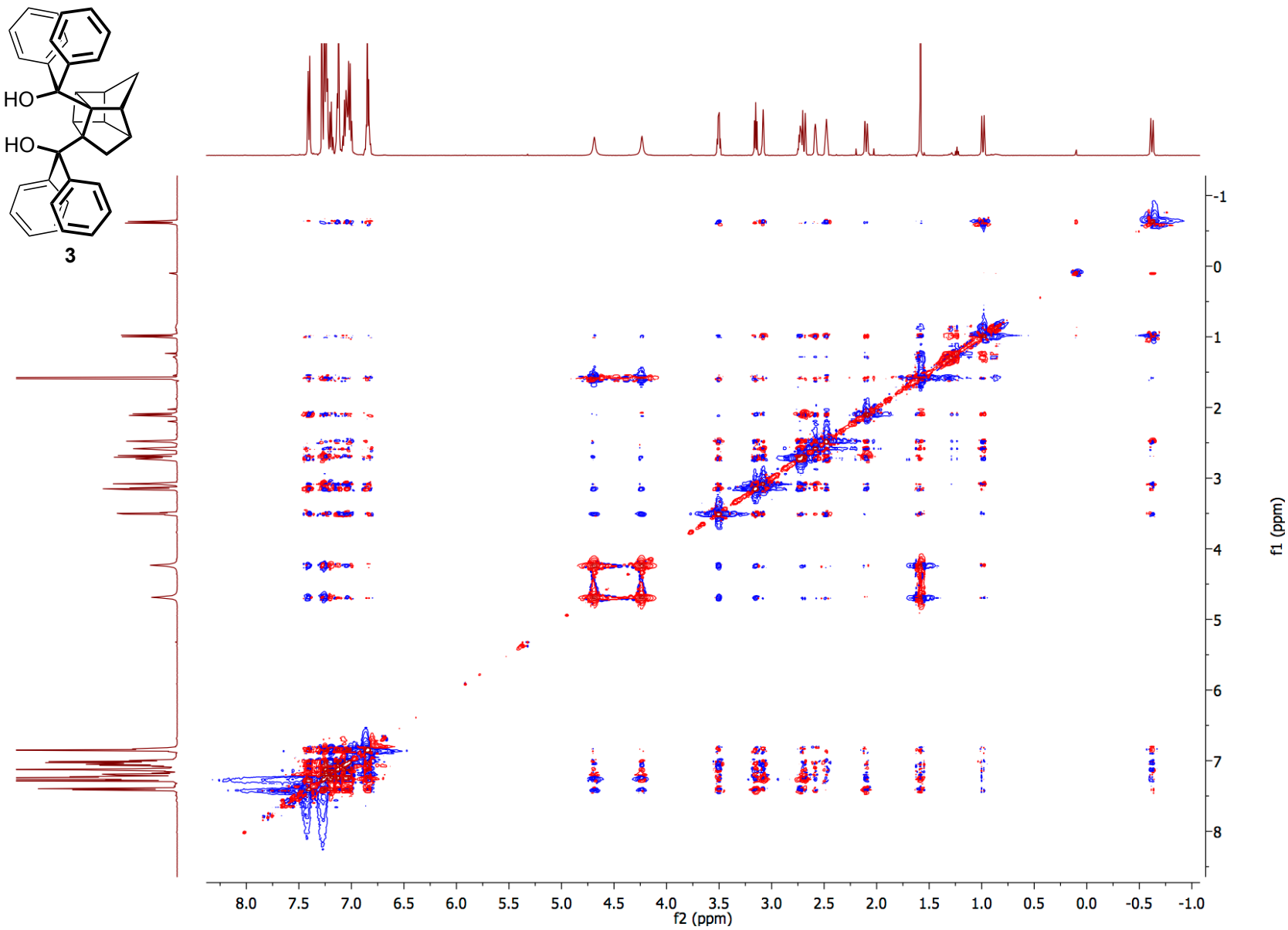

Figure S38. Gradient NOESY spectrum of compound **3** (500.27 MHz, $CDCl_3$).

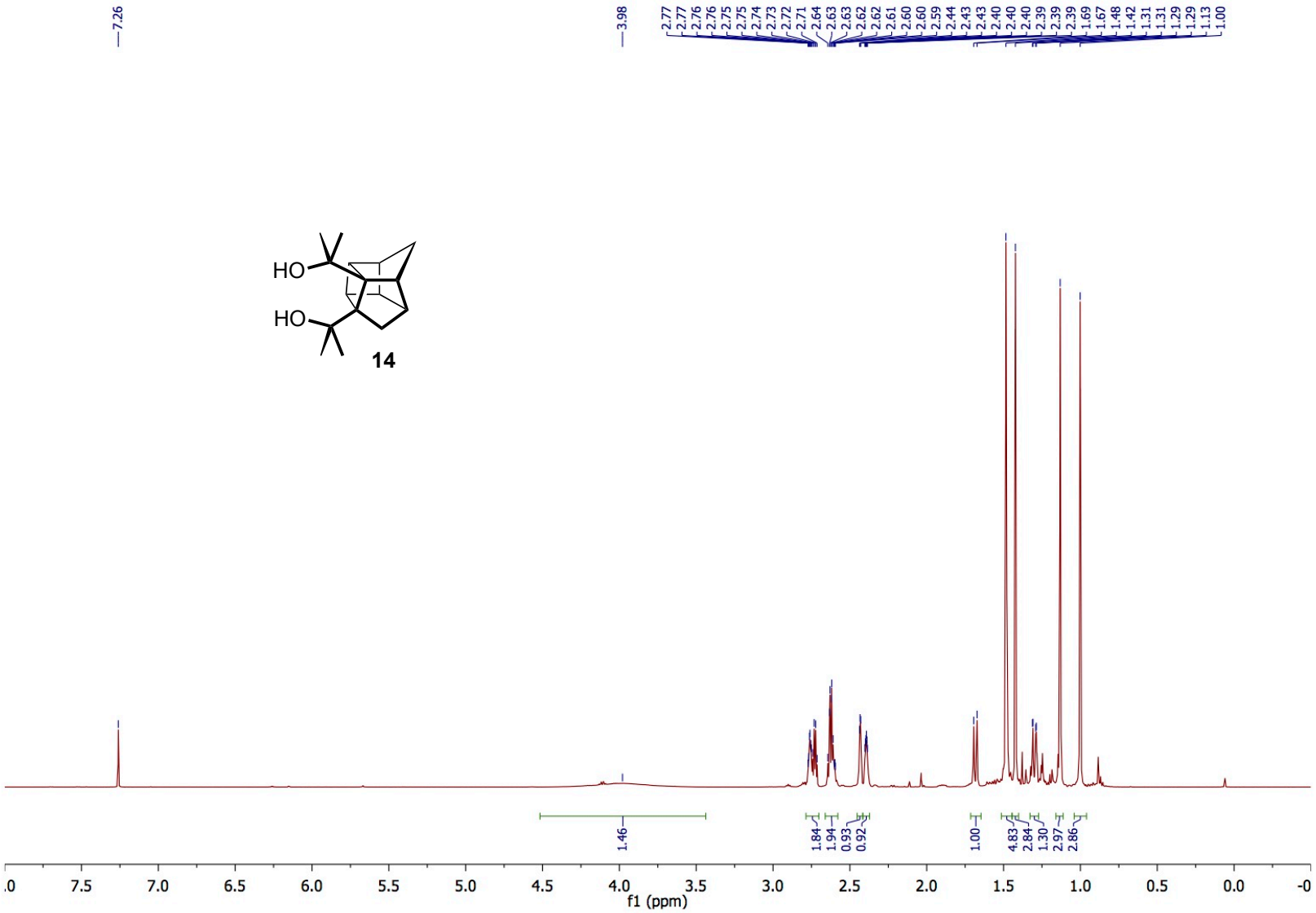

Figure S39. ^{1}H NMR of compound **14** (500.27 MHz, $CDCl_3$).

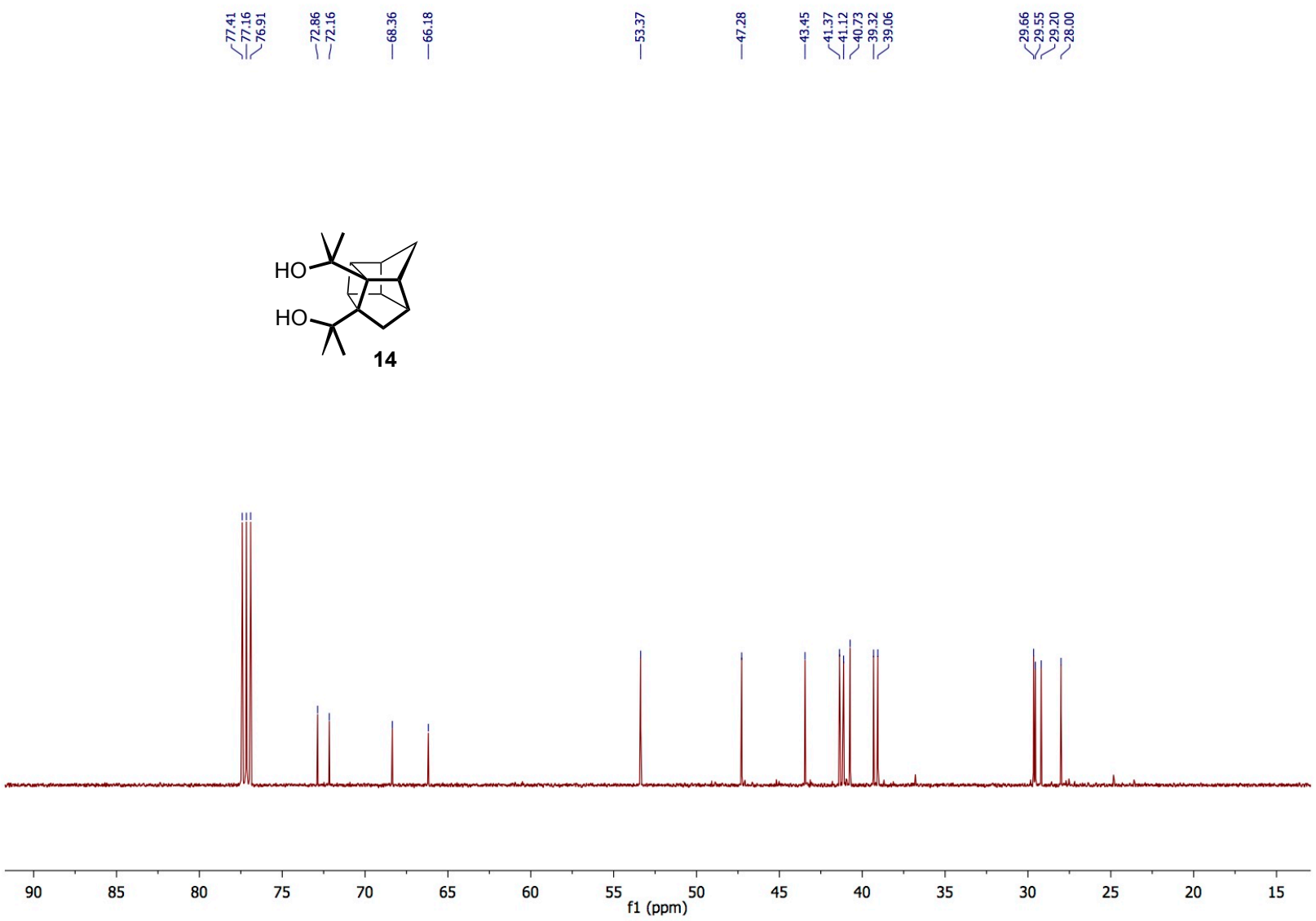

Figure S40. ^{13}C NMR of compound **14** (125.81 MHz, $CDCl_3$).

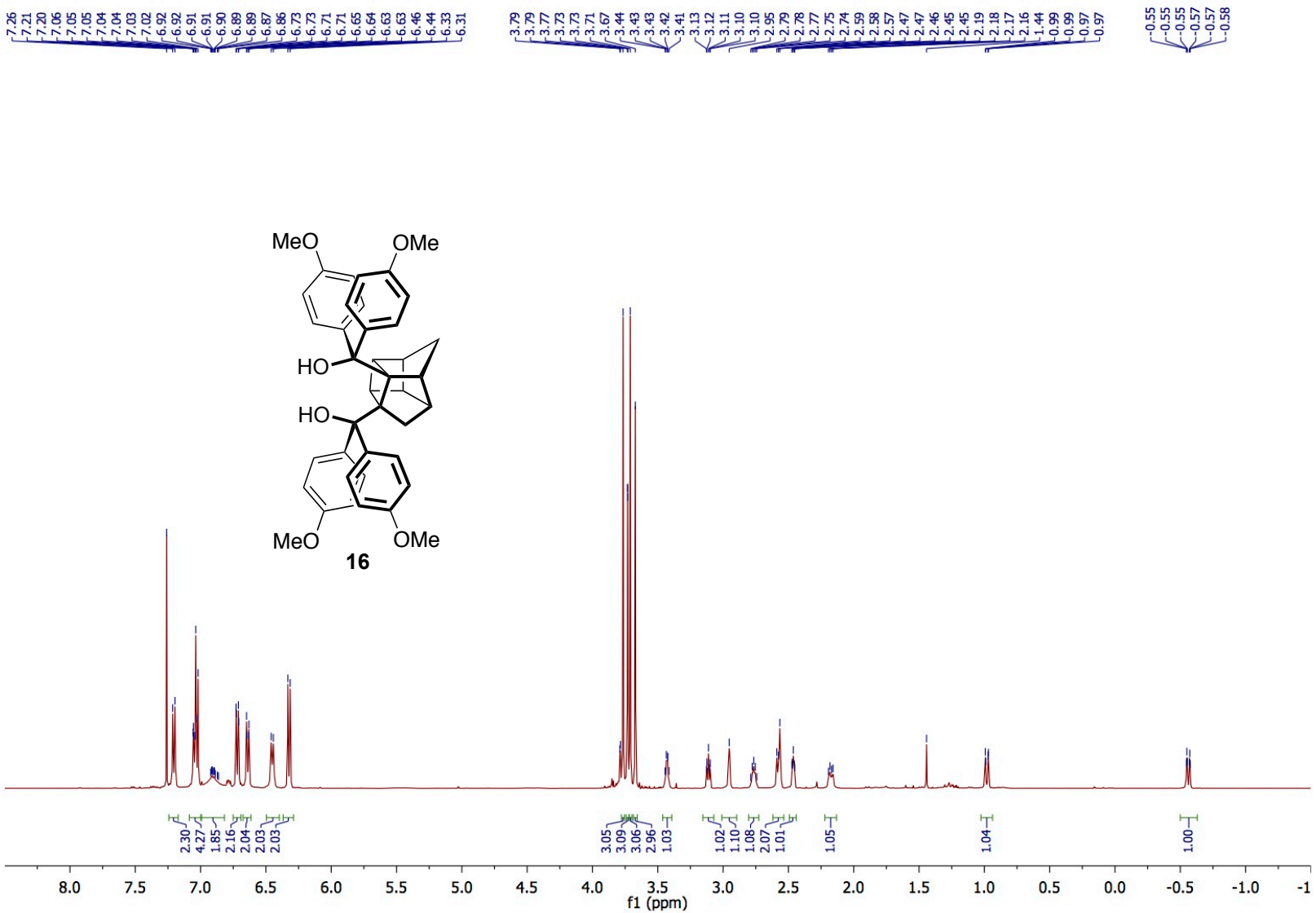

Figure S41. ^{1}H NMR of compound **16** (500.27 MHz, $CDCl_3$).

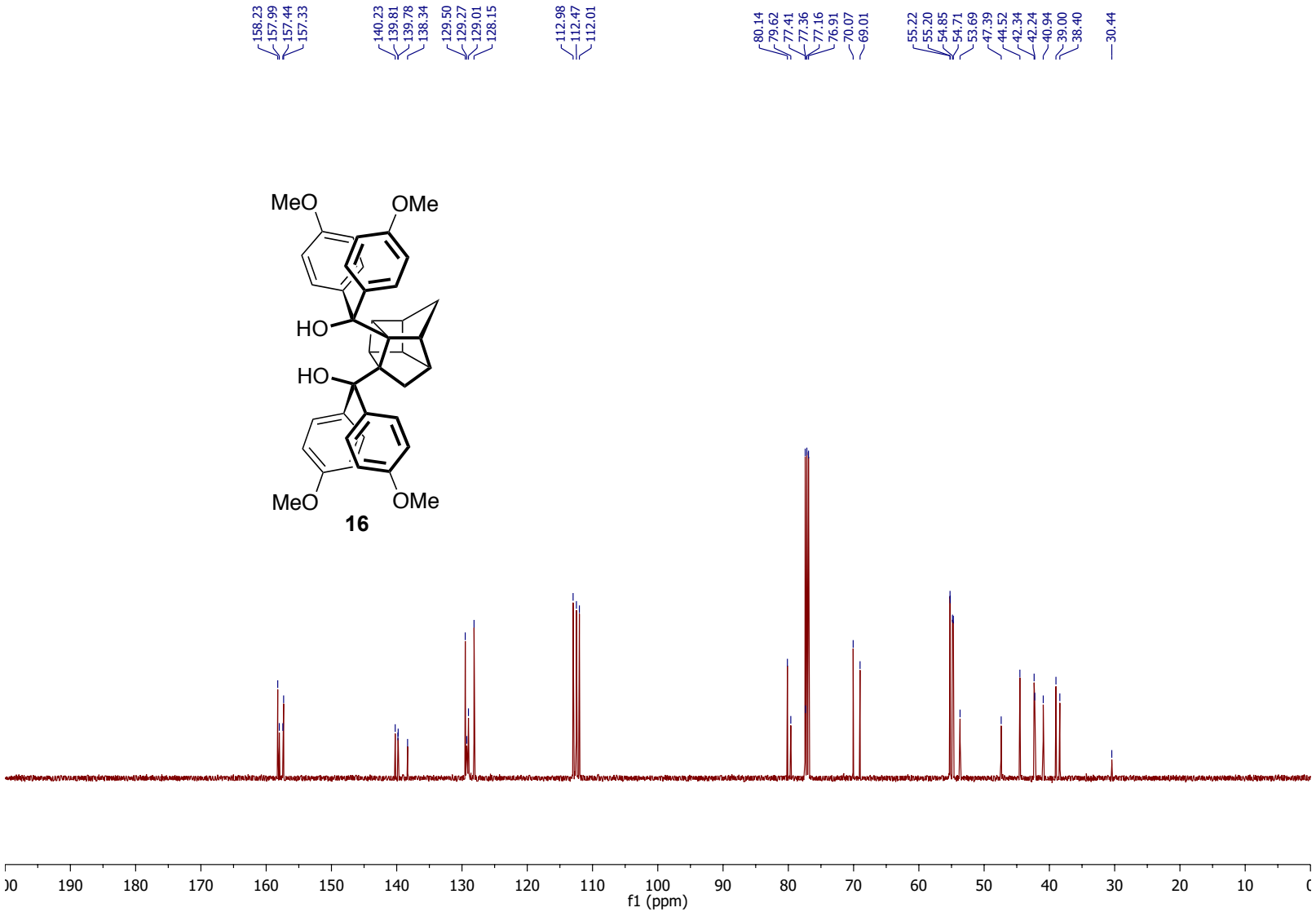

Figure S42. ^{13}C NMR of compound **16** (125.81 MHz, $CDCl_3$).

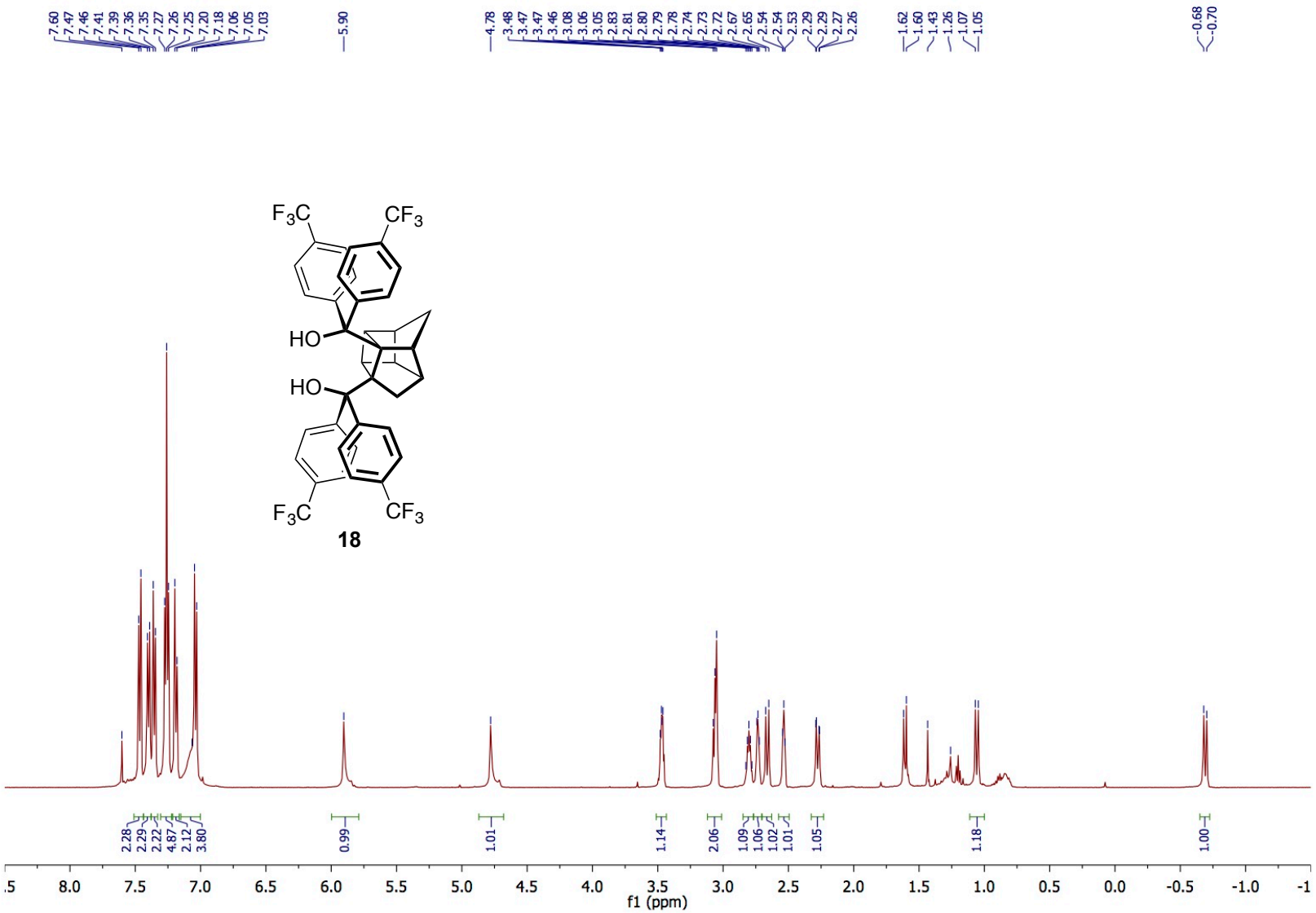

Figure S43. ^{1}H NMR of compound **18** (500.27 MHz, $CDCl_3$).

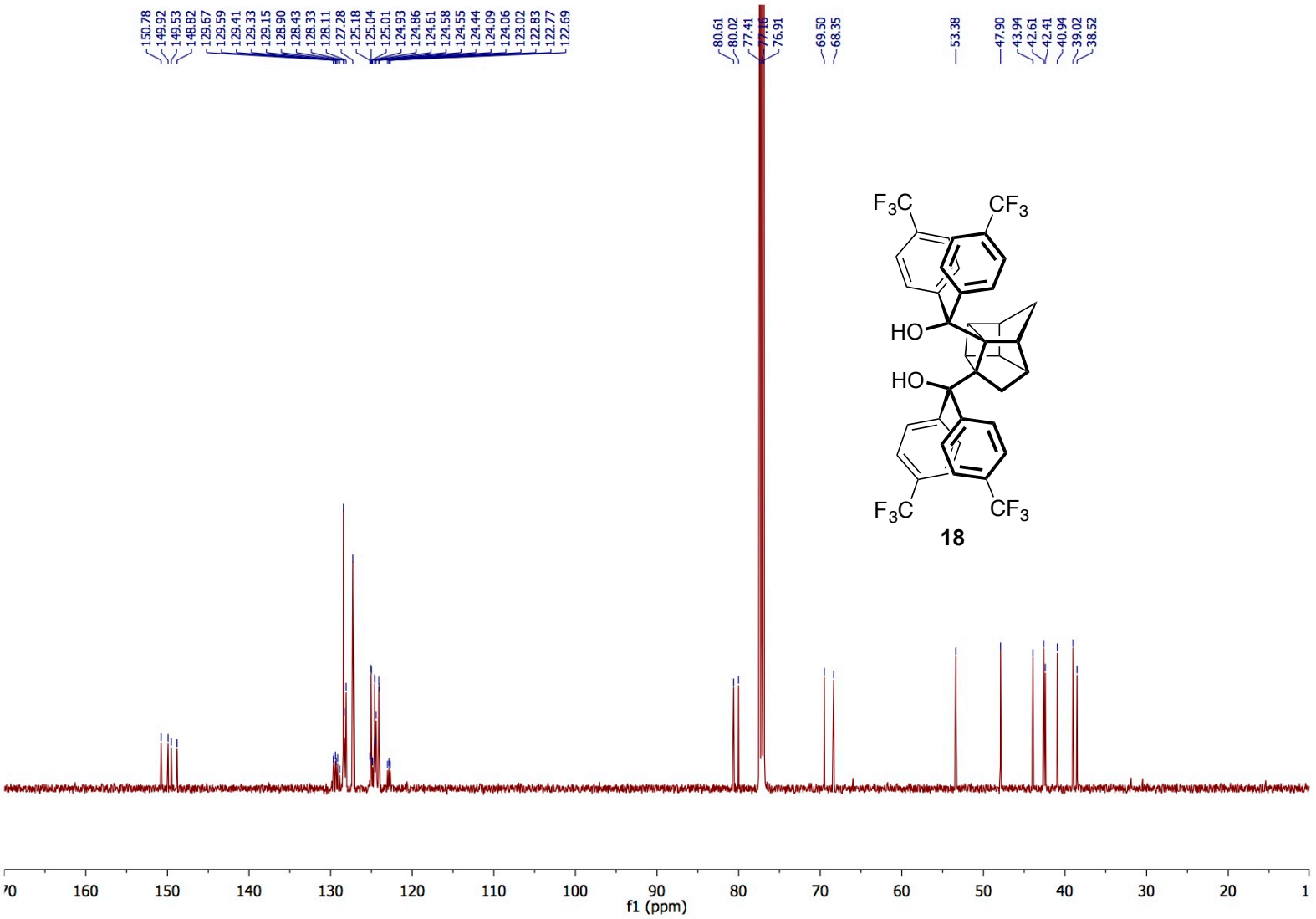

Figure S44. ^{13}C NMR of compound **18** (125.81 MHz, $CDCl_3$).

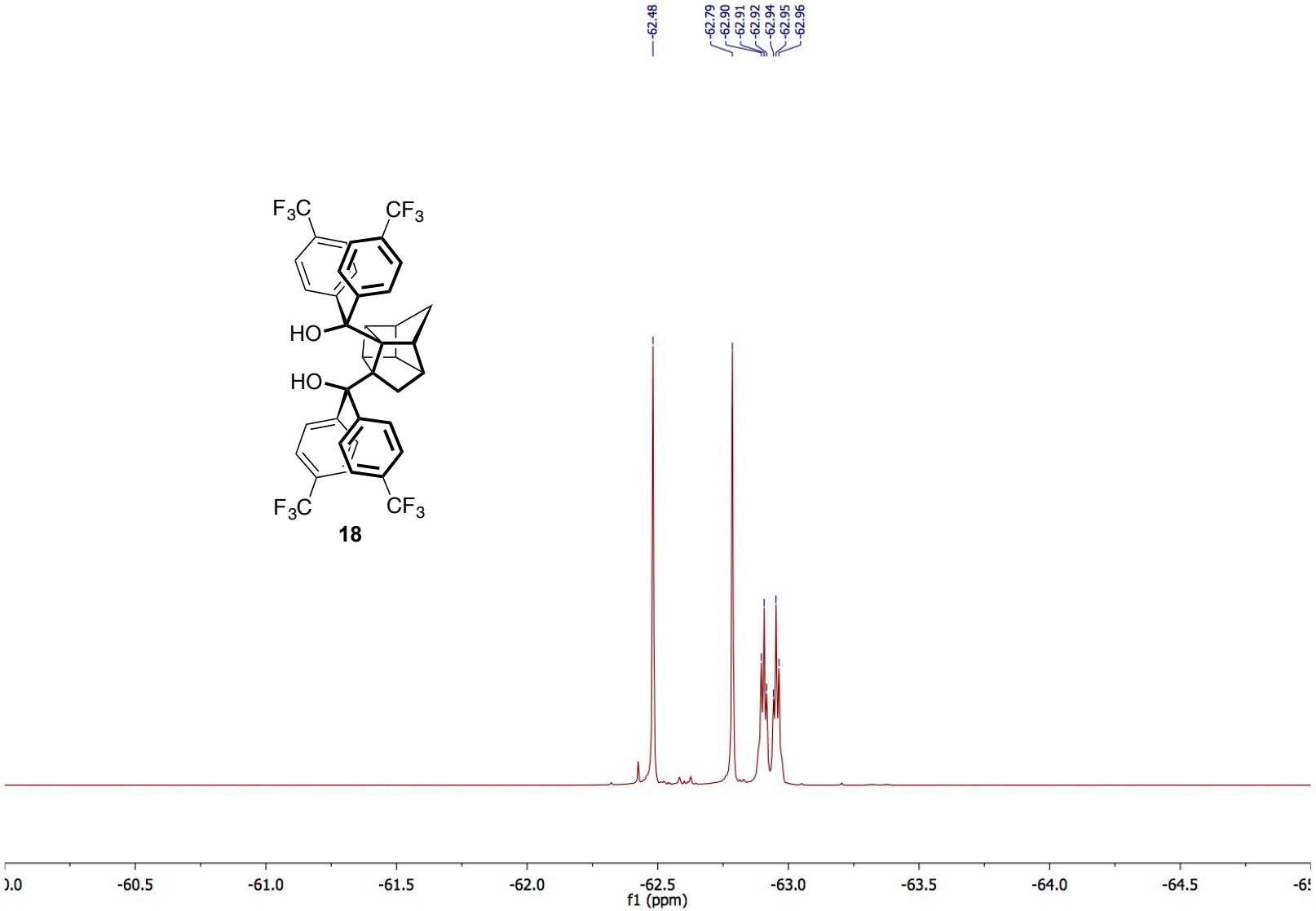

Figure S45. ^{19}F NMR of compound **18** (470.68 MHz, $CDCl_3$).

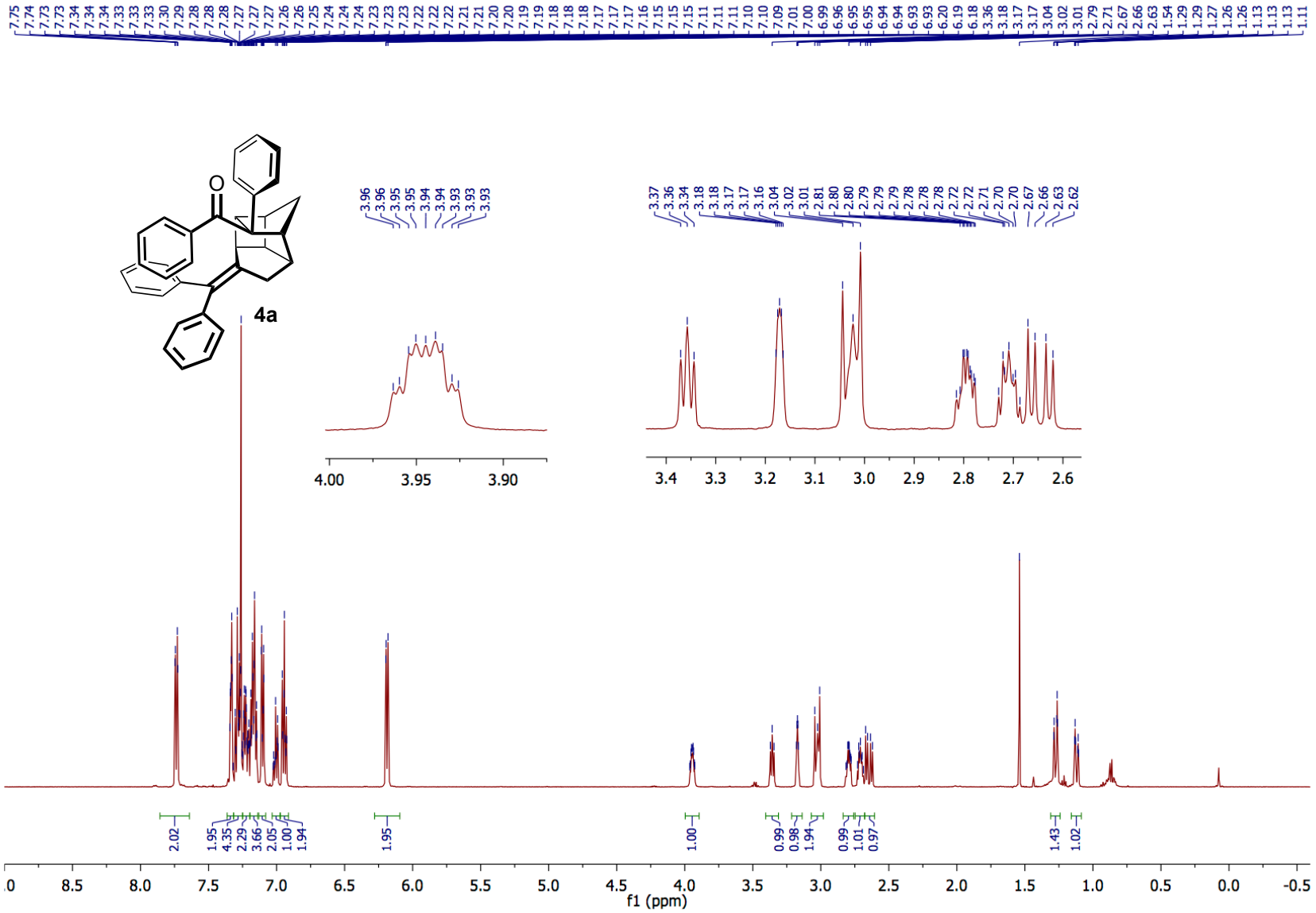

Figure S46. ^{1}H NMR of compound **4a** (500.27 MHz, $CDCl_3$).

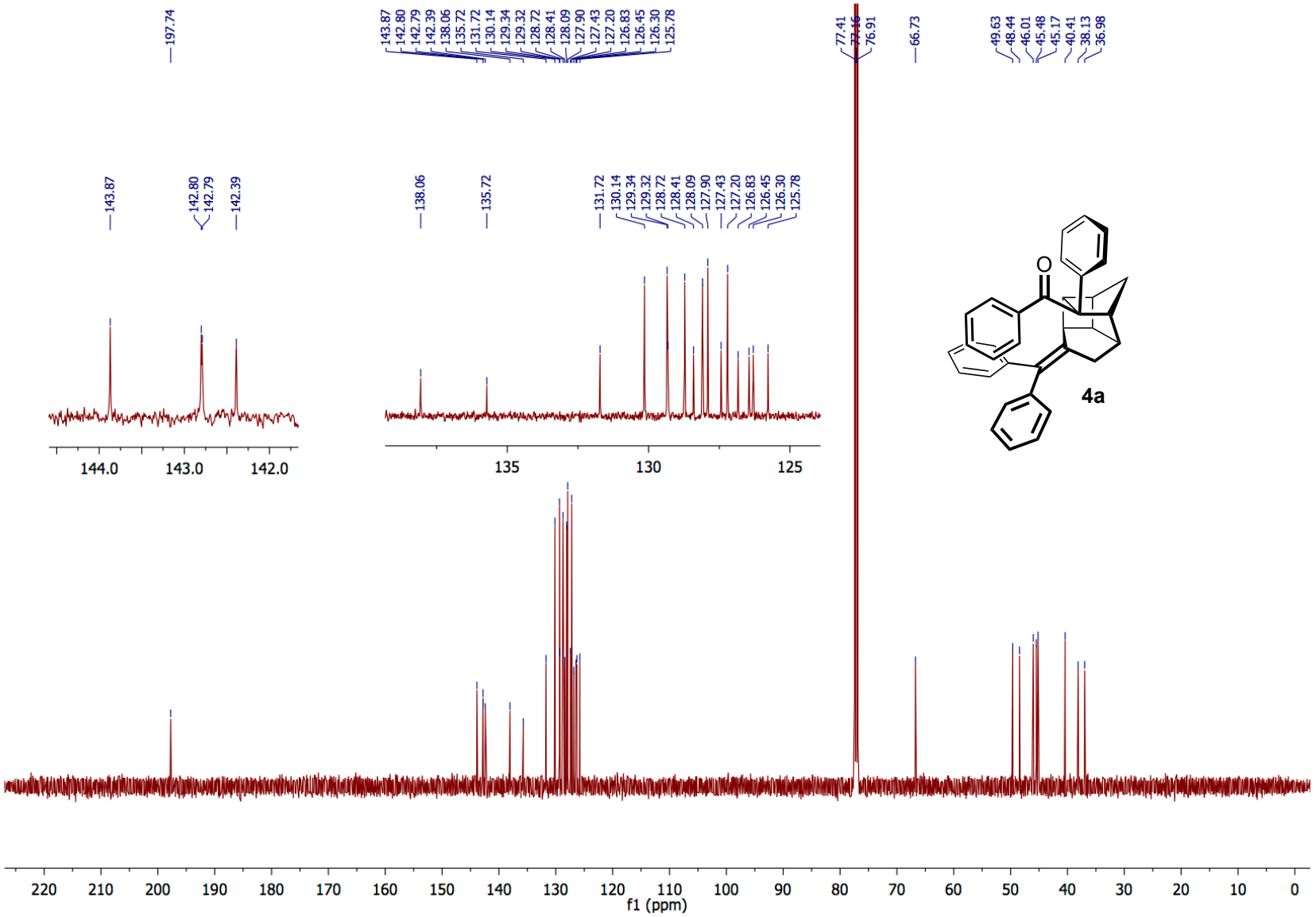

Figure S47. ^{13}C NMR of compound **4a** (125.81 MHz, $CDCl_3$).

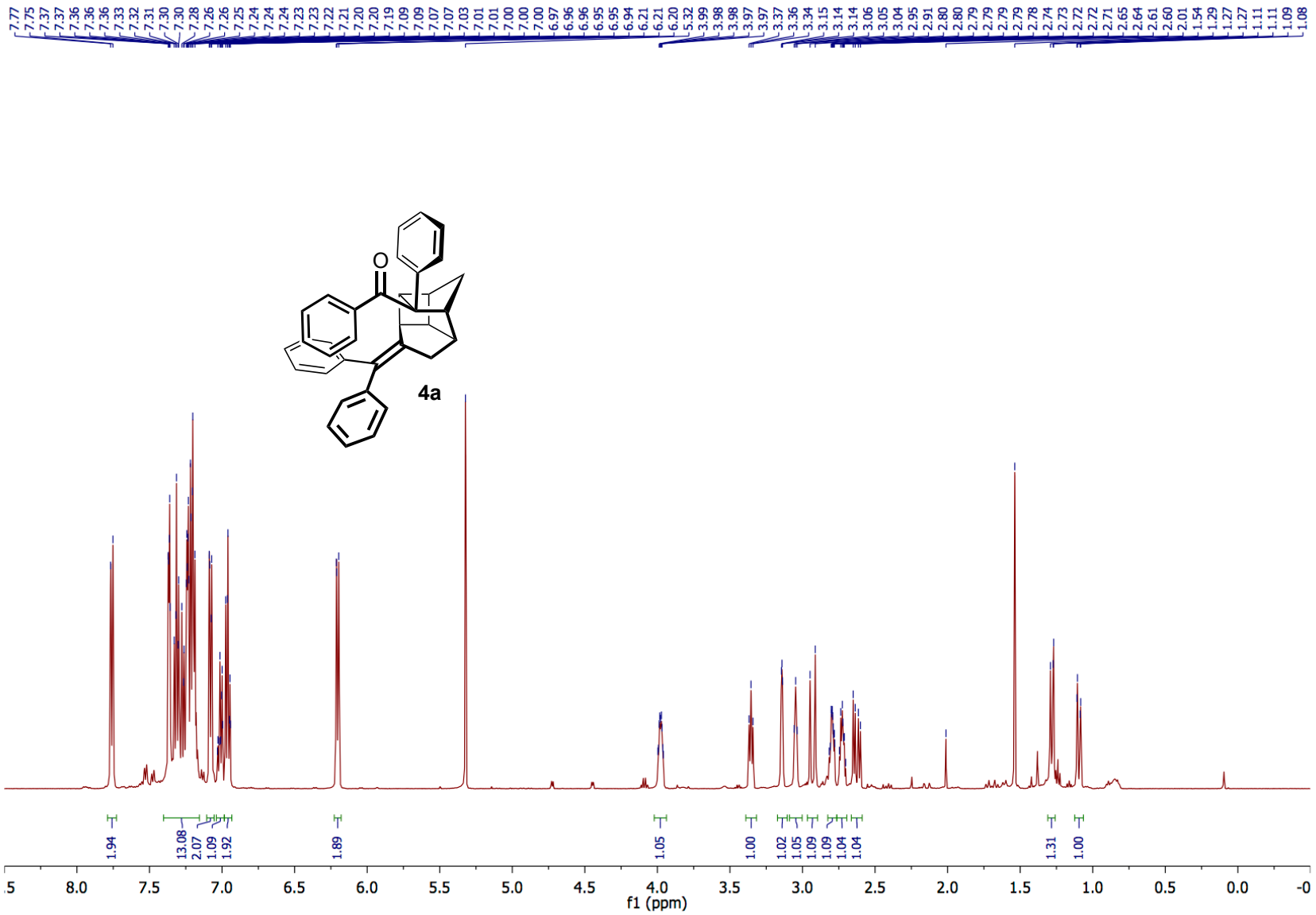

Figure S48. ^{1}H NMR of compound **4a** (500.27 MHz, CD_2Cl_2).

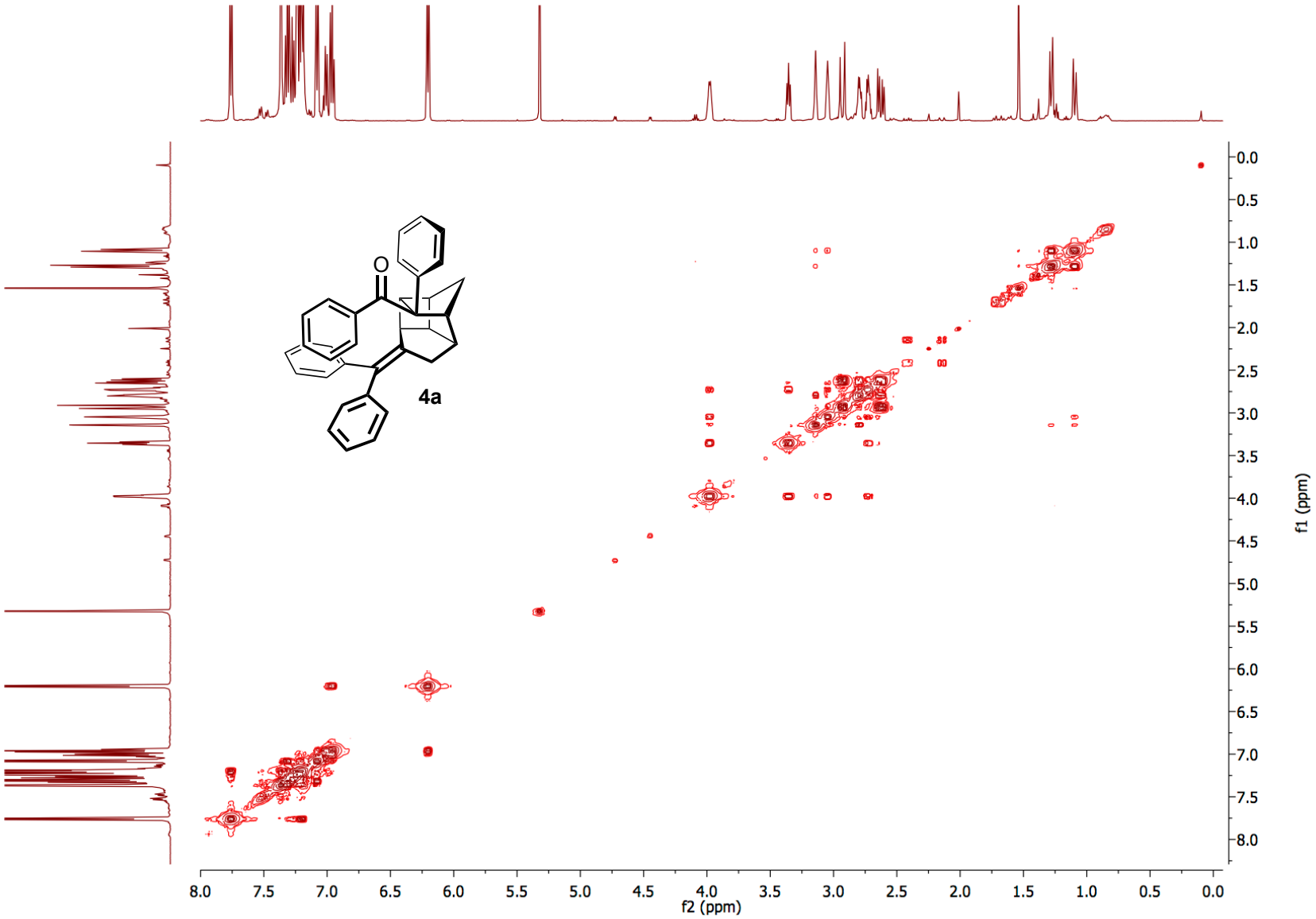

Figure S49. Gradient COSY spectrum of compound **4a** (500.27 MHz, CD_2Cl_2).

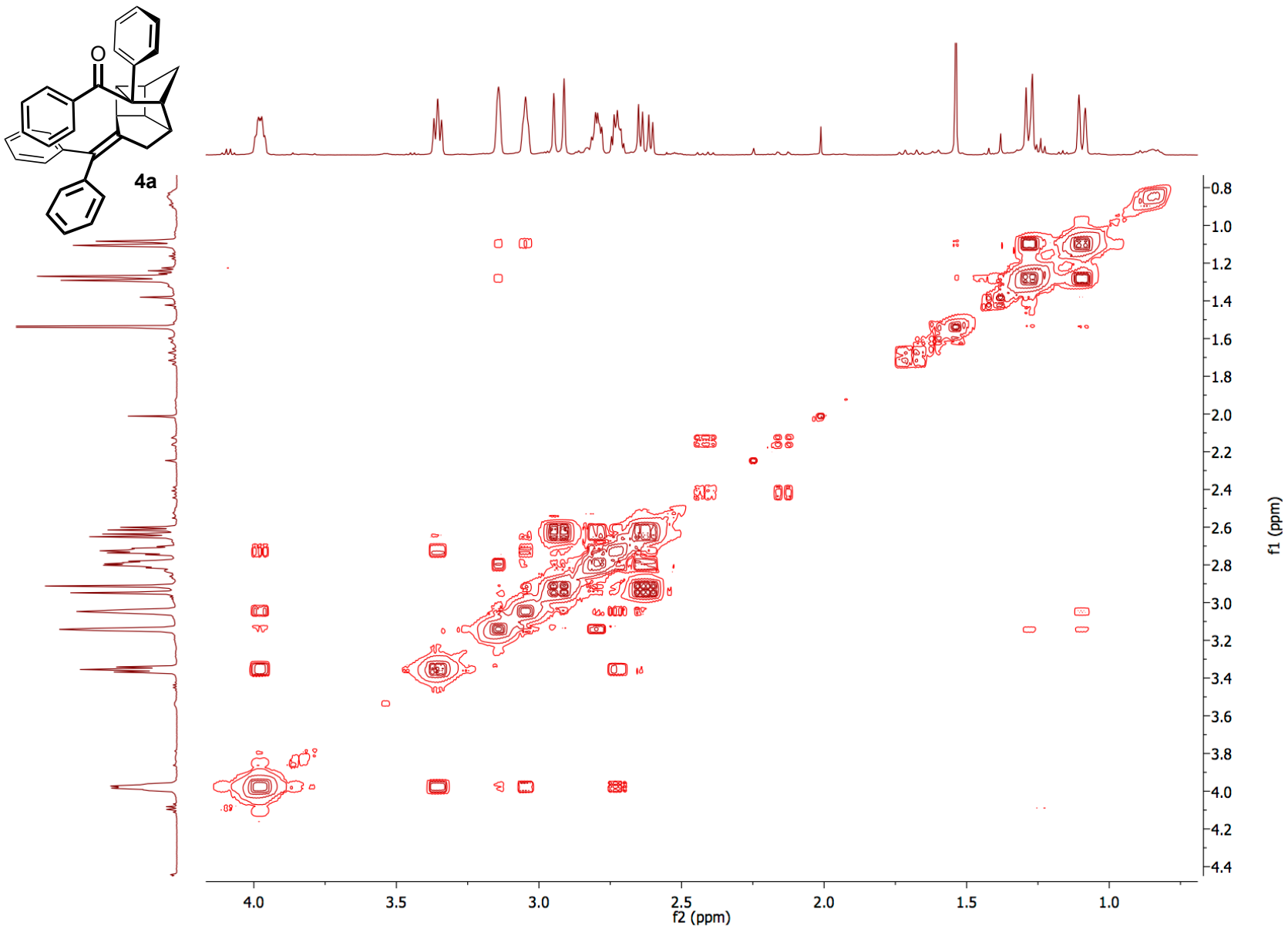

Figure S50. Gradient COSY spectrum of compound **4a** (500.27 MHz, CD_2Cl_2).

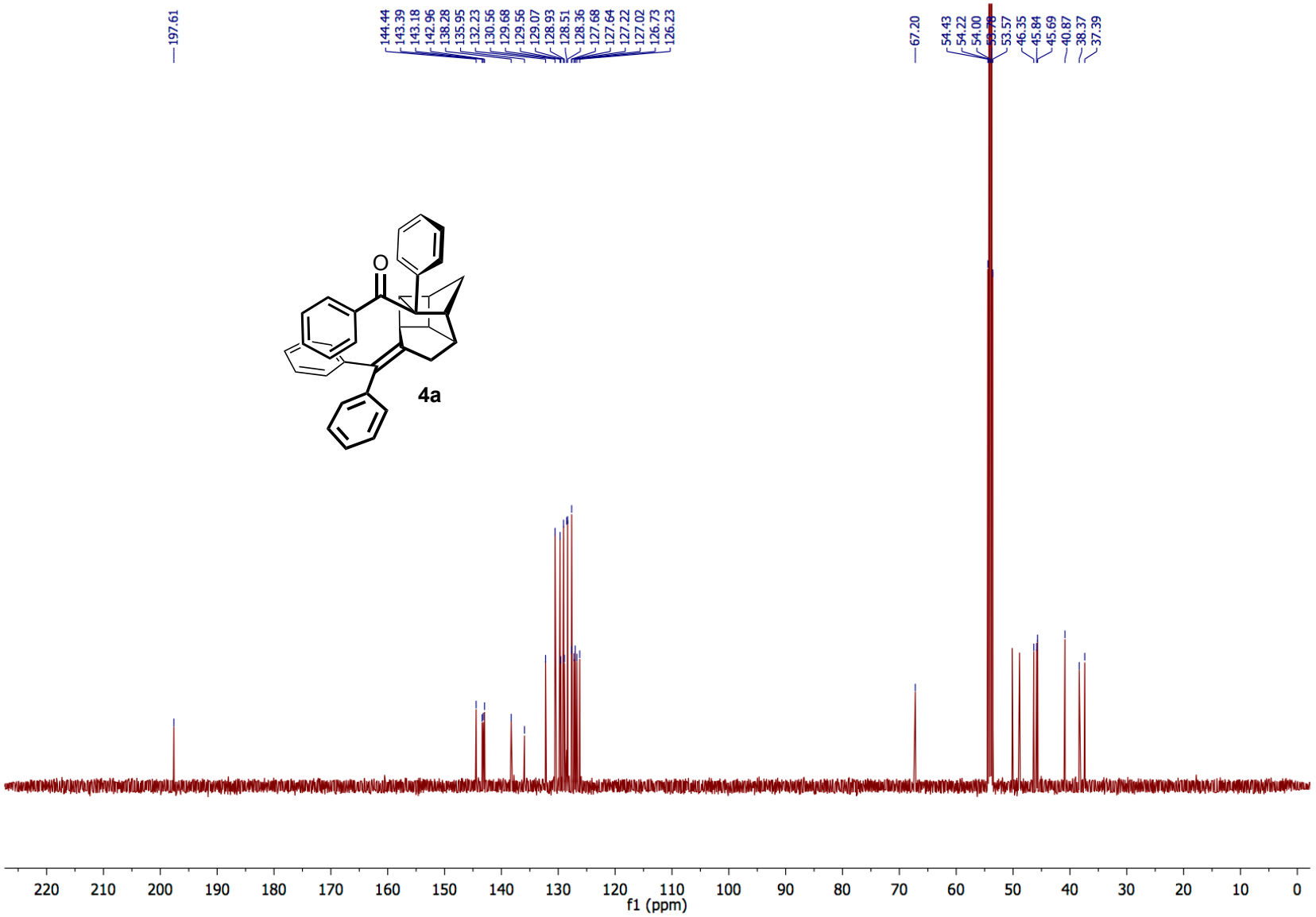

Figure S51. ^{13}C NMR of compound **4a** (125.81 MHz, CD_2Cl_2).

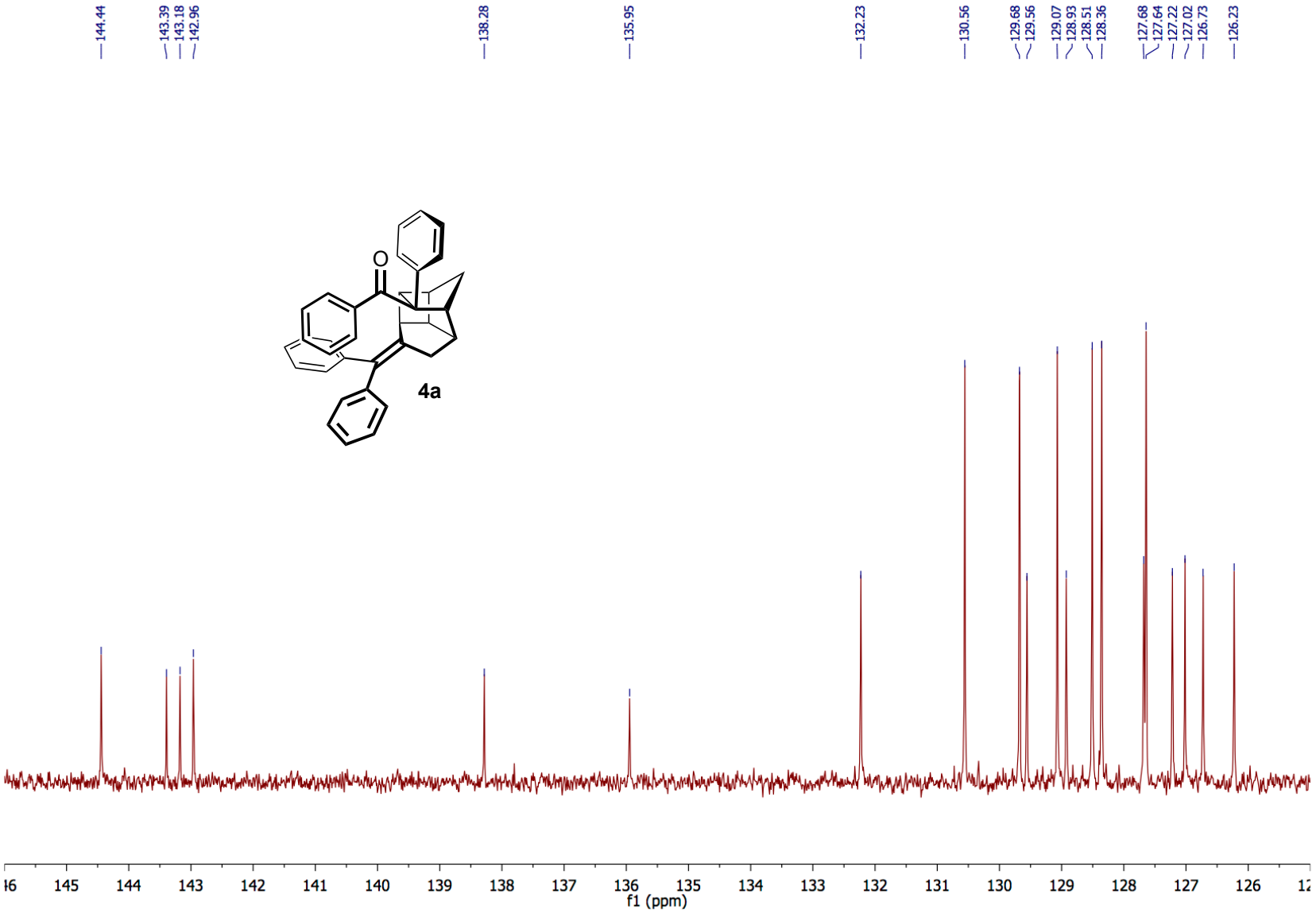

Figure S52. Downfield region of the ^{13}C NMR of compound **4a** (125.81 MHz, CD_2Cl_2).

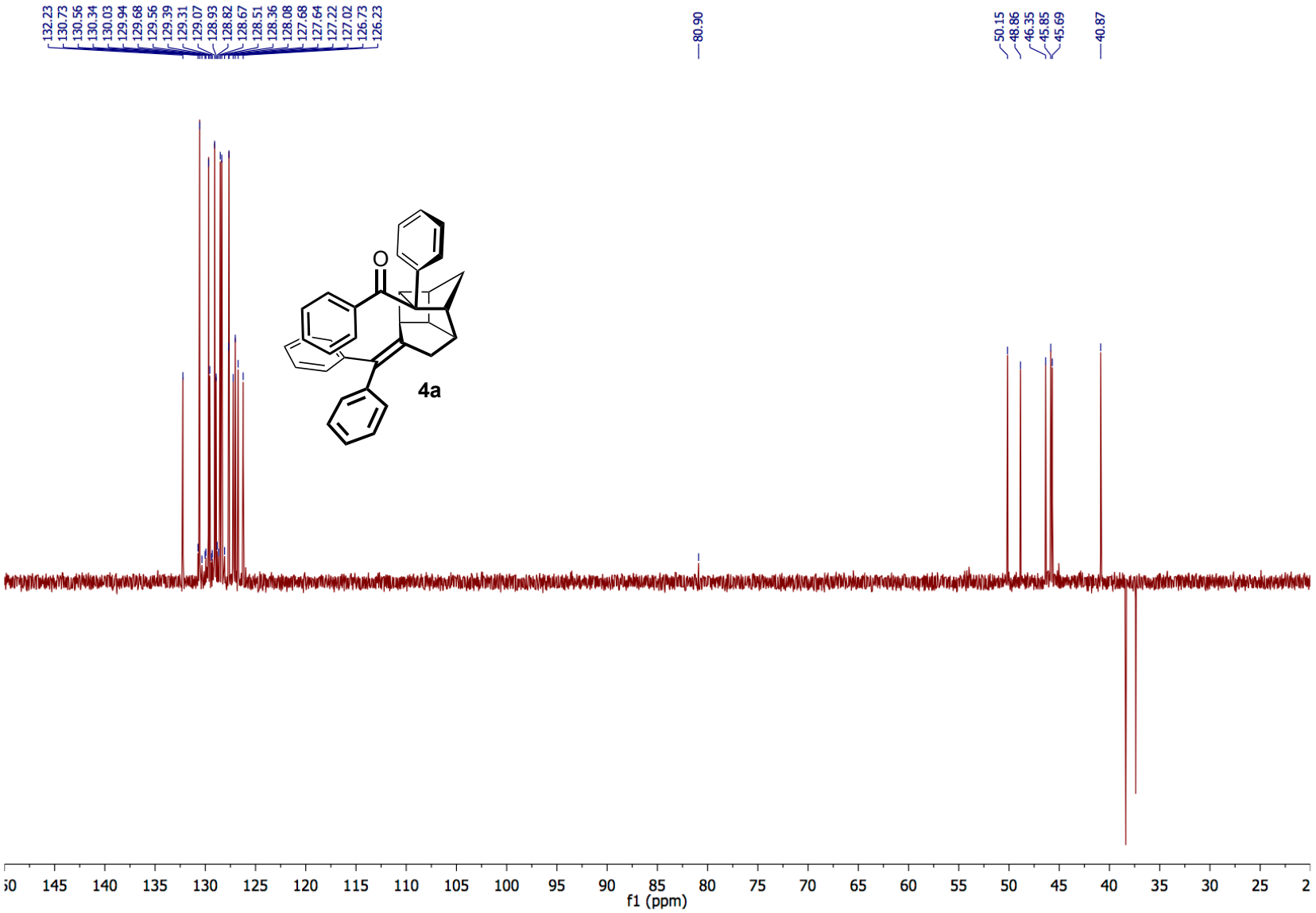

Figure S53. ^{13}C DEPT-135 spectrum of compound **4a** (125.81 MHz, CD_2Cl_2).

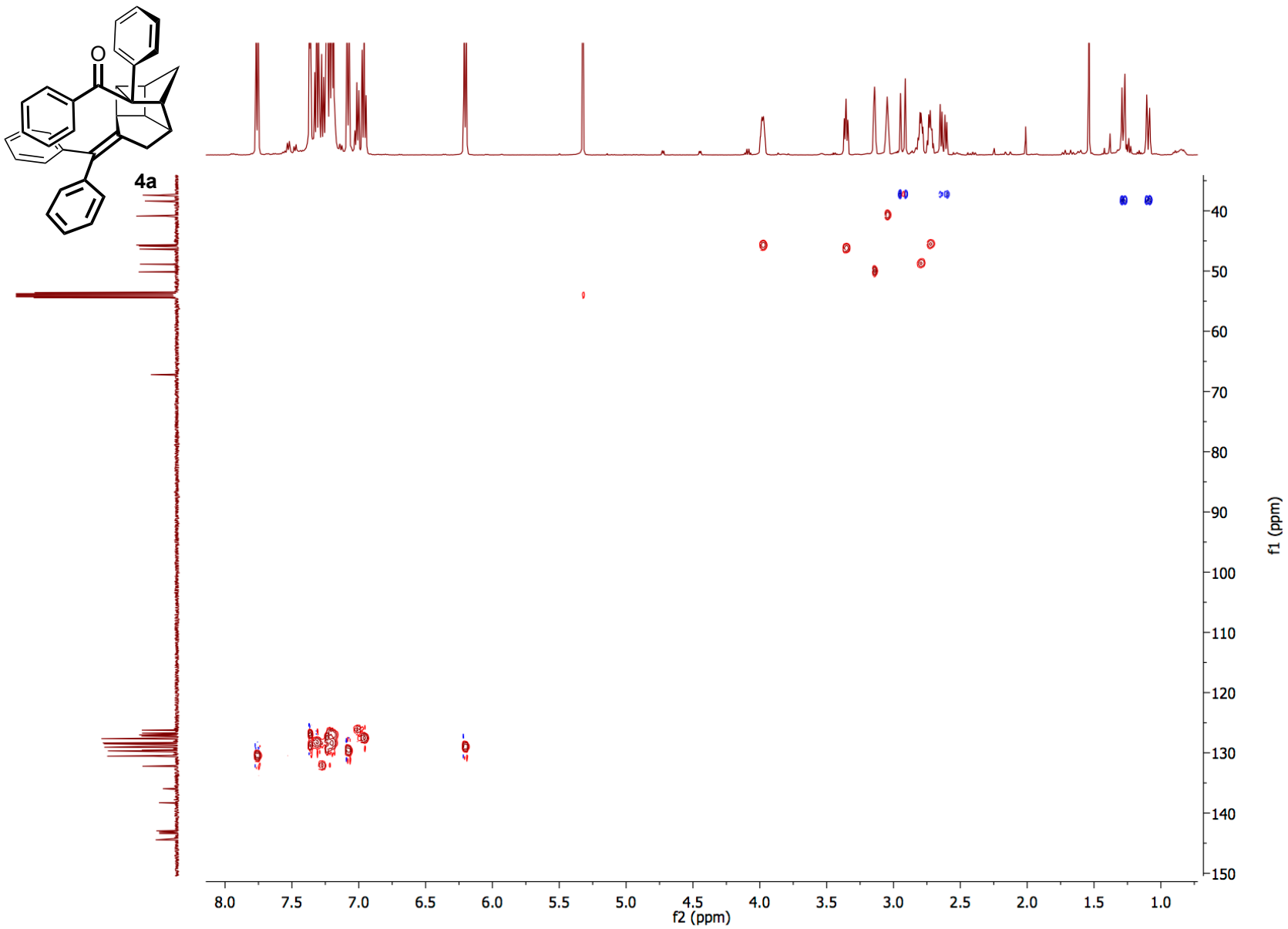

Figure S54. Gradient HSQC spectrum of compound **4a** (500.27, 125.81 MHz, CD_2Cl_2).

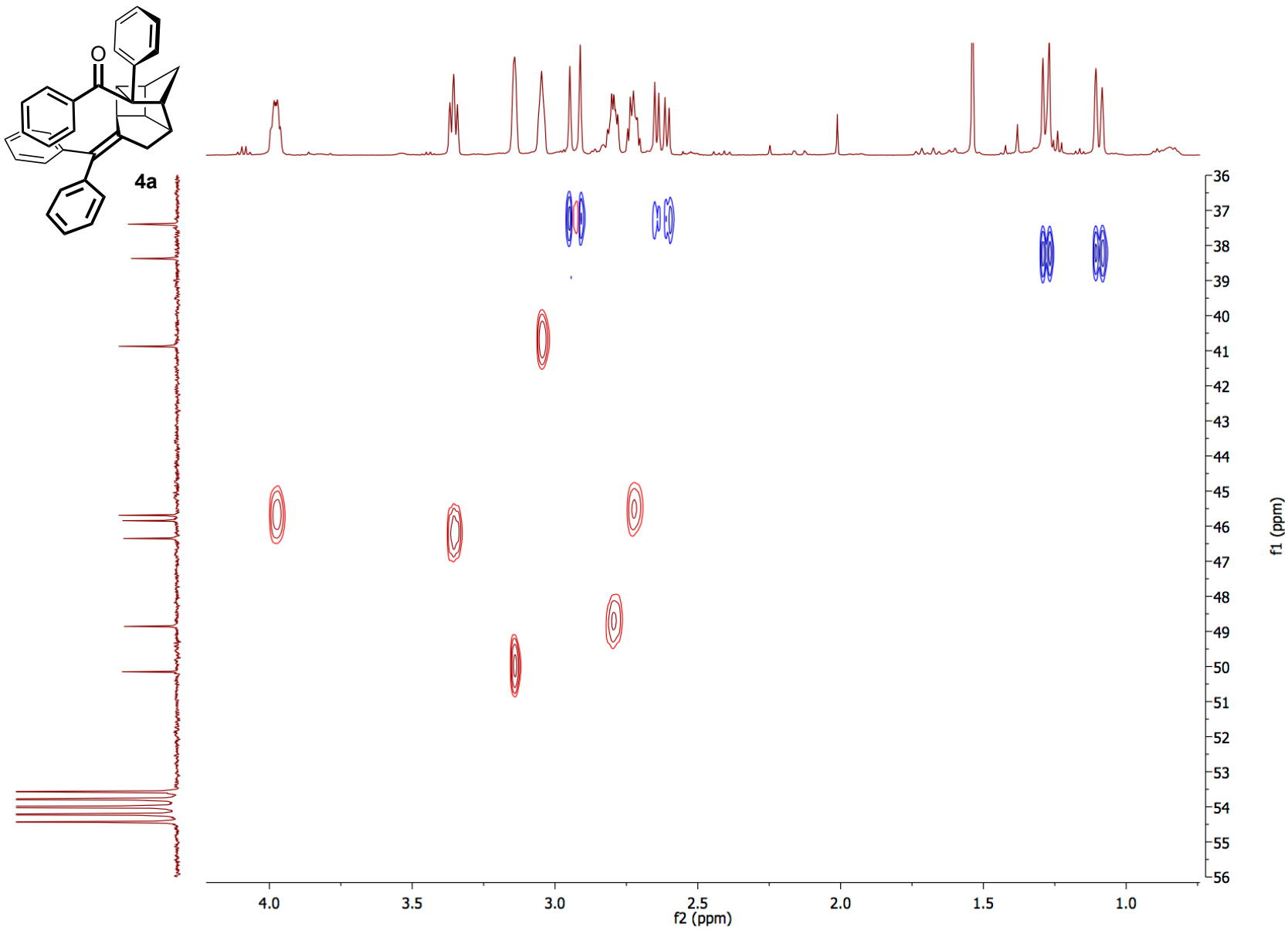

Figure S55. Gradient HSQC spectrum of compound **4a** (500.27, 125.81 MHz, CD_2Cl_2).

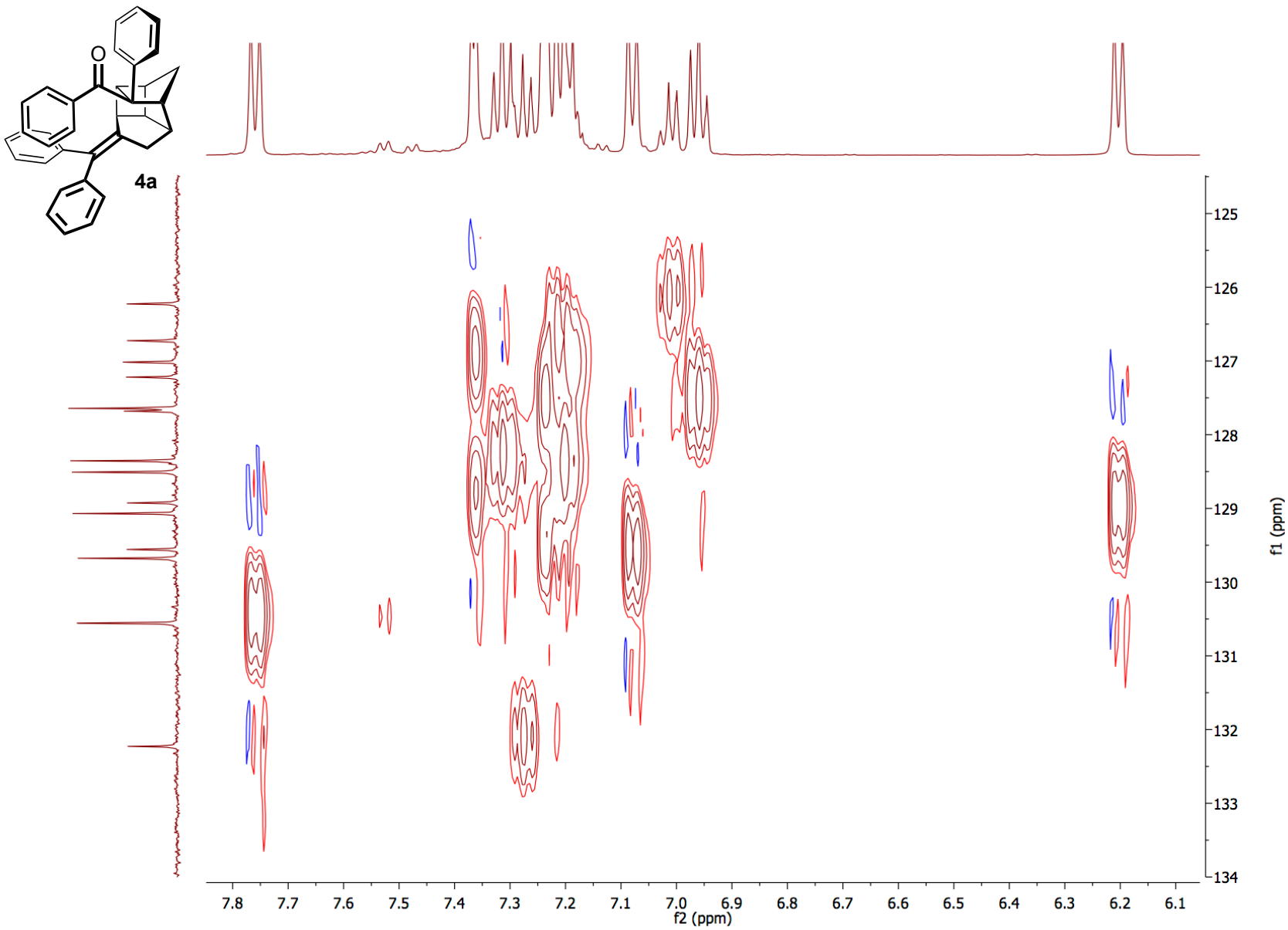

Figure S56. Gradient HSQC spectrum of compound **4a** (500.27, 125.81 MHz, CD_2Cl_2).

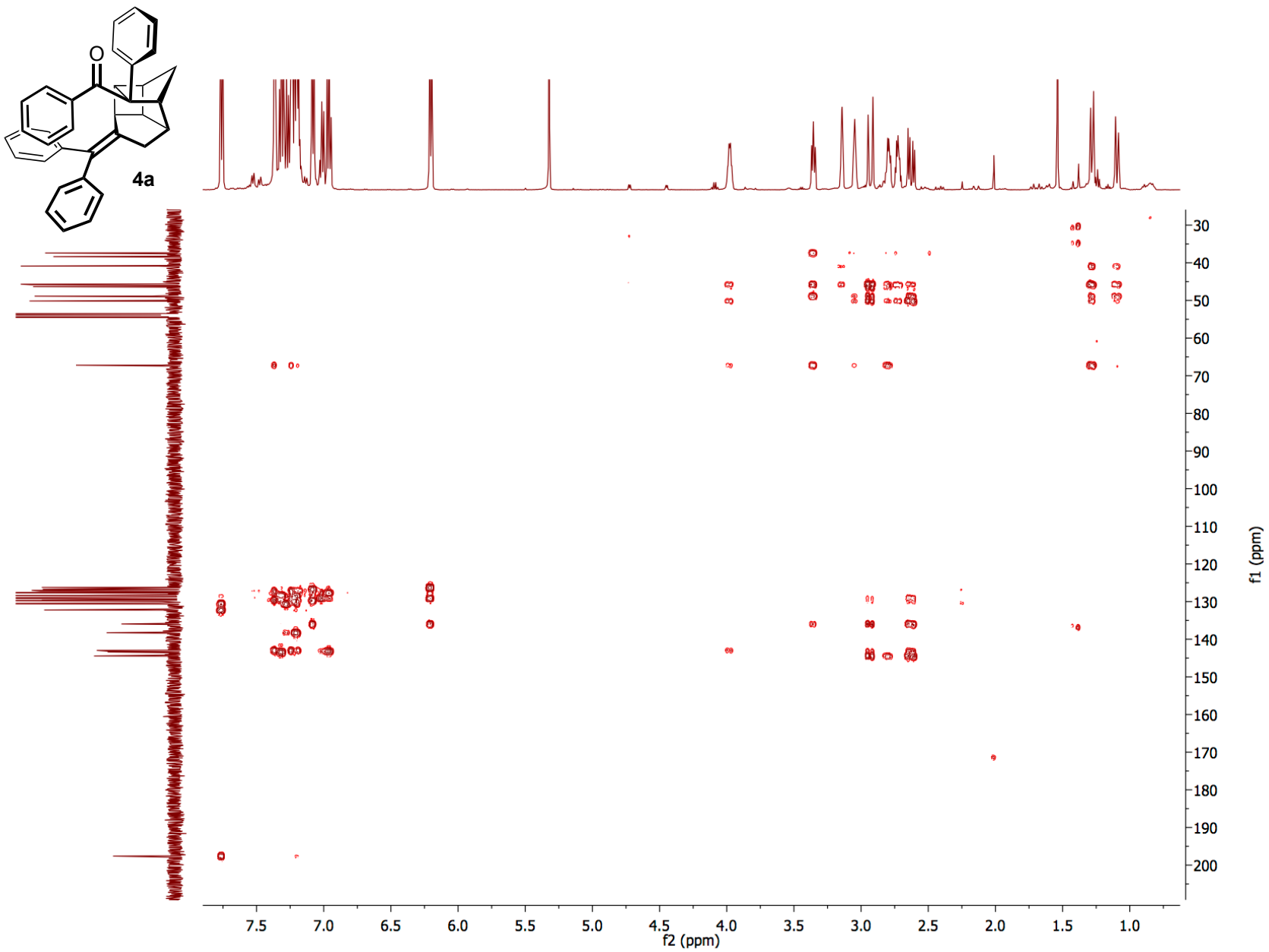

Figure S57. Gradient HMBC spectrum of compound **4a** (500.27, 125.81 MHz, CD_2Cl_2).

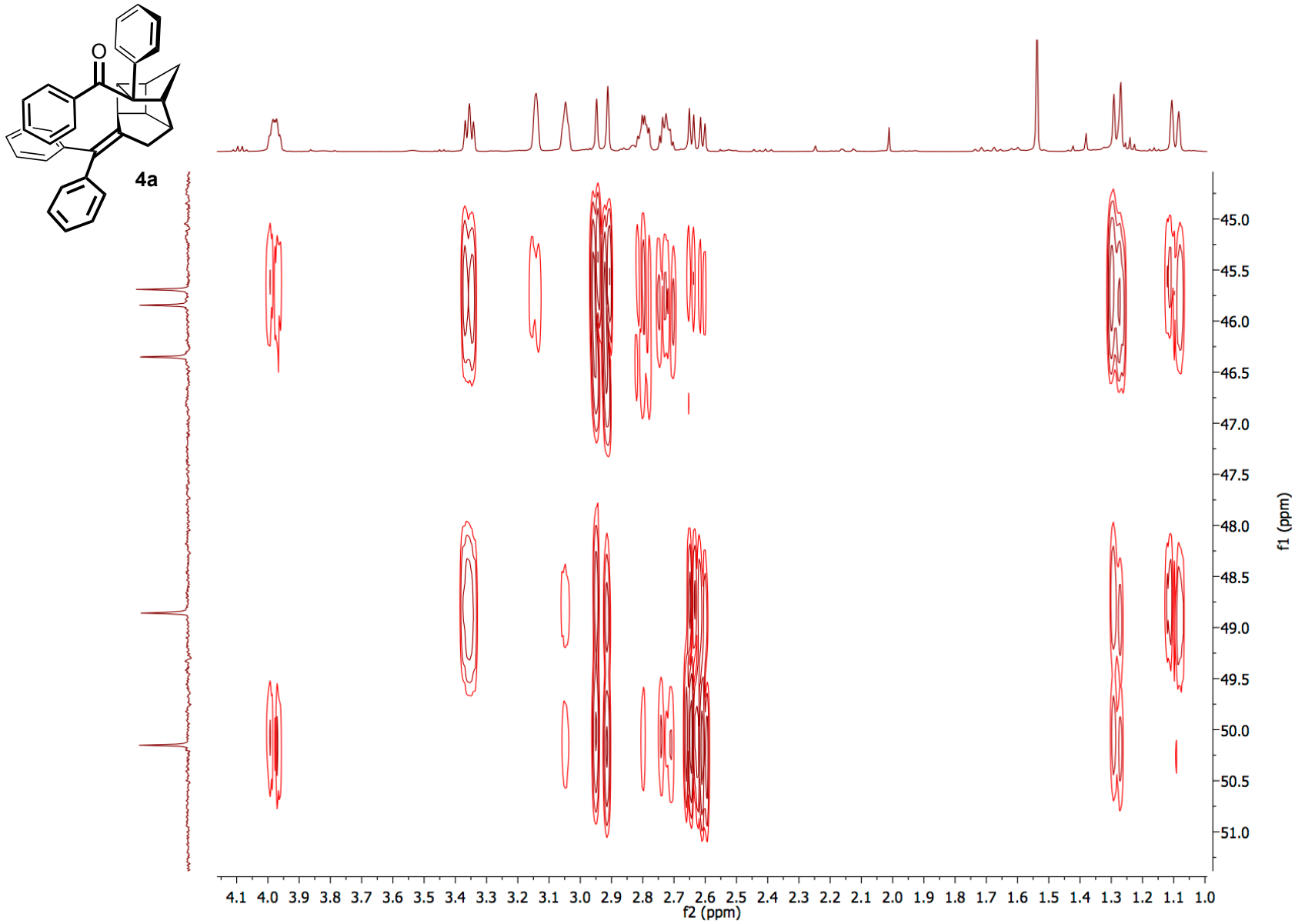

Figure S58. Gradient HMBC spectrum of compound **4a** (500.27, 125.81 MHz, CD_2Cl_2).

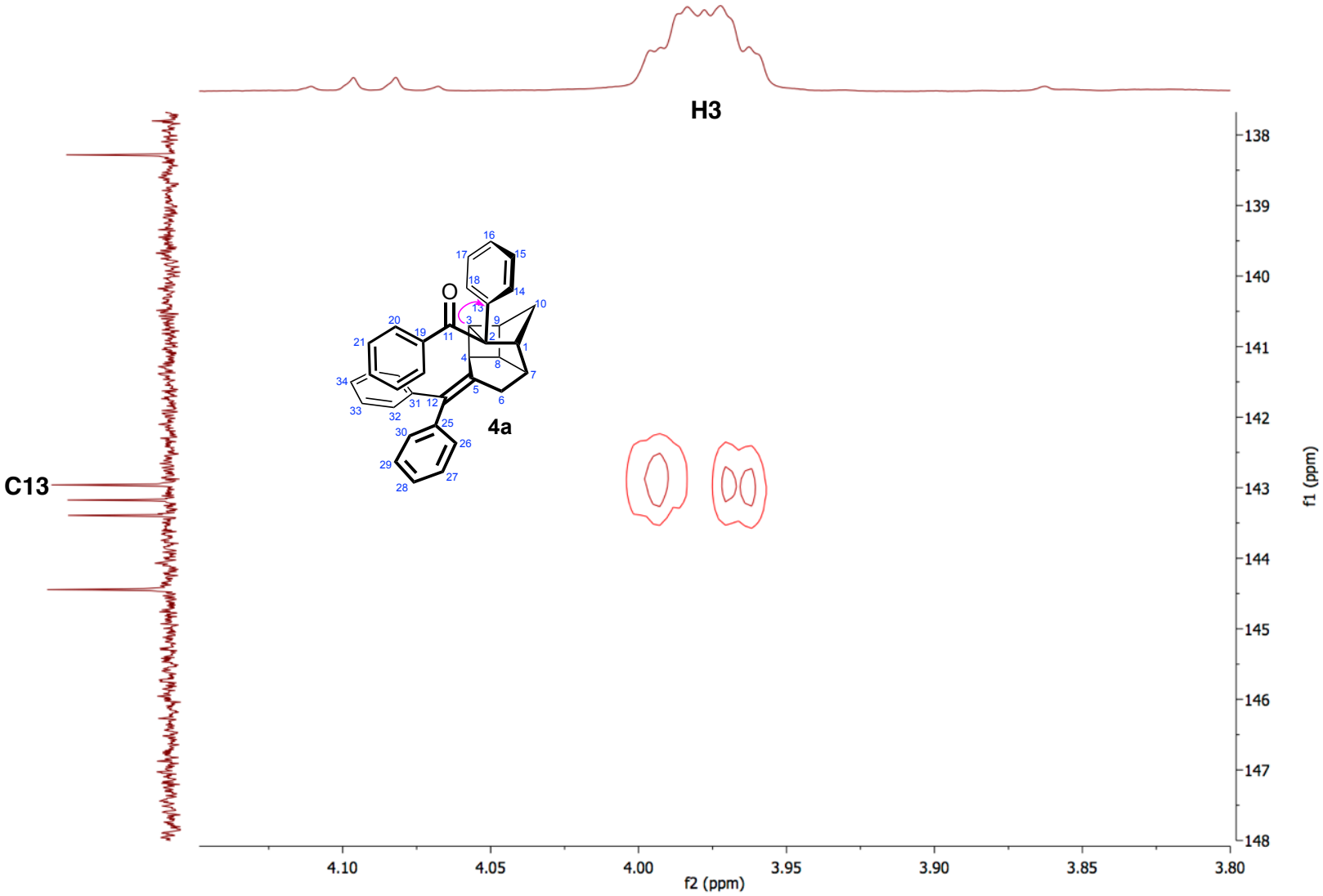

Figure S59. Gradient HMBC spectrum of compound **4a** highlighting the H3/C13 correlation (500.27, 125.81 MHz, CD_2Cl_2).

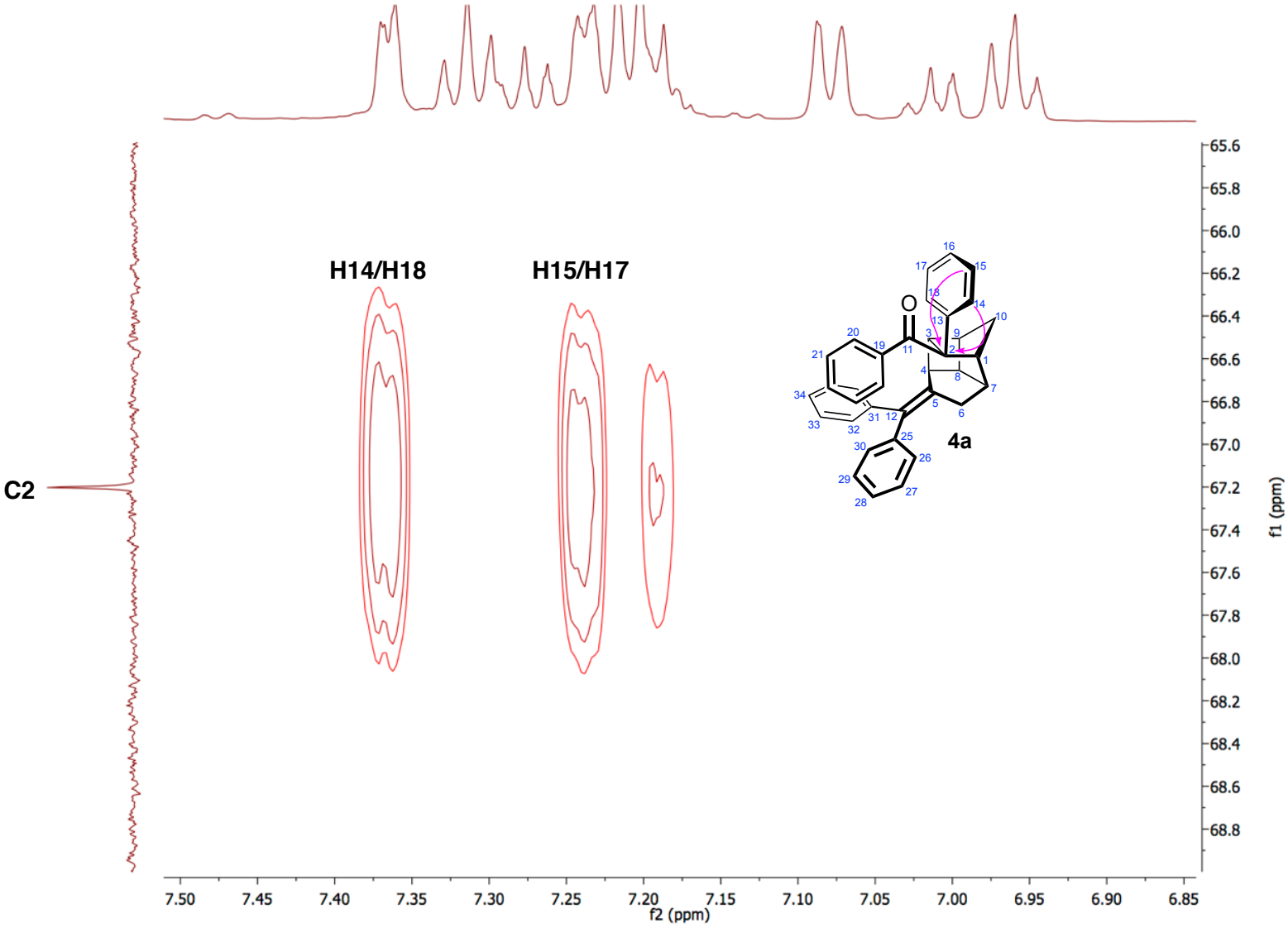

Figure S60. Gradient HMBC spectrum of compound **4a** showing relevant correlations to C2 (500.27, 125.81 MHz, CD_2Cl_2).

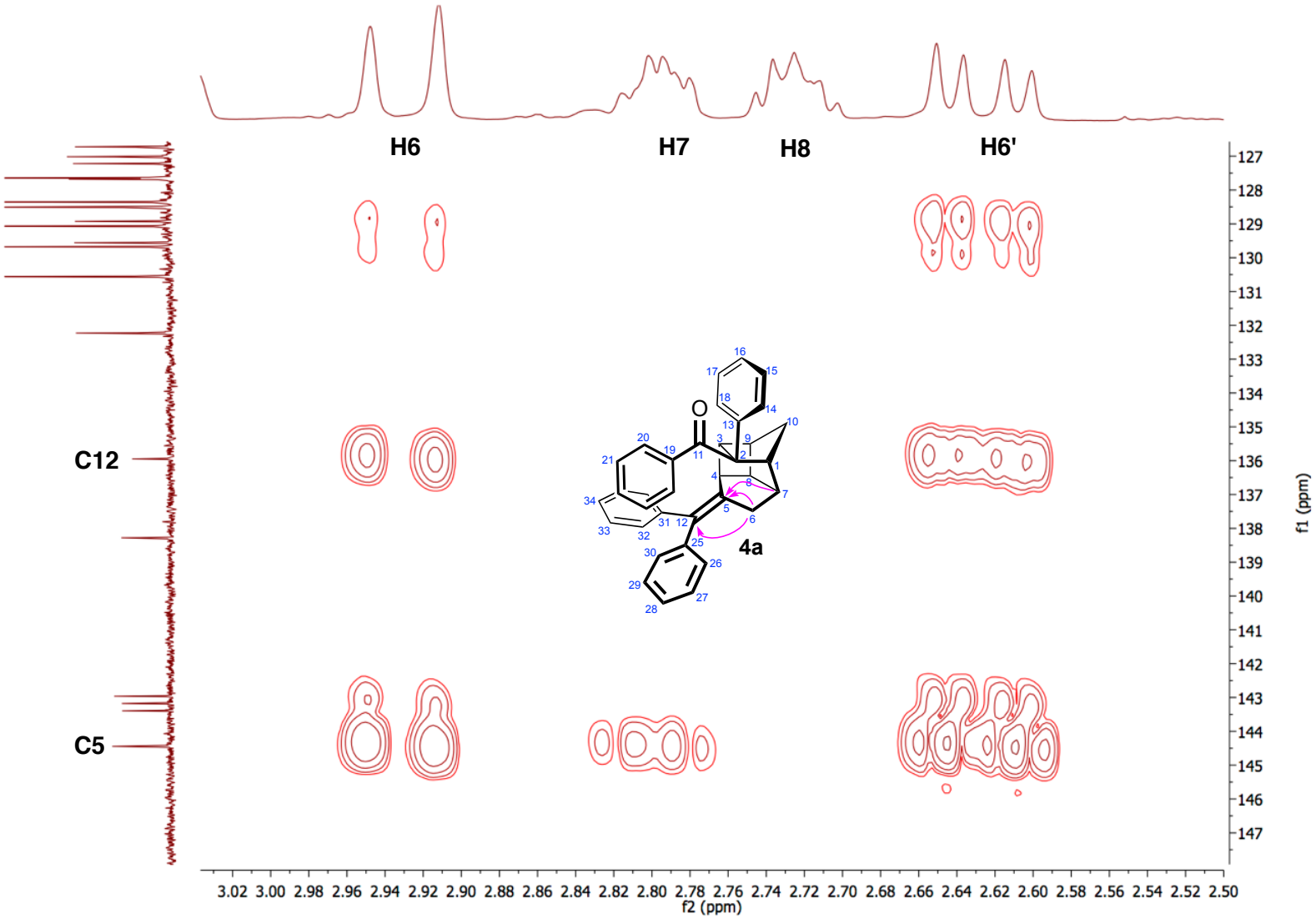

Figure S61. Gradient HMBC spectrum of compound **4a** showing correlations to C5 and C12 of the diphenyl alkylidene (500.27, 125.81 MHz, CD_2Cl_2).

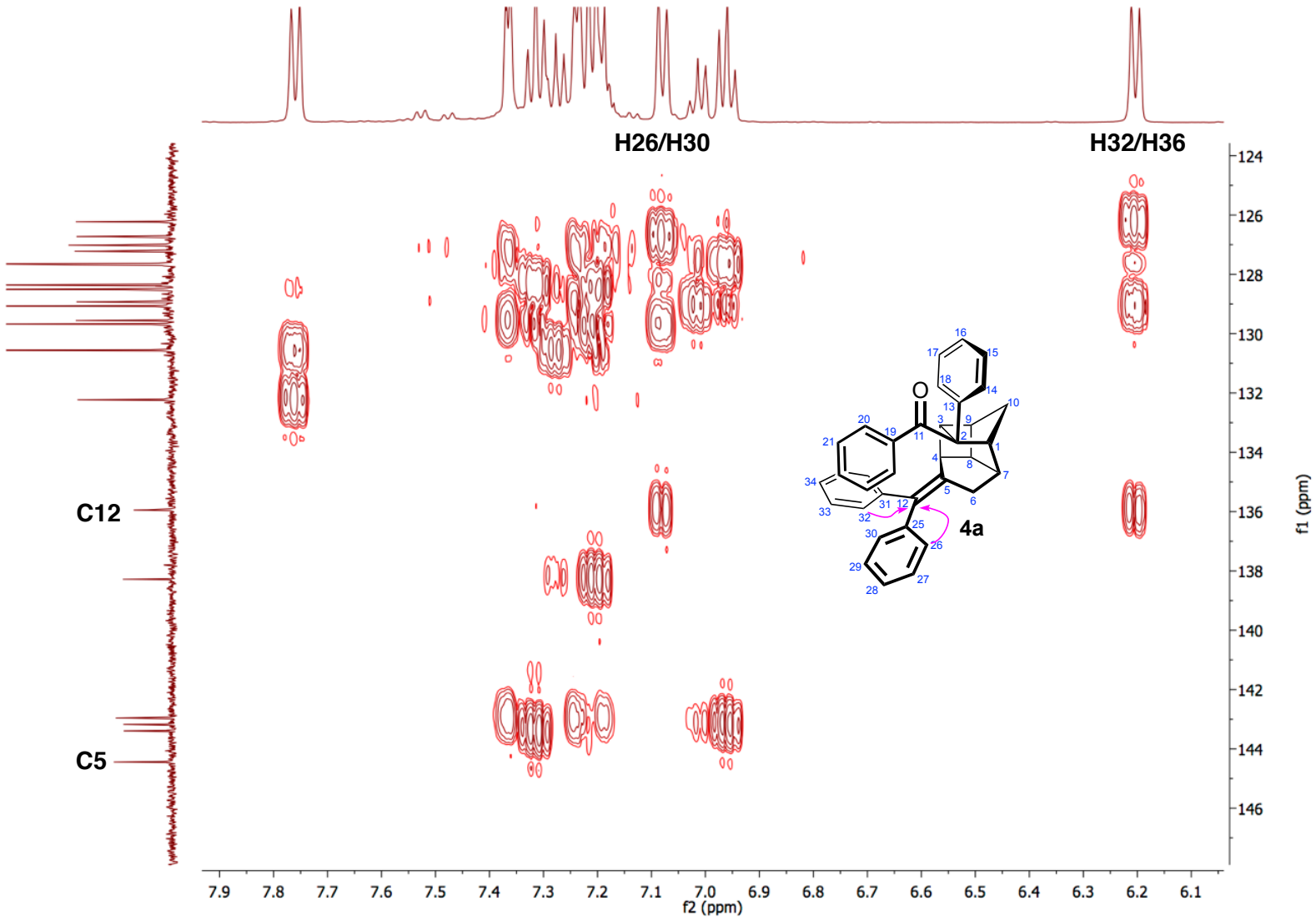

Figure S62. Gradient HMBC spectrum of compound **4a** showing correlations from H26/H30 and H32/H36 to C12 of the diphenyl alkylidene (500.27, 125.81 MHz, CD_2Cl_2).

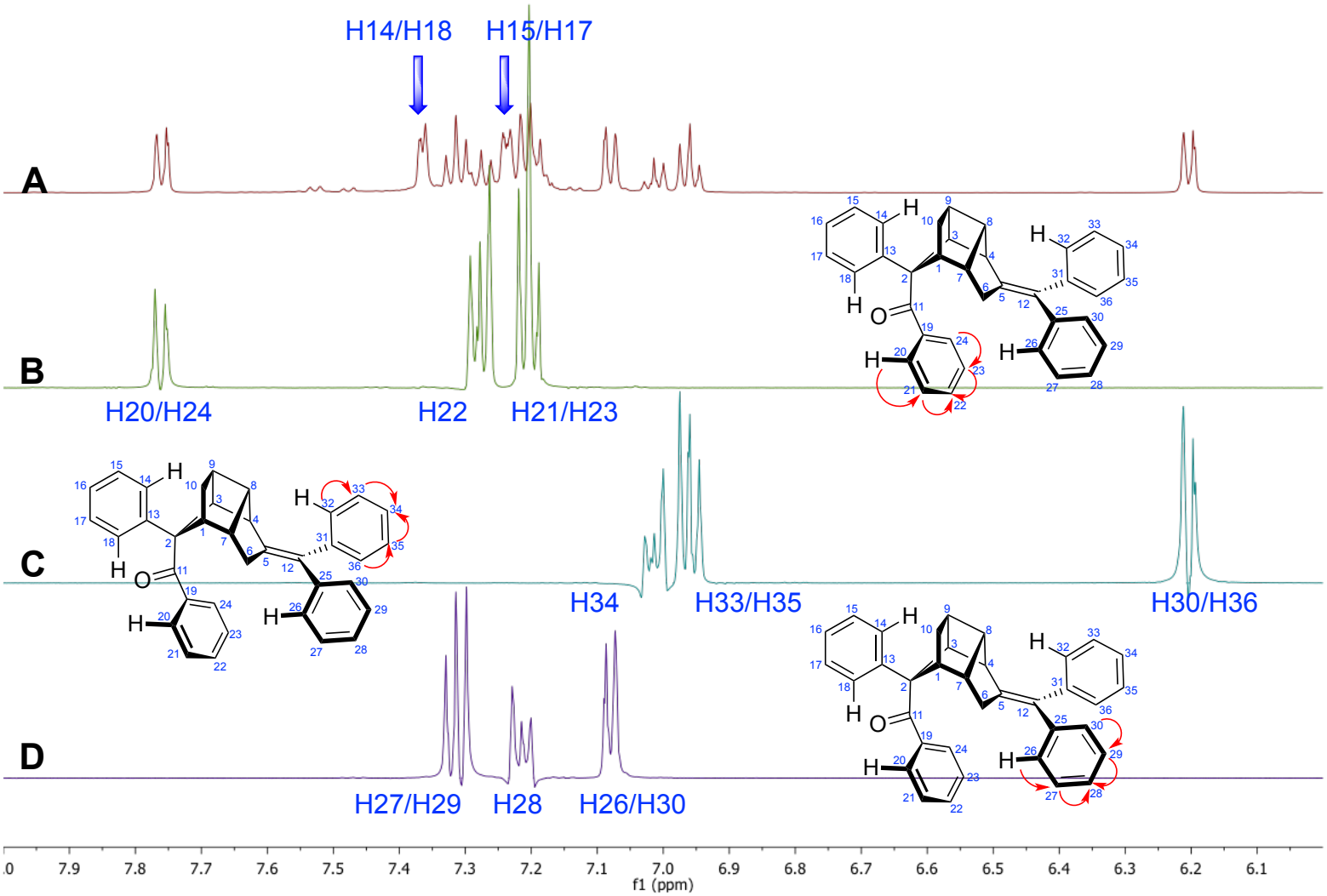

Figure S63. A) ^{1}H NMR of compound **4a**. 1D selective gradient TOCSY spectra of compound **4a** (500.27 MHz, CD_2Cl_2) from irradiation of H20/H24 **(B)**, H30/H36 **(C)**, and H26/H30 **(D)**.

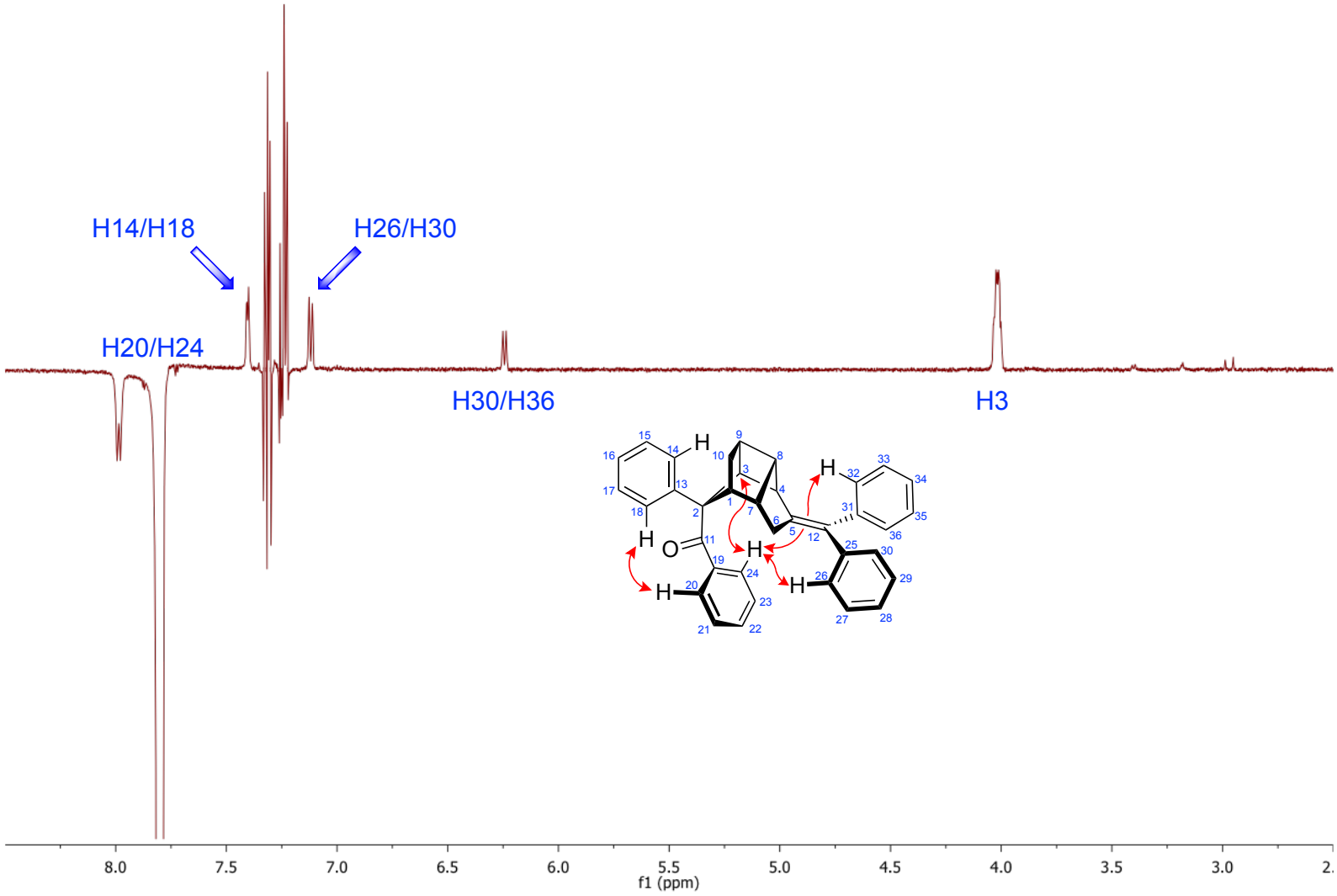

Figure S64. 1D selective gradient NOESY spectrum of compound **4a** (500.27 MHz, CD_2Cl_2) from irradiation of H20/H24.

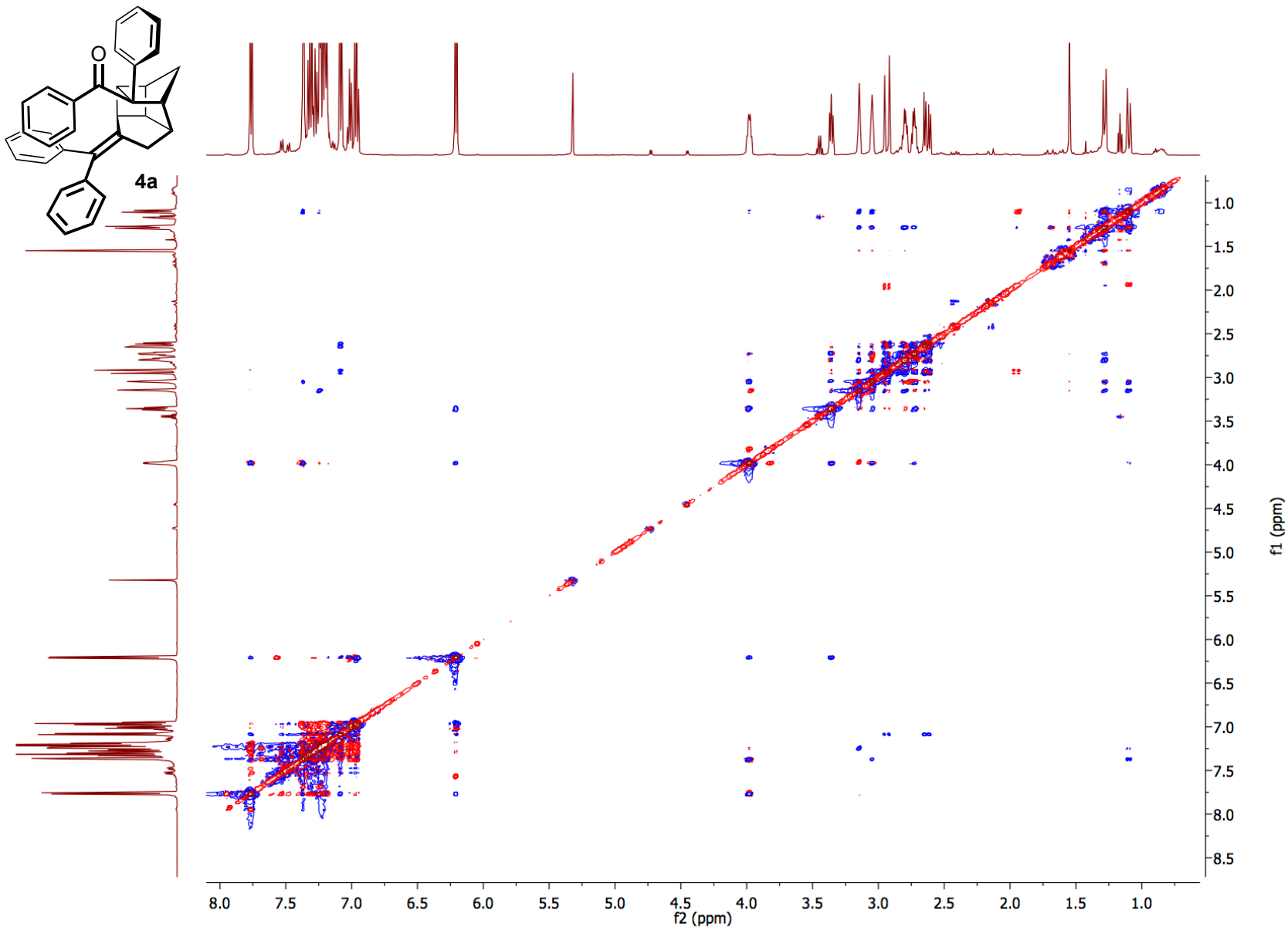

Figure S65. Gradient NOESY spectrum of compound **4a** (500.27 MHz, CD_2Cl_2).

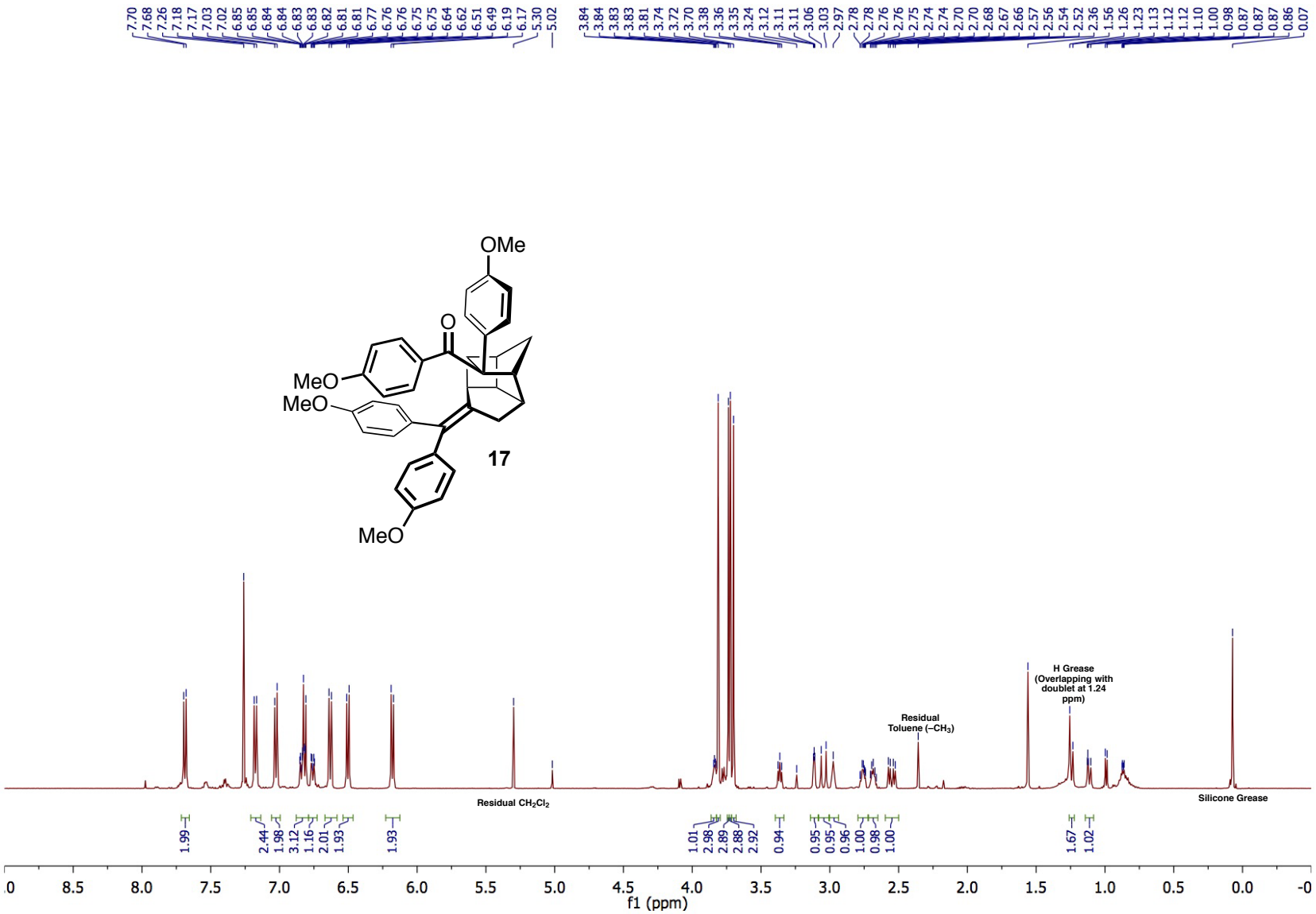

Figure S66. ^{1}H NMR of compound **17** (500.27 MHz, $CDCl_3$).

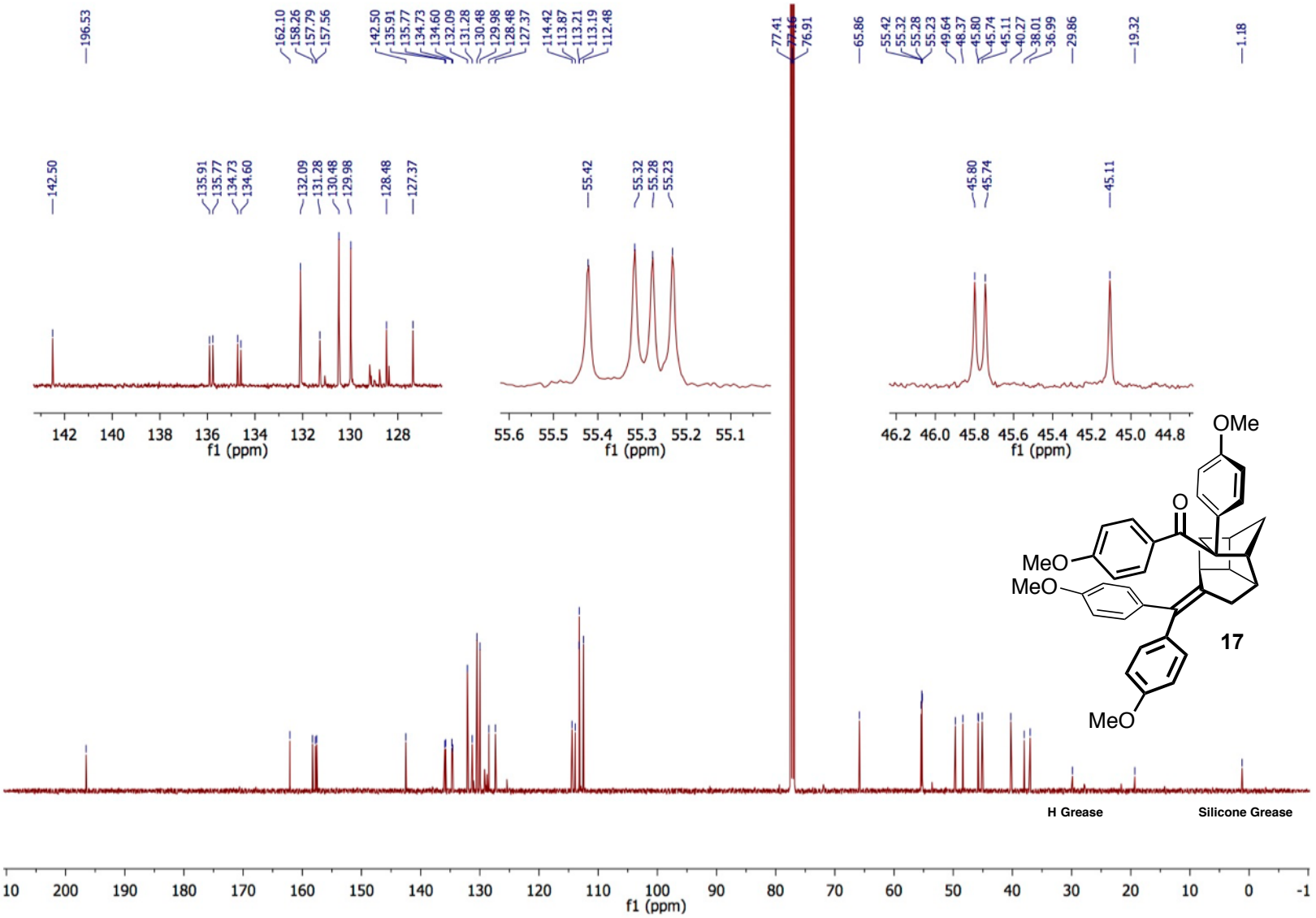

Figure S67. ^{13}C NMR of compound **17** (125.81 MHz, $CDCl_3$).

X-ray Structure Report

DISCUSSION

The compound crystallizes as colorless block-like crystals. There are four molecules of the compound in the unit cell of the primitive, centrosymmetric, monoclinic space group $P2_1/n$.

The structure of the compound is as expected (see Figures). The hydroxyl hydrogen atoms were located from a difference Fourier map and refined freely. At each site two positions for the hydrogen atoms were observed. As such, they were included in two, half-occupancy positions. Presumably this is disorder associated with the intra- and inter-molecular hydrogen-bonding this compound exhibits. The compound crystallizes as hydrogen-bonded dimers (see Table of Hydrogen Bonds for details) about a center of symmetry.

Due to the strain imposed by the fused, polycyclic ring system, two bonds about C2 (C2-C5 and C1-C2) are longer than expected [1.6610(13) and 1.5750(13) Å, respectively, see Tables of Bond Distances]. Likewise, bond angles about the fused rings are also strained beyond typical sp^3 geometries (see Table of Bond Angles). Other bond distances and angles within the molecular are typical.

CRYSTAL SUMMARY

Crystal data for $C_{36}H_{32}O_2$; M_r = 496.61; Monoclinic; space group $P2_1/n$; a = 13.7581(14) Å; b = 9.9466(10) Å; c = 18.8561(19) Å; α = 90°; β = 97.7032(16)°; γ = 90°; V = 2557.1(4) $Å^3$; Z = 4; T = 120(2) K; λ(Mo-Kα) = 0.71073 Å; μ(Mo-Kα) = 0.078 mm^{-1}; d_{calc} = 1.290 $g.cm^{-3}$; 54865 reflections collected; 7798 unique (R_{int} = 0.0299); giving R_1 = 0.0403, wR_2 = 0.1040 for 6432 data with [I>2σ(I)] and R_1 = 0.0521, wR_2 = 0.1113 for all 7798 data. Residual electron density ($e^-.Å^{-3}$) max/min: 0.386/-0.219.

An arbitrary sphere of data was collected on a colorless block-like crystal, having approximate dimensions of 0.390 × 0.192 × 0.122 mm, on a Bruker APEX-II diffractometer using a combination of ω- and φ-scans of 0.5° [1]. Data were corrected for absorption and polarization effects and analyzed for space group determination [2]. The structure was solved by dual-space methods and expanded routinely [3]. The model was refined by full-matrix least-squares analysis of F^2 against all reflections [4]. All non-hydrogen atoms were refined with anisotropic atomic displacement parameters. Unless otherwise noted, hydrogen atoms were included in calculated positions. Atomic displacement parameters for the hydrogens were tied to the equivalent isotropic displacement parameter of the atom to which they are bonded (U_{iso}(H) = 1.5U_{eq}(C) for methyl, 1.2U_{eq}(C) for all others).

REFERENCES

[1] *APEX-3*. Bruker AXS. Madison, Wisconsin, USA. **2016**.
[2] L. Krause, R. Herbst-Irmer, G. M. Sheldrick, & D. Stalke. *J. Appl. Cryst.* **2015** *48*, 3.
[3] G. M. Sheldrick. *Acta Cryst.*, **2015**, *A71*, 3.
[4] G. M. Sheldrick. *Acta Cryst.*, **2015**, *C71*, 3.

Table S6. Crystal Data and Structure Refinement for UVIC1813.

Identification code	uvic1813	
Empirical formula	$C_{36}H_{32}O_2$	
Formula weight	496.61	
Temperature	120(2) K	
Wavelength	0.71073 Å	
Crystal system	Monoclinic	
Space group	$P2_1/n$	
Unit cell dimensions	*a* = 13.7581(14) Å	α = 90°
	b = 9.9466(10) Å	β = 97.7032(16)°
	c = 18.8561(19) Å	γ = 90°
Volume	2557.1(4) $Å^3$	
Z	4	
Density (calculated)	1.290 $g.cm^{-3}$	
Absorption coefficient (μ)	0.078 mm^{-1}	
F(000)	1056	
Crystal color, habit	colorless, block	
Crystal size	0.390 × 0.192 × 0.122 mm^3	
θ range for data collection	1.727 to 30.560°	
Index ranges	-19 ≤ h ≤ 19, -14 ≤ k ≤ 14, -26 ≤ l ≤ 26	
Reflections collected	54865	
Independent reflections	7798 [R_{int} = 0.0299]	
Completeness to θ = 25.242°	100.0 %	
Absorption correction	Numerical	
Max. and min. transmission	1.0000 and 0.9666	
Refinement method	Full-matrix least-squares on F^2	
Data / restraints / parameters	7798 / 0 / 359	
Goodness-of-fit on F^2	1.022	
Final R indices [I>2σ(I)]	R_1 = 0.0403, wR_2 = 0.1040	
R indices (all data)	R_1 = 0.0521, wR_2 = 0.1113	
Extinction coefficient	n/a	
Largest diff. peak and hole	0.386 and -0.219 $e^-.Å^{-3}$	

Table S7. Atomic Coordinates and Equivalent Isotropic Displacement Parameters ($Å^2$) for UVIC1813. U(eq) is defined as one third of the trace of the orthogonalized U_{ij} tensor.

	x	y	z	U(eq)
O(1)	0.61959(5)	0.53409(7)	0.53970(5)	0.021(1)
O(2)	0.54596(6)	0.53095(7)	0.40298(5)	0.022(1)
C(1)	0.87245(7)	0.55990(10)	0.47601(5)	0.018(1)
C(2)	0.75788(7)	0.55762(9)	0.47537(5)	0.015(1)
C(3)	0.73222(7)	0.71004(9)	0.46013(5)	0.019(1)
C(4)	0.71785(7)	0.67815(9)	0.37970(5)	0.018(1)
C(5)	0.71570(6)	0.52286(9)	0.39066(5)	0.014(1)
C(6)	0.80584(7)	0.47045(9)	0.35947(5)	0.016(1)
C(7)	0.87886(7)	0.57262(10)	0.39518(5)	0.019(1)
C(8)	0.82911(8)	0.71155(10)	0.37972(6)	0.021(1)
C(9)	0.83268(8)	0.77759(10)	0.45542(6)	0.023(1)
C(10)	0.90778(8)	0.69865(10)	0.50470(6)	0.023(1)
C(11)	0.72071(7)	0.49600(9)	0.54291(5)	0.015(1)
C(12)	0.61478(6)	0.45904(9)	0.36573(5)	0.015(1)
C(13)	0.77620(7)	0.56158(10)	0.61003(5)	0.018(1)
C(14)	0.86140(8)	0.50442(11)	0.64554(6)	0.022(1)
C(15)	0.91756(8)	0.57227(13)	0.70139(6)	0.028(1)
C(16)	0.88787(9)	0.69743(13)	0.72288(6)	0.031(1)
C(17)	0.80057(9)	0.75187(12)	0.69067(6)	0.029(1)
C(18)	0.74461(8)	0.68469(10)	0.63464(6)	0.023(1)
C(19)	0.72803(7)	0.34290(9)	0.54961(5)	0.016(1)
C(20)	0.78426(7)	0.26424(10)	0.51005(5)	0.019(1)
C(21)	0.78710(8)	0.12535(10)	0.51779(6)	0.023(1)
C(22)	0.73380(8)	0.06245(10)	0.56527(6)	0.024(1)
C(23)	0.67882(8)	0.13977(10)	0.60632(6)	0.024(1)
C(24)	0.67649(7)	0.27869(10)	0.59898(6)	0.020(1)
C(25)	0.60906(6)	0.30685(9)	0.37873(5)	0.015(1)
C(26)	0.65640(7)	0.21719(10)	0.33767(5)	0.018(1)
C(27)	0.64435(8)	0.07919(10)	0.34401(5)	0.021(1)
C(28)	0.58227(8)	0.02806(10)	0.38975(6)	0.022(1)
C(29)	0.53472(7)	0.11626(10)	0.43017(6)	0.021(1)
C(30)	0.54919(7)	0.25410(10)	0.42566(5)	0.018(1)
C(31)	0.57733(7)	0.48020(10)	0.28530(5)	0.018(1)
C(32)	0.48742(8)	0.42018(11)	0.25951(6)	0.025(1)
C(33)	0.44651(8)	0.43229(12)	0.18864(7)	0.030(1)
C(34)	0.49450(9)	0.50579(12)	0.14094(6)	0.028(1)
C(35)	0.58285(8)	0.56651(11)	0.16548(6)	0.024(1)
C(36)	0.62413(7)	0.55382(10)	0.23684(5)	0.020(1)
H(1OA)	0.590(3)	0.502(4)	0.570(2)	0.045(9)

H(1OB)	0.585(3)	0.526(4)	0.497(2)	0.050(10)
H(2OA)	0.562(2)	0.534(3)	0.443(2)	0.028(8)
H(2OB)	0.489(3)	0.499(3)	0.3988(17)	0.033(8)
H(1)	0.90838	0.48156	0.50026	0.021
H(3)	0.68016	0.75645	0.48327	0.022
H(4)	0.66605	0.72450	0.34615	0.022
H(6A)	0.82295	0.37721	0.37472	0.019
H(6B)	0.79799	0.47669	0.30661	0.019
H(7)	0.94658	0.56515	0.38181	0.023
H(8)	0.84856	0.76706	0.33970	0.025
H(9)	0.83591	0.87792	0.45825	0.027
H(10A)	0.90065	0.71093	0.55585	0.028
H(10B)	0.97596	0.71842	0.49663	0.028
H(14)	0.88154	0.41814	0.63156	0.027
H(15)	0.97616	0.53281	0.72472	0.034
H(16)	0.92739	0.74548	0.75960	0.037
H(17)	0.77863	0.83561	0.70684	0.035
H(18)	0.68454	0.72269	0.61295	0.027
H(20)	0.82139	0.30593	0.47717	0.022
H(21)	0.82606	0.07319	0.49017	0.028
H(22)	0.73482	-0.03269	0.56973	0.029
H(23)	0.64258	0.09759	0.63961	0.028
H(24)	0.63936	0.33084	0.62791	0.024
H(26)	0.69734	0.25103	0.30502	0.021
H(27)	0.67876	0.01949	0.31691	0.025
H(28)	0.57261	-0.06616	0.39322	0.026
H(29)	0.49173	0.08229	0.46134	0.025
H(30)	0.51774	0.31307	0.45504	0.021
H(32)	0.45371	0.36992	0.29144	0.030
H(33)	0.38552	0.39034	0.17250	0.036
H(34)	0.46684	0.51403	0.09220	0.033
H(35)	0.61587	0.61746	0.13341	0.028
H(36)	0.68513	0.59602	0.25270	0.024

Table S8. Anisotropic Displacement Parameters ($Å^2$) for UVIC1813.
The anisotropic displacement factor exponent takes the form:
$-2\pi^2[h^2a^{*2}U_{11} + ... + 2hka^*b^*U_{12}]$

	U_{11}	U_{22}	U_{33}	U_{23}	U_{13}	U_{12}
O(1)	0.0137(3)	0.0193(3)	0.0324(4)	0.0012(3)	0.0112(3)	0.0031(3)
O(2)	0.0184(4)	0.0181(3)	0.0316(5)	0.0021(3)	0.0143(3)	0.0042(3)
C(1)	0.0136(4)	0.0182(4)	0.0220(4)	-0.0040(3)	0.0066(3)	-0.0023(3)
C(2)	0.0149(4)	0.0118(4)	0.0186(4)	-0.0013(3)	0.0073(3)	0.0001(3)
C(3)	0.0222(4)	0.0121(4)	0.0232(5)	-0.0010(3)	0.0102(4)	0.0003(3)
C(4)	0.0215(4)	0.0127(4)	0.0219(5)	0.0017(3)	0.0094(4)	0.0000(3)
C(5)	0.0138(4)	0.0127(4)	0.0176(4)	0.0005(3)	0.0061(3)	-0.0001(3)
C(6)	0.0141(4)	0.0158(4)	0.0192(4)	-0.0020(3)	0.0072(3)	-0.0010(3)
C(7)	0.0155(4)	0.0191(4)	0.0237(5)	-0.0038(4)	0.0096(3)	-0.0042(3)
C(8)	0.0244(5)	0.0161(4)	0.0244(5)	-0.0012(3)	0.0121(4)	-0.0059(3)
C(9)	0.0288(5)	0.0142(4)	0.0281(5)	-0.0043(4)	0.0125(4)	-0.0066(4)
C(10)	0.0223(5)	0.0218(5)	0.0268(5)	-0.0071(4)	0.0090(4)	-0.0092(4)
C(11)	0.0130(4)	0.0136(4)	0.0195(4)	-0.0004(3)	0.0067(3)	0.0017(3)
C(12)	0.0131(4)	0.0139(4)	0.0189(4)	0.0016(3)	0.0063(3)	0.0015(3)
C(13)	0.0198(4)	0.0175(4)	0.0188(4)	-0.0022(3)	0.0086(3)	-0.0021(3)
C(14)	0.0206(5)	0.0252(5)	0.0216(5)	-0.0044(4)	0.0060(4)	-0.0006(4)
C(15)	0.0251(5)	0.0379(6)	0.0221(5)	-0.0060(4)	0.0038(4)	-0.0032(4)
C(16)	0.0369(6)	0.0362(6)	0.0217(5)	-0.0102(4)	0.0079(4)	-0.0108(5)
C(17)	0.0420(6)	0.0231(5)	0.0249(5)	-0.0080(4)	0.0134(5)	-0.0040(5)
C(18)	0.0286(5)	0.0183(4)	0.0227(5)	-0.0025(4)	0.0108(4)	0.0000(4)
C(19)	0.0151(4)	0.0143(4)	0.0175(4)	0.0003(3)	0.0020(3)	0.0000(3)
C(20)	0.0218(4)	0.0157(4)	0.0188(4)	0.0003(3)	0.0041(3)	0.0024(3)
C(21)	0.0318(5)	0.0160(4)	0.0206(5)	-0.0014(4)	0.0012(4)	0.0061(4)
C(22)	0.0337(6)	0.0146(4)	0.0219(5)	0.0017(4)	-0.0038(4)	-0.0005(4)
C(23)	0.0282(5)	0.0195(5)	0.0229(5)	0.0050(4)	0.0018(4)	-0.0040(4)
C(24)	0.0213(4)	0.0187(4)	0.0217(5)	0.0018(4)	0.0057(4)	-0.0006(3)
C(25)	0.0126(4)	0.0149(4)	0.0166(4)	0.0014(3)	0.0019(3)	-0.0001(3)
C(26)	0.0182(4)	0.0175(4)	0.0178(4)	-0.0009(3)	0.0048(3)	-0.0016(3)
C(27)	0.0236(5)	0.0171(4)	0.0210(5)	-0.0036(3)	0.0034(4)	-0.0003(4)
C(28)	0.0239(5)	0.0155(4)	0.0255(5)	0.0025(4)	0.0013(4)	-0.0016(3)
C(29)	0.0197(4)	0.0195(4)	0.0249(5)	0.0071(4)	0.0057(4)	-0.0006(3)
C(30)	0.0155(4)	0.0177(4)	0.0208(4)	0.0033(3)	0.0054(3)	0.0018(3)
C(31)	0.0153(4)	0.0172(4)	0.0206(4)	0.0034(3)	0.0036(3)	0.0022(3)
C(32)	0.0180(4)	0.0277(5)	0.0285(5)	0.0088(4)	0.0005(4)	-0.0021(4)
C(33)	0.0220(5)	0.0339(6)	0.0319(6)	0.0086(5)	-0.0054(4)	-0.0030(4)
C(34)	0.0285(5)	0.0298(5)	0.0237(5)	0.0061(4)	-0.0023(4)	0.0026(4)
C(35)	0.0272(5)	0.0224(5)	0.0221(5)	0.0046(4)	0.0055(4)	0.0021(4)
C(36)	0.0197(4)	0.0191(4)	0.0218(5)	0.0019(4)	0.0055(4)	0.0002(3)

Table S9. Bond Lengths [Å] for UVIC1813.

atom-atom	distance	atom-atom	distance
O(1)-C(11)	1.4353(11)	O(1)-H(1OA)	0.80(4)
O(1)-H(1OB)	0.88(4)	O(2)-C(12)	1.4422(11)
O(2)-H(2OA)	0.75(4)	O(2)-H(2OB)	0.84(4)
C(1)-C(10)	1.5372(13)	C(1)-C(7)	1.5437(14)
C(1)-C(2)	1.5750(13)	C(1)-H(1)	1.0000
C(2)-C(11)	1.5600(13)	C(2)-C(3)	1.5743(13)
C(2)-C(5)	1.6610(13)	C(3)-C(4)	1.5360(14)
C(3)-C(9)	1.5500(14)	C(3)-H(3)	1.0000
C(4)-C(5)	1.5592(12)	C(4)-C(8)	1.5663(14)
C(4)-H(4)	1.0000	C(5)-C(6)	1.5334(12)
C(5)-C(12)	1.5417(13)	C(6)-C(7)	1.5211(13)
C(6)-H(6A)	0.9900	C(6)-H(6B)	0.9900
C(7)-C(8)	1.5523(14)	C(7)-H(7)	1.0000
C(8)-C(9)	1.5660(14)	C(8)-H(8)	1.0000
C(9)-C(10)	1.5133(16)	C(9)-H(9)	1.0000
C(10)-H(10A)	0.9900	C(10)-H(10B)	0.9900
C(11)-C(19)	1.5302(13)	C(11)-C(13)	1.5333(14)
C(12)-C(25)	1.5372(13)	C(12)-C(31)	1.5494(14)
C(13)-C(14)	1.3910(15)	C(13)-C(18)	1.3992(13)
C(14)-C(15)	1.3940(15)	C(14)-H(14)	0.9500
C(15)-C(16)	1.3876(17)	C(15)-H(15)	0.9500
C(16)-C(17)	1.3817(19)	C(16)-H(16)	0.9500
C(17)-C(18)	1.3919(16)	C(17)-H(17)	0.9500
C(18)-H(18)	0.9500	C(19)-C(20)	1.3862(13)
C(19)-C(24)	1.3979(13)	C(20)-C(21)	1.3892(13)
C(20)-H(20)	0.9500	C(21)-C(22)	1.3808(16)
C(21)-H(21)	0.9500	C(22)-C(23)	1.3856(16)
C(22)-H(22)	0.9500	C(23)-C(24)	1.3887(14)
C(23)-H(23)	0.9500	C(24)-H(24)	0.9500
C(25)-C(30)	1.3900(12)	C(25)-C(26)	1.3979(13)
C(26)-C(27)	1.3897(13)	C(26)-H(26)	0.9500
C(27)-C(28)	1.3892(14)	C(27)-H(27)	0.9500
C(28)-C(29)	1.3828(15)	C(28)-H(28)	0.9500
C(29)-C(30)	1.3897(14)	C(29)-H(29)	0.9500
C(30)-H(30)	0.9500	C(31)-C(36)	1.3940(13)
C(31)-C(32)	1.4005(14)	C(32)-C(33)	1.3839(16)
C(32)-H(32)	0.9500	C(33)-C(34)	1.3923(17)
C(33)-H(33)	0.9500	C(34)-C(35)	1.3803(16)
C(34)-H(34)	0.9500	C(35)-C(36)	1.3945(15)
C(35)-H(35)	0.9500	C(36)-H(36)	0.9500

Table S10. Bond Angles [°] for UVIC1813.

atom-atom-atom	angle	atom-atom-atom	angle
C(11)-O(1)-H(1OA)	116(2)	C(11)-O(1)-H(1OB)	115(2)
C(12)-O(2)-H(2OA)	112(2)	C(12)-O(2)-H(2OB)	116(2)
C(10)-C(1)-C(7)	102.51(8)	C(10)-C(1)-C(2)	106.53(7)
C(7)-C(1)-C(2)	100.55(7)	C(10)-C(1)-H(1)	115.2
C(7)-C(1)-H(1)	115.2	C(2)-C(1)-H(1)	115.2
C(11)-C(2)-C(3)	115.94(7)	C(11)-C(2)-C(1)	115.89(8)
C(3)-C(2)-C(1)	100.79(7)	C(11)-C(2)-C(5)	126.35(7)
C(3)-C(2)-C(5)	89.08(7)	C(1)-C(2)-C(5)	103.34(7)
C(4)-C(3)-C(9)	91.75(7)	C(4)-C(3)-C(2)	88.70(7)
C(9)-C(3)-C(2)	104.36(8)	C(4)-C(3)-H(3)	121.4
C(9)-C(3)-H(3)	121.4	C(2)-C(3)-H(3)	121.4
C(3)-C(4)-C(5)	94.35(7)	C(3)-C(4)-C(8)	87.69(8)
C(5)-C(4)-C(8)	104.25(7)	C(3)-C(4)-H(4)	121.1
C(5)-C(4)-H(4)	121.1	C(8)-C(4)-H(4)	121.1
C(6)-C(5)-C(12)	118.99(8)	C(6)-C(5)-C(4)	104.78(7)
C(12)-C(5)-C(4)	113.57(8)	C(6)-C(5)-C(2)	104.08(7)
C(12)-C(5)-C(2)	124.28(7)	C(4)-C(5)-C(2)	84.89(6)
C(7)-C(6)-C(5)	97.08(7)	C(7)-C(6)-H(6A)	112.3
C(5)-C(6)-H(6A)	112.3	C(7)-C(6)-H(6B)	112.3
C(5)-C(6)-H(6B)	112.3	H(6A)-C(6)-H(6B)	109.9
C(6)-C(7)-C(1)	105.10(7)	C(6)-C(7)-C(8)	105.26(8)
C(1)-C(7)-C(8)	100.15(7)	C(6)-C(7)-H(7)	114.9
C(1)-C(7)-H(7)	114.9	C(8)-C(7)-H(7)	114.9
C(7)-C(8)-C(9)	104.07(8)	C(7)-C(8)-C(4)	102.56(7)
C(9)-C(8)-C(4)	90.02(7)	C(7)-C(8)-H(8)	118.5
C(9)-C(8)-H(8)	118.5	C(4)-C(8)-H(8)	118.5
C(10)-C(9)-C(3)	106.29(8)	C(10)-C(9)-C(8)	106.11(8)
C(3)-C(9)-C(8)	87.20(7)	C(10)-C(9)-H(9)	117.6
C(3)-C(9)-H(9)	117.6	C(8)-C(9)-H(9)	117.6
C(9)-C(10)-C(1)	95.29(8)	C(9)-C(10)-H(10A)	112.7
C(1)-C(10)-H(10A)	112.7	C(9)-C(10)-H(10B)	112.7
C(1)-C(10)-H(10B)	112.7	H(10A)-C(10)-H(10B)	110.2
O(1)-C(11)-C(19)	108.59(7)	O(1)-C(11)-C(13)	107.16(7)
C(19)-C(11)-C(13)	109.59(8)	O(1)-C(11)-C(2)	106.48(8)
C(19)-C(11)-C(2)	115.67(7)	C(13)-C(11)-C(2)	108.98(7)
O(2)-C(12)-C(25)	111.09(7)	O(2)-C(12)-C(5)	105.69(8)
C(25)-C(12)-C(5)	114.84(7)	O(2)-C(12)-C(31)	104.80(8)
C(25)-C(12)-C(31)	105.81(7)	C(5)-C(12)-C(31)	114.22(7)
C(14)-C(13)-C(18)	118.51(9)	C(14)-C(13)-C(11)	121.17(8)

C(18)-C(13)-C(11)	120.24(9)	C(13)-C(14)-C(15)	120.78(10)
C(13)-C(14)-H(14)	119.6	C(15)-C(14)-H(14)	119.6
C(16)-C(15)-C(14)	119.99(11)	C(16)-C(15)-H(15)	120.0
C(14)-C(15)-H(15)	120.0	C(17)-C(16)-C(15)	119.72(11)
C(17)-C(16)-H(16)	120.1	C(15)-C(16)-H(16)	120.1
C(16)-C(17)-C(18)	120.35(10)	C(16)-C(17)-H(17)	119.8
C(18)-C(17)-H(17)	119.8	C(17)-C(18)-C(13)	120.47(10)
C(17)-C(18)-H(18)	119.8	C(13)-C(18)-H(18)	119.8
C(20)-C(19)-C(24)	118.03(9)	C(20)-C(19)-C(11)	123.54(8)
C(24)-C(19)-C(11)	118.42(8)	C(19)-C(20)-C(21)	120.97(9)
C(19)-C(20)-H(20)	119.5	C(21)-C(20)-H(20)	119.5
C(22)-C(21)-C(20)	120.58(10)	C(22)-C(21)-H(21)	119.7
C(20)-C(21)-H(21)	119.7	C(21)-C(22)-C(23)	119.20(9)
C(21)-C(22)-H(22)	120.4	C(23)-C(22)-H(22)	120.4
C(22)-C(23)-C(24)	120.24(10)	C(22)-C(23)-H(23)	119.9
C(24)-C(23)-H(23)	119.9	C(23)-C(24)-C(19)	120.93(9)
C(23)-C(24)-H(24)	119.5	C(19)-C(24)-H(24)	119.5
C(30)-C(25)-C(26)	118.14(9)	C(30)-C(25)-C(12)	121.37(8)
C(26)-C(25)-C(12)	120.15(8)	C(27)-C(26)-C(25)	120.84(9)
C(27)-C(26)-H(26)	119.6	C(25)-C(26)-H(26)	119.6
C(28)-C(27)-C(26)	120.35(9)	C(28)-C(27)-H(27)	119.8
C(26)-C(27)-H(27)	119.8	C(29)-C(28)-C(27)	119.06(9)
C(29)-C(28)-H(28)	120.5	C(27)-C(28)-H(28)	120.5
C(28)-C(29)-C(30)	120.66(9)	C(28)-C(29)-H(29)	119.7
C(30)-C(29)-H(29)	119.7	C(29)-C(30)-C(25)	120.89(9)
C(29)-C(30)-H(30)	119.6	C(25)-C(30)-H(30)	119.6
C(36)-C(31)-C(32)	117.42(9)	C(36)-C(31)-C(12)	126.21(9)
C(32)-C(31)-C(12)	116.38(8)	C(33)-C(32)-C(31)	121.60(10)
C(33)-C(32)-H(32)	119.2	C(31)-C(32)-H(32)	119.2
C(32)-C(33)-C(34)	120.18(10)	C(32)-C(33)-H(33)	119.9
C(34)-C(33)-H(33)	119.9	C(35)-C(34)-C(33)	119.06(10)
C(35)-C(34)-H(34)	120.5	C(33)-C(34)-H(34)	120.5
C(34)-C(35)-C(36)	120.68(10)	C(34)-C(35)-H(35)	119.7
C(36)-C(35)-H(35)	119.7	C(31)-C(36)-C(35)	121.05(10)
C(31)-C(36)-H(36)	119.5	C(35)-C(36)-H(36)	119.5

Table S11. Torsion angles [°] for UVIC1813.

atom-atom-atom-atom	angle	atom-atom-atom-atom	angle
C(10)-C(1)-C(2)-C(11)	-94.26(9)	C(7)-C(1)-C(2)-C(11)	159.17(7)
C(10)-C(1)-C(2)-C(3)	31.72(9)	C(7)-C(1)-C(2)-C(3)	-74.85(8)
C(10)-C(1)-C(2)-C(5)	123.35(8)	C(7)-C(1)-C(2)-C(5)	16.78(8)
C(11)-C(2)-C(3)-C(4)	-143.42(8)	C(1)-C(2)-C(3)-C(4)	90.64(7)
C(5)-C(2)-C(3)-C(4)	-12.77(7)	C(11)-C(2)-C(3)-C(9)	125.11(8)
C(1)-C(2)-C(3)-C(9)	-0.84(9)	C(5)-C(2)-C(3)-C(9)	-104.24(7)
C(9)-C(3)-C(4)-C(5)	117.98(7)	C(2)-C(3)-C(4)-C(5)	13.65(7)
C(9)-C(3)-C(4)-C(8)	13.87(7)	C(2)-C(3)-C(4)-C(8)	-90.46(7)
C(3)-C(4)-C(5)-C(6)	-116.22(8)	C(8)-C(4)-C(5)-C(6)	-27.50(10)
C(3)-C(4)-C(5)-C(12)	112.32(8)	C(8)-C(4)-C(5)-C(12)	-158.96(8)
C(3)-C(4)-C(5)-C(2)	-12.98(7)	C(8)-C(4)-C(5)-C(2)	75.74(7)
C(11)-C(2)-C(5)-C(6)	-121.29(9)	C(3)-C(2)-C(5)-C(6)	116.61(7)
C(1)-C(2)-C(5)-C(6)	15.73(8)	C(11)-C(2)-C(5)-C(12)	19.58(13)
C(3)-C(2)-C(5)-C(12)	-102.52(9)	C(1)-C(2)-C(5)-C(12)	156.60(8)
C(11)-C(2)-C(5)-C(4)	134.72(9)	C(3)-C(2)-C(5)-C(4)	12.62(6)
C(1)-C(2)-C(5)-C(4)	-88.26(7)	C(12)-C(5)-C(6)-C(7)	174.97(8)
C(4)-C(5)-C(6)-C(7)	46.72(9)	C(2)-C(5)-C(6)-C(7)	-41.62(8)
C(5)-C(6)-C(7)-C(1)	55.76(9)	C(5)-C(6)-C(7)-C(8)	-49.48(8)
C(10)-C(1)-C(7)-C(6)	-155.54(8)	C(2)-C(1)-C(7)-C(6)	-45.80(9)
C(10)-C(1)-C(7)-C(8)	-46.56(9)	C(2)-C(1)-C(7)-C(8)	63.18(8)
C(6)-C(7)-C(8)-C(9)	126.59(8)	C(1)-C(7)-C(8)-C(9)	17.73(9)
C(6)-C(7)-C(8)-C(4)	33.36(9)	C(1)-C(7)-C(8)-C(4)	-75.49(8)
C(3)-C(4)-C(8)-C(7)	90.71(8)	C(5)-C(4)-C(8)-C(7)	-3.20(9)
C(3)-C(4)-C(8)-C(9)	-13.72(7)	C(5)-C(4)-C(8)-C(9)	-107.62(8)
C(4)-C(3)-C(9)-C(10)	-119.85(8)	C(2)-C(3)-C(9)-C(10)	-30.74(10)
C(4)-C(3)-C(9)-C(8)	-13.87(7)	C(2)-C(3)-C(9)-C(8)	75.23(8)
C(7)-C(8)-C(9)-C(10)	16.79(9)	C(4)-C(8)-C(9)-C(10)	119.75(8)
C(7)-C(8)-C(9)-C(3)	-89.37(8)	C(4)-C(8)-C(9)-C(3)	13.60(7)
C(3)-C(9)-C(10)-C(1)	48.20(9)	C(8)-C(9)-C(10)-C(1)	-43.61(9)
C(7)-C(1)-C(10)-C(9)	55.96(8)	C(2)-C(1)-C(10)-C(9)	-49.20(9)
C(3)-C(2)-C(11)-O(1)	47.88(10)	C(1)-C(2)-C(11)-O(1)	165.75(7)
C(5)-C(2)-C(11)-O(1)	-61.75(10)	C(3)-C(2)-C(11)-C(19)	168.62(8)
C(1)-C(2)-C(11)-C(19)	-73.51(10)	C(5)-C(2)-C(11)-C(19)	58.99(11)
C(3)-C(2)-C(11)-C(13)	-67.41(10)	C(1)-C(2)-C(11)-C(13)	50.46(10)
C(5)-C(2)-C(11)-C(13)	-177.04(8)	C(6)-C(5)-C(12)-O(2)	-178.79(8)
C(4)-C(5)-C(12)-O(2)	-54.73(10)	C(2)-C(5)-C(12)-O(2)	45.62(11)
C(6)-C(5)-C(12)-C(25)	58.40(11)	C(4)-C(5)-C(12)-C(25)	-177.54(7)
C(2)-C(5)-C(12)-C(25)	-77.19(10)	C(6)-C(5)-C(12)-C(31)	-64.12(11)
C(4)-C(5)-C(12)-C(31)	59.94(10)	C(2)-C(5)-C(12)-C(31)	160.29(8)
O(1)-C(11)-C(13)-C(14)	152.47(9)	C(19)-C(11)-C(13)-C(14)	34.81(12)

C(2)-C(11)-C(13)-C(14)	-92.68(10)	O(1)-C(11)-C(13)-C(18)	-30.93(12)
C(19)-C(11)-C(13)-C(18)	-148.59(9)	C(2)-C(11)-C(13)-C(18)	83.91(10)
C(18)-C(13)-C(14)-C(15)	-4.14(15)	C(11)-C(13)-C(14)-C(15)	172.51(9)
C(13)-C(14)-C(15)-C(16)	1.00(17)	C(14)-C(15)-C(16)-C(17)	2.58(17)
C(15)-C(16)-C(17)-C(18)	-2.93(17)	C(16)-C(17)-C(18)-C(13)	-0.29(16)
C(14)-C(13)-C(18)-C(17)	3.79(15)	C(11)-C(13)-C(18)-C(17)	-172.90(9)
O(1)-C(11)-C(19)-C(20)	134.91(10)	C(13)-C(11)-C(19)-C(20)	-108.33(10)
C(2)-C(11)-C(19)-C(20)	15.32(13)	O(1)-C(11)-C(19)-C(24)	-46.07(12)
C(13)-C(11)-C(19)-C(24)	70.69(11)	C(2)-C(11)-C(19)-C(24)	-165.66(8)
C(24)-C(19)-C(20)-C(21)	1.79(15)	C(11)-C(19)-C(20)-C(21)	-179.19(9)
C(19)-C(20)-C(21)-C(22)	-0.03(16)	C(20)-C(21)-C(22)-C(23)	-1.30(16)
C(21)-C(22)-C(23)-C(24)	0.84(16)	C(22)-C(23)-C(24)-C(19)	0.96(16)
C(20)-C(19)-C(24)-C(23)	-2.25(15)	C(11)-C(19)-C(24)-C(23)	178.68(9)
O(2)-C(12)-C(25)-C(30)	-4.74(13)	C(5)-C(12)-C(25)-C(30)	115.12(10)
C(31)-C(12)-C(25)-C(30)	-117.93(9)	O(2)-C(12)-C(25)-C(26)	168.47(9)
C(5)-C(12)-C(25)-C(26)	-71.66(11)	C(31)-C(12)-C(25)-C(26)	55.28(11)
C(30)-C(25)-C(26)-C(27)	-0.41(14)	C(12)-C(25)-C(26)-C(27)	-173.84(9)
C(25)-C(26)-C(27)-C(28)	2.11(15)	C(26)-C(27)-C(28)-C(29)	-1.65(16)
C(27)-C(28)-C(29)-C(30)	-0.47(16)	C(28)-C(29)-C(30)-C(25)	2.19(15)
C(26)-C(25)-C(30)-C(29)	-1.72(14)	C(12)-C(25)-C(30)-C(29)	171.62(9)
O(2)-C(12)-C(31)-C(36)	112.53(10)	C(25)-C(12)-C(31)-C(36)	-129.98(10)
C(5)-C(12)-C(31)-C(36)	-2.66(13)	O(2)-C(12)-C(31)-C(32)	-66.90(10)
C(25)-C(12)-C(31)-C(32)	50.60(11)	C(5)-C(12)-C(31)-C(32)	177.91(8)
C(36)-C(31)-C(32)-C(33)	0.42(16)	C(12)-C(31)-C(32)-C(33)	179.90(10)
C(31)-C(32)-C(33)-C(34)	-0.19(18)	C(32)-C(33)-C(34)-C(35)	-0.28(18)
C(33)-C(34)-C(35)-C(36)	0.50(17)	C(32)-C(31)-C(36)-C(35)	-0.20(15)
C(12)-C(31)-C(36)-C(35)	-179.62(9)	C(34)-C(35)-C(36)-C(31)	-0.26(16)

Table S12. Hydrogen bonds for uvic1813 [Å and °].

D-H...A	d(D-H)	d(H...A)	d(D...A)	<(DHA)
O(1)-H(1OA^a)...O(2)#1	0.80(4)	2.04(4)	2.7266(10)	144(3)
O(1)-H(1OB^b)...O(2)	0.88(4)	1.78(4)	2.6406(13)	163(4)
O(2)-H(2OA^a)...O(1)	0.75(4)	1.89(4)	2.6406(13)	172(3)
O(2)-H(2OB^b)...O(1)#1	0.84(4)	2.04(3)	2.7266(10)	139(3)

Symmetry transformations used to generate equivalent atoms:
#1 -x+1,-y+1,-z+1